DOI:10.14753/SE.2021.2460

MORPHOLOGICAL AND FUNCTIONAL CHARACTERIZATION OF THE ATHLETE'S HEART USING ADVANCED ECHOCARDIOGRAPHIC TECHNIQUES

Ph.D. Thesis

Bálint Károly Lakatos MD

Doctoral School of Basic and Translational Medicine
Semmelweis University

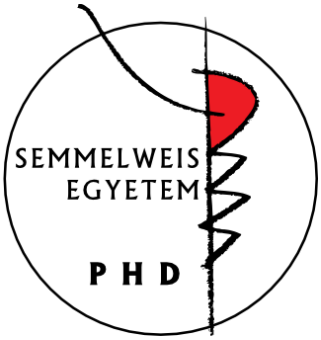

Supervisors: Attila Kovács, MD, Ph.D.
Béla Merkely, MD, Ph.D., DSc.

Official reviewers: Zsuzsanna Miklós MD, Ph.D.
Eszter Csajági MD, Ph.D.

Head of the Complex Examination Committee: Tivadar Tulassay MD, D.Sc

Members of the Complex Examination Committee: Péter Andréka MD, Ph.D.
Attila Patócs MD, Ph.D.

Budapest, 2020

DOI:10.14753/SE.2021.2460

Table of contents

DOI:10.14753/SE.2021.2460

DOI:10.14753/SE.2021.2460

DOI:10.14753/SE.2021.2460

LIST OF ABBREVIATIONS

2D – two dimensional

3D – three dimensional

A – late diastolic filling velocity

a’ – mitral anular late diastolic peak velocity

AEF – anteroposterior ejection fraction

AF – atrial fibrillation

ANOVA – analysis of variance

ARVC – arrhythmogenic right ventricular cardiomyopathy

AV – atrioventricular

AWT – anterior wall thickness

BSA – body surface area

BW – body weight

CI – cardiac index

cMR – cardiac magnetic resonance imaging

CO – cardiac output

CPET – cardiopulmonary exercise testing

CSr – circumferential strain rate

DCM – dilated cardiomyopathy

dP/dtmax – the maximal slope of left ventricular systolic pressure increment

dP/dtmin – the maximal slope of left ventricular diastolic pressure increment

DT – deceleration time

E – early diastolic filling velocity

e’ – mitral anular early diastolic peak velocity

ECG – electrocardiography

EDV – end-diastolic volume

EF – ejection fraction

ESPVR – end-systolic pressure-volume relationship

ESV – end-systolic volume

FAC – fractional area change

FS – fractional shortening

FWLS – free wall longitudinal strain

GCS – global circumferential strain

GLS – global longitudinal strain

HCM – hypertrophic cardiomyopathy

HR – heart rate

HW – heart weight

IGF – insulin-like growth factor

ICC – intraclass correlation coefficient

JAK – Janus kinase

LA – left atrium

LEF – longitudinal ejection fraction

LSr – longitudinal strain rate

LV – left ventricle

LVEDD – left ventricular end-diastolic diameter

LVEDP – left ventricular end-diastolic pressure

LVESD – left ventricular end-systolic diameter

LVESP – left ventricular end-systolic pressure

M – mass

MAP – mean arterial pressure

PLAX – parasternal long-axis

preAV – volume prior to the late diastolic emptying

PRSW – preload recruitable stroke work

P-V – pressure-volume

PWT – posterior wall thickness

RA – right atrium

REF – radial ejection fraction

RIMP – right ventricular index of myocardial performance

RV – right ventricle

RWT – relative wall thickness

s’ – mitral anular systolic peak velocity

SCD – sudden cardiac death

SR – strain rate

STAT – signal transducer and activator of transcription protein

DOI:10.14753/SE.2021.2460

STE – speckle-tracking echocardiography

SV – stroke volume

SW – stroke work

TAPSE – tricuspid anular plane systolic excursion

Vmax – maximal atrial volume

Vmin – minimal atrial volume

VO2/kg – peak oxygen uptake

DOI:10.14753/SE.2021.2460

1. INTRODUCTION

1.1 Historical perspective

The adaptation of the cardiovascular system to regular physical exercise has been a subject of research for over a century. The first studies reporting the enlargement of the heart in athletes were published in the end of the 19th century (1,2). While the initial observations were based on chest percussion, a few years later chest X-ray examinations also confirmed these findings (3). Palpation of the radial artery pulse, and later electrocardiographic (ECG) studies revealed significant resting bradycardia in athletes. Along with the extension of the cardiovascular diagnostic modalities (echocardiography, cardiac magnetic resonance, etc.), data were exponentially growing regarding the morphological and functional remodeling of the heart in response to chronic exercise. This was also supported by the substantial changes in athletic training: the hobby sportsmen of the first Olympics were gradually replaced by professional athletes. As a result of scientifically designed training regimes, diets and schedules, the cardiac adaptation in elite athletes may be considered as the absolute peak of exercise-induced remodeling.

In parallel with the novel findings of exercise physiology, alarming observations about the possibly harmful consequences of intense training brought sports cardiology to life. The death of Philippides, the soldier running from Marathon to Athens may be the first documented exercise-related sudden cardiac death (SCD), and even in the 18. century it was thought that intense regular exercise is generally harmful. This concept was mainly defeated; however, the existence of “athletic heart syndrome” – cardiomyopathy solely on the basis of regular exercise is still a matter of debate.

Nowadays, sports cardiology is an important subspecialty of heart- and vascular medicine incorporating various fields, such as cardiovascular imaging, electrophysiology, or even experimental cardiology. The “larger heart for a better performance” concept is dissected to the level of distinct changes in myocardial mechanics, histological features, and gene expressions.

1.2 Cardiac chamber mechanics and their measurement: systolic function beyond left ventricular ejection fraction

Undoubtedly, left ventricular (LV) ejection fraction (EF) is the mainstay parameter of LV function: numerous guidelines incorporate its measurement to support clinical decisions due to its robustly established prognostic role. Nevertheless, it only represents the systolic function of the LV from a geometric point of view, and its significant load dependency and suboptimal reproducibility are also established limitations of the measurement (4). Importantly, a decline in LVEF typically marks advanced myocardial damage, when even optimal therapeutic choices may offer only limited reversibility. Due to these issues, significant efforts were made to identify more sensitive markers of myocardial (dys)function. In order to properly interpret these state-of-the-art parameters, a better understanding of cardiac mechanics is essential.

1.2.1 Left ventricular deformation

LV ejection is generated by a complex interplay of different myofiber layers. The subendocardial layer consists of mainly longitudinally oriented fibers, which extend to the obliquely oriented fibers of the subepicardium through the LV apical vortex. A horizontal, middle layer is also present, contracting mainly circumferentially. In physiological conditions, the circumferential shortening contributes twice as much more to LV ejection compared to the longitudinal contraction (5).

The LV subendocardial fibers have the highest oxygen demand; therefore, they are the most prone to ischaemia, and also hemodynamic overload states affect more this layer (4). Hence, the vast majority of cardiac diseases damage longitudinal shortening first, giving the possibility to detect early stages of myocardial dysfunction by the measurement of this deformation component. A decrease in longitudinal contraction can be effectively compensated by an increase in circumferential shortening, which maintains LVEF, while changes in chamber volume and wall thickness may also alter this interrelation (5).

1.2.2 Right ventricular deformation

Three main mechanisms generate the right ventricular (RV) ejection: shortening along the longitudinal axis with the traction of the tricuspid annulus towards the apex

(longitudinal motion); inward movement of the RV free wall (radial motion) and traction of the RV free wall insertion points by the circumferential deformation of LV myocardium (anteroposterior motion) (6). These motion components also correspond to the architecture of the RV myocardium. The latter consists of two main layers: a predominantly longitudinally aligned subendocardial layer and a dominantly circumferentially oriented subepicardial layer. By the shared interventricular septum and the fibers crossing the interventricular groove, LV contraction also has a significant impact on RV performance. Traditionally, the longitudinal motion is considered to be the main determinant of RV ejection; however, recent data suggest that the non-longitudinal motion components may have a more significant role than previously thought (6).

1.2.3 Atrial deformation

The function of the thin-walled atria in health and disease was neglected for a long time. Indubitably, the atrial function is tightly coupled to the function of the corresponding ventricle. Nevertheless, evidence is growing about a more reciprocal relationship: while ventricular dysfunction markedly hampers atrial function, atrial dysfunction also has a significant effect on ventricular performance (7).

The wall of the atria consists of two layers, longitudinally aligned fibers can be found in the subendocardium, while the subepicardial layer consists of circumferentially oriented fibers. Assessment of longitudinal and circumferential function separately may be of high interest; however, a similarly interesting (and easier to measure) aspect of atrial performance is its phasic function (7). During ventricular systole, the atria act as reservoirs of blood. In early diastole, they serve as passive conduits of the diastolic blood flow into the ventricles, while at late diastole active contraction of the atria create a booster pump function to complete ventricular filling. These distinct phases can be quantified either by the volumetric changes (Figure 1) and also by the deformation of the atria throughout the cardiac cycle.

DOI:10.14753/SE.2021.2460

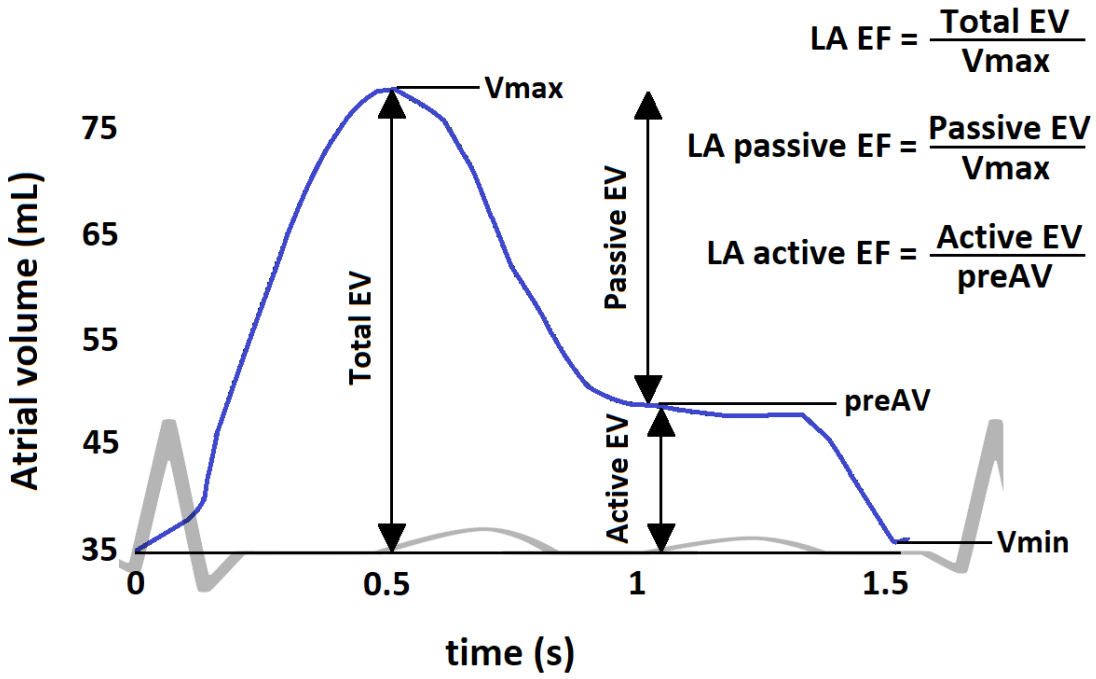

Figure 1: Left atrial (LA) volume-time curve with the phasic volumes and the calculation of LA functional indices. The curve in synchronized with an electrocardiogram. Vmax = maximal atrial volume, Vmin = minimal atrial volume, EV = ejection volume, preAV = preA-wave volume. LA EF = left atrial total emptying fraction (reservoir function); LA passive EF = left atrial passive emptying fraction (conduit function); LA active EF = left atrial active emptying fraction (contractile function). These metrics were used in our third study regarding LA function in athletes

1.2.4 Conventional echocardiographic indices and their inherent limitations

Standard one- and two dimensional (2D) and Doppler-based echocardiographic methods revolutionized the examination of the heart (8). Quantification of cardiac morphology using chest X-ray and by physical examination, assessment of valvular function by auscultation, and the estimation of cardiac function by indirect physical signs and symptoms were replaced with much more objective and reproducible measures. The largest body of data originate from these parameters, providing numerous important observations regarding the nature of physiological adaptation to exercise. Still, simple linear dimensions or calculated volumes using geometric formulas do not effectively characterize the complex three-dimensional (3D) structure of the cardiac chambers. Moreover, the functional measures derived from these parameters carry the same errors

along with other additional fundamental limitations as well (e.g., limited sensitivity, significant load dependency, modest reproducibility). These issues brought novel cardiovascular imaging methods, such as speckle-tracking echocardiography (STE) or 3D echocardiography to life. Beyond the management of various cardiovascular diseases, these state-of-the-art techniques can also be implemented in the practice of sports cardiology.

1.2.5 Speckle-tracking echocardiography

The measurement of myocardial deformation offers the opportunity to assess myocardial function from another aspect compared to the traditional functional parameters. STE quantifies myocardial deformation by the frame-by-frame tracking of the region of interest. The myocardium consists of a complex structure of different histological components, causing scattering, reflection, and interference of the ultrasound beams: on a standard 2D greyscale image, these phenomena appear as “speckles”. The movement of these stable imaging markers serves as a surrogate of myocardial function. Myocardial deformation can be quantified as strain values by tracking the speckle pattern throughout the cardiac cycle. Strain represents the relative change in the length of the region of interest (measured in %). Negative strain represents shortening, while positive values represent lengthening. The 3D myocardial deformation has different elemental components, such as longitudinal and circumferential shortening, which can be quantified by strain measurement. Global LV myocardial strain, especially global longitudinal strain (GLS), has proven to have incremental value compared to traditional functional measures in almost every cardiovascular disease (9). GLS may effectively reflect the function of the longitudinally aligned LV subendocardial myofibers, which are, as previously mentioned, typically damaged initially in disease processes. STE assessment of the RV and the atria is also feasible, and clinical data are growing regarding the quantification of myocardial deformation in these cardiac chambers as well (10,11). Nevertheless, significantly less studies investigated RV and atrial deformation in health and disease.

1.2.6 3D echocardiography

The tomographic imaging of conventional 2D echocardiography is a major limitation of the technique: the cardiac chambers are complex 3D structures; therefore, conventional

geometric assumptions only give a rough estimation of actual morphology. The one-dimensional measurement of LV volumes, such as the Teichholz formula, or the 2D Simpson's method tends to work with acceptable measurement errors in the case of normal LV geometry. Still, when abnormal LV geometry is present (which are the clinically most relevant scenarios), the errors of volumetric estimation are far from negligible (12). This issue gains special importance in the case of the RV and the atria, where the complex anatomy of these chambers undermines the feasibility of such simple geometric formulas. In everyday clinical practice, the assessment of RV function generally relies on simple linear measurements with subsequent limitations, while the volumetric measurement of the atrial function is usually not even part of a standard echocardiographic examination. 3D echocardiography may overcome these issues by examining the exact volumes and also 3D deformation of cardiac chambers. Using 3D reconstruction of the RV, the detailed assessment of RV mechanical pattern is feasible, and the importance of such motion directions that are usually neglected in clinical routine can also be evaluated (i.e., radial "bellows" motion of the free wall or anteroposterior RV shortening). Semi-automatic 3D measurement of the atria offers incremental value in terms of accuracy and reproducibility, characterizing the phasic function of these cardiac chambers.

Nowadays, 3D echocardiography is widely available, and the usage of 3D post-processing techniques is also strongly recommended by the most recent chamber quantification guideline (13). Several vendors provide semi-automatic or even fully automatic solutions for 3D measurements, which significantly reduces the length of the quantification process (Figure 2). 3D-based measurements have already proven their additive diagnostic and prognostic value compared to 2D assessment, and with the constantly improving hardware and software environment, it may become an essential part of the everyday echocardiographic protocols (14).

3D volumes of cardiac chambers are significantly higher compared to those measured by 2D estimates; therefore, normative values derived from 2D studies are not applicable to 3D-based measurements. Nevertheless, evidence suggests that compared to the gold standard cardiac magnetic resonance (cMR), a systematic underestimation of chamber volumes is still present (14).

DOI:10.14753/SE.2021.2460

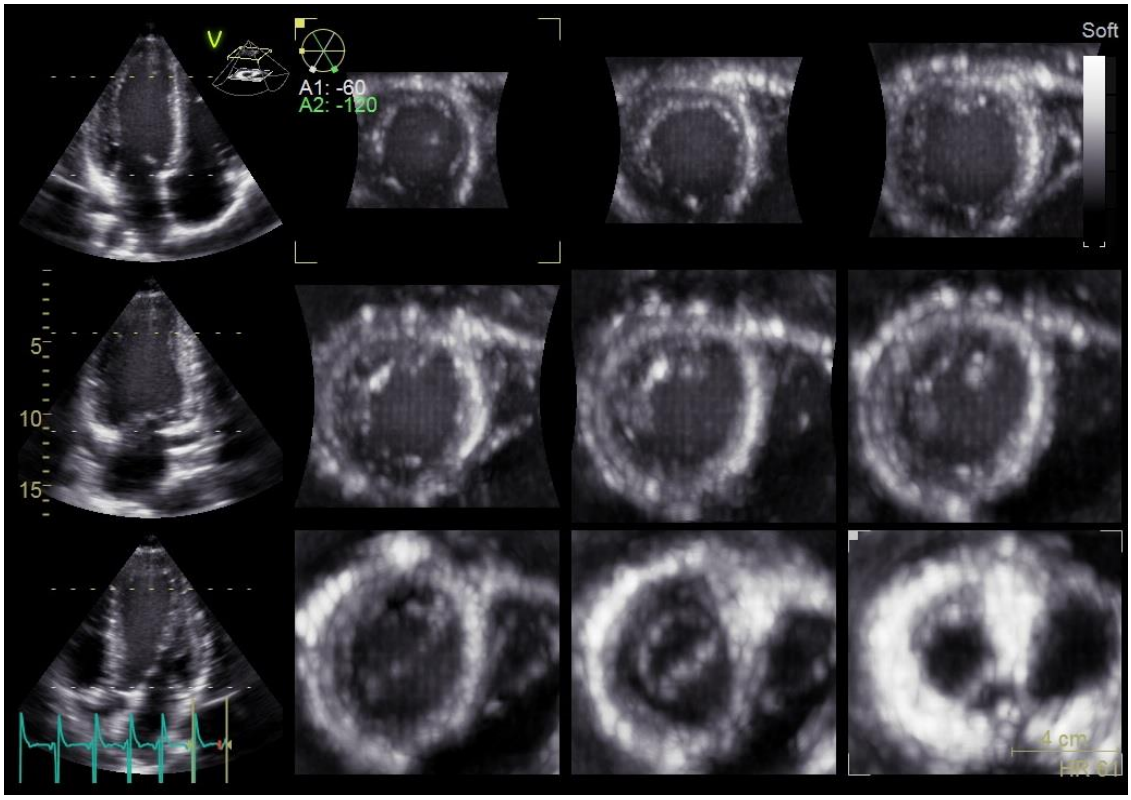

Figure 2: 3D echocardiography of the left ventricle and the left atrium. The software shows long-axis and short-axis views of the chambers simultaneously. Various vendor-dependent or even independent software solutions are available to extract volumetric and deformation data from raw 3D images.

1.3 The cardiac adaptation to regular physical exercise

High-intensity exercise training has significant hemodynamic demands: depending on the sport discipline, a 5-6-fold increase in cardiac output (CO) and/or significant elevation in the systemic blood pressure is needed during peak performance (15). To cope with such an increase in workload, the stroke volume (SV) is increased by 25-50%, along with a 4-fold increase in heart rate (HR). These changes require complex cardiac remodeling, also referred to as the athlete's heart (Figures 3 and 4). The rationale of this physiological adaptation follows simple physical principles. According to the law of Laplace, the wall tension is determined as follows:

$$T = \frac{Pr}{2h}$$

T: tension; P: pressure; r: circumference of the chamber; h: wall thickness

Considering that the cardiomyocytes have extremely limited proliferation potential, changes in the cardiac mass are based on the increase in cardiomyocyte size and/or accumulation of the extracellular tissue. In opposed to pathological states, physiological remodeling is characterized by elevated myocyte mass with only a proportional increase in the absolute extracellular tissue mass (16).

Sport disciplines can be classified along with the intensity of their isotonic (percent of peak oxygen uptake) and isometric (percent of voluntary peak contraction) component, which influence the nature of the observed cardiac hypertrophy (17). In the case of isotonic, dynamic exercise (e.g., long-distance running, swimming), CO is elevated, resulting in increased preload and decreased systemic resistance. In order to maintain wall tension, chamber volumes increase, while wall thickness remains unaltered (excentric hypertrophy, Figure 3). In the case of isometric, static exercise (e.g., weightlifting, wrestling), systemic resistance is markedly elevated, while CO only modestly changes. Wall tension is compensated by the increase in wall thickness, while chamber volumes do not change significantly (concentric hypertrophy, Figure 3). The most prominent remodeling is observed in endurance athletes (e.g., cycling, triathlon), where both types

of hemodynamic stress are combined: high CO has to be achieved against increased systemic resistance. Based on the classical concept of Morganroth and colleagues, the nature of exercise-induced cardiac remodeling reflects these principles (18). Nevertheless, initially, it was only applied to the LV, and several results suggest that these theoretical categories are rarely seen in practice. Irrespective of the sport discipline, professional athletic training usually incorporates dynamic and static components as well; therefore, a wide range of changes can be seen regarding cardiac morphology and function (19). Moreover, several other factors, such as age, training load and intensity, gender, ethnicity, and personal genetic factors, may also influence cardiac adaptation (20).

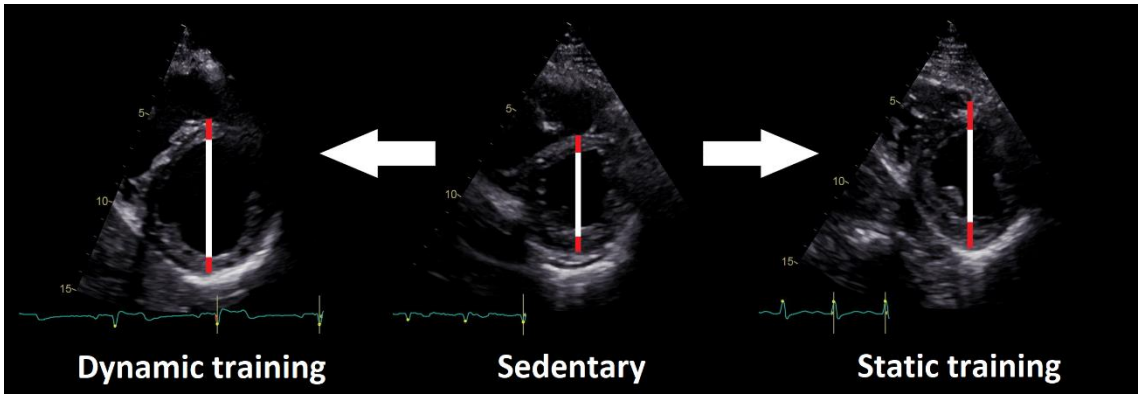

Figure 3: The Morganroth hypothesis in clinical practice. Dynamic (isotonic) training is associated with significant excentric hypertrophy, as seen on the left echocardiogram of a professional swimmer. Static (isometric) training results in concentric hypertrophy of the left ventricle, demonstrated by the echocardiogram of a powerlifter athlete on the right (parasternal short-axis views). White lines: end-diastolic diameter, Red lines: septal and posterior wall thickness

1.3.1 Molecular pathways of the exercise-induced cardiac remodeling

The nature of the hemodynamic stimuli is fundamentally the same in the physiological and pathological cardiac remodeling. Significant LV pressure- (e.g., aortic stenosis, hypertension) and volume overload (mitral regurgitation, aortic regurgitation) are associated with morphologically similar changes of the myocardium; however, the molecular pathways are markedly different. As it is widely known, these differences also translate into substantial prognostic consequences.

According to our current knowledge, the Insulin-like growth factor (IGF) – Phosphoinositide 3-kinase – Akt is the most important signalization pathway in the physiological remodeling (21). Besides that, cytokine-driven pathways, such as the gp130 – JAK – STAT (22) and the thyroid hormone signalization, may also have a role in this process (23). The expression of several anti-apoptotic and anti-fibrotic proteins are increased (24).

In contrast with that, pathological remodeling is mainly initiated through Gs and Gq-protein coupled pathways by the increased levels of certain circulating hormones (e.g., catecholamines, angiotensin II, endothelin-1). These transmitters promote the upregulation of the fetal genetic program with enhanced apoptosis, necrosis, and extracellular matrix accumulation (24).

1.3.2 Left ventricular adaptation to exercise

As the "engine" of the systemic circulation, the vast majority of data regarding the training-induced cardiac changes are focusing on the LV. The above-discussed theory of Morganroth et al. is at least partially confirmed by clinical experience: meta-analyses have shown that dynamic exercise is associated with increased LV diameters, while strength-trained athletes have significantly higher relative wall thickness compared to sedentary individuals or dynamic athletes (25,26). Therefore, the increase in LV mass (M) is similar in the athlete groups, while the relative wall thickness (RWT) shows the different nature of LV hypertrophy in dynamic and static athletes. Still, as previously stated, numerous studies suggest that this dichotomous distinction between isometric and isotonic training-related remodeling does not reflect the real-life experience, and the classification of sports by Mitchell et al. only gives a rough estimation of the expected physiological LV adaptation (20).

The degree of LV dilation may be quite prominent (Figure 4): a considerable proportion of elite athletes fulfill the criteria of mild or even moderate LV dilation, which was also confirmed by more advanced imaging modalities, such as 3D echocardiography or cMR (27,28). Mildly increased LV wall thickness is also not an uncommon finding (25). Moreover, certain authors suggest that even extreme LV dilation (LV end-diastolic diameter > 70 mm) and/or severe LV wall thickening (Septal thickness > 16 mm) may be associated with physiological remodeling (29).

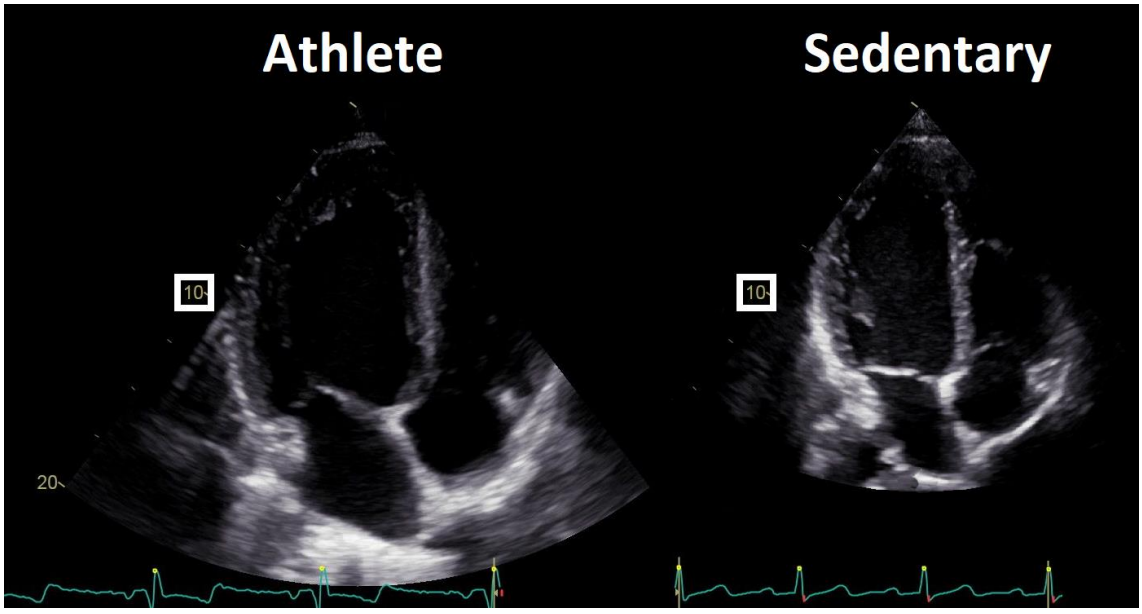

Figure 4: Left ventricular and atrial adaptation in athletes. Two echocardiograms (apical four-chamber view) are shown, a professional male athlete (swimmer, 25 hours of training/week), and a sedentary male with comparable height. Note the spectacular difference in chamber dimensions.

Beyond morphological adaptation, alterations in LV systolic function are also well known; however, results are far less consistent. The most robust body of data are derived from echocardiographic studies, and a large number of cMR studies are also available. Meta-analyses of both modalities have shown comparable resting LV ejection fraction (EF) values between athletes and sedentary controls (25,28). Nevertheless, the low-normal or even reduced LV EF of professional athletes is not an uncommon finding (30,31). Reduced LV systolic function at rest is usually associated with more advanced morphological remodeling, suggesting that if significant chamber enlargement is present, a less vigorous contractile function is required at rest to maintain CO even in the presence of the characteristic sinus bradycardia (20).

Measurement of more advanced markers of LV systolic performance, such as STE-derived strain values, also demonstrate conflicting data (32). Some studies report enhanced deformation values compared to sedentary individuals (33), while comparable (34) and lower strains (35) are also reported in the scientific literature. A meta-analysis of STE in athletes showed deformation values in the normal range; however, a significant heterogeneity of GLS values was seen across studies (32). Overall, similarly to LV EF,

maintained strain values are expected in association with exercise-induced remodeling, with a considerable amount of athletes presenting low-normal LV systolic deformation.
Functional adaptation to long-term exercise training also involves changes in the diastolic function. During exercise, the diastolic function should support adequate LV load even when increased heart rates significantly shorten the period of diastole. Pulsed-wave Doppler interrogation of the transmitral diastolic inflow in athletes often demonstrates higher early filling velocity (E) and/or decreased atrial contraction flow (A), resulting in higher E/A ratio (36,37). This pattern is even more pronounced in master athletes: it appears that regular physical exercise prevents or at least blunts the physiological shift towards a lower E/A ratio in the elderly (36). Similarly to the assessment of LV systolic function, STE studies also showed inconsistent results: in the majority of cases, comparable resting early diastolic strain rates were seen along with lower late diastolic strain rate (35). Still, studies examining LV rotational mechanics suggest that enhanced diastolic untwisting can be seen in response to regular exercise training, as a sign of supernormal LV diastolic function at rest (38,39). Nevertheless, the significant effect of resting bradycardia in diastolic filling properties should also be emphasized (36).

1.3.3 Right ventricular adaptation to exercise

Compared to its left counterpart, significantly less data are available regarding RV remodeling in athletes. Traditionally it is believed that intense dynamic training is considered to be a sole volume overload for the RV, while pure strength training has little to no effect on the right side of the heart. However, according to recent studies, concomitant pressure overload is remarkably present during high-intensity dynamic training. Left atrial pressure progressively increases with CO, which is transferred back directly to the pulmonary circulation (40,41). Moreover, compared to the high-resistance systemic circulation, the pulmonary vascular bed has a limited reserve for flow-mediated reduction of resistance (41). These factors result in elevated pulmonary arterial stiffness and increased RV wall stress (30, 31). Considering that in top-level athletes, CO can reach a 5-7-fold increase during peak exercise, markedly elevated pulmonary pressures may develop (15). Therefore, dynamic exercise can be perceived as a combined pressure-volume overload to the RV.

Recent studies suggest that right-sided dilation may be comparably significant to LV dilation, and it becomes even more pronounced with longer training history and higher intensity (42-44). RV dimensions may exceed the normal limits, and other peculiar morphological features, such as rounded apex, hyperreflective moderator band, and hypertrabeculation, are also relatively common (45). cMR studies confirm these findings: a recent meta-analysis found more significant RV dilation compared to the LV; moreover, RV remodeling was present irrespective of the training regime (28). Evidence suggests that increased RV wall thickness can be seen in endurance athletes as an adaptive response to the elevated pulmonary pressures during exercise (46).

The incidence and the physiological nature of RV scarring is also a matter of debate. While the presence of focal late gadolinium enhancement on cMR in a minority of professional athletes is a known phenomenon (47), a previous study enrolling master athletes with a very high cumulative training load found no signs of RV myocardial scarring (42).

In terms of global function measured by EF, the lower resting contractile state of the RV is similar to its left counterpart in this population (45). However, the majority of studies demonstrate preserved (48,49), or even enhanced (44) STE-derived GLS compared to sedentary controls presuming a shift in the deformation pattern. Still, data are lacking about the detailed assessment of RV mechanical pattern in athletes. Results are also inconsistent regarding RV diastolic function; however, increased early diastolic strain rate was demonstrated in athletes suggesting enhanced resting diastolic function similarly to the LV (48).

1.3.4 Atrial adaptation to exercise

Cardiac adaptation to intense training is not limited to the level of the ventricles. The atria are also subjects of volume- and pressure overload during high-level exercise (40). Two meta-analyses demonstrated higher left atrial (LA) volumes compared to controls (50,51), while several studies showed enlargement of the right atrium (RA) as well (52,53). A significant proportion of athletes fulfill the criteria of mild or even moderate atrial enlargement (Figure 4), showing that the changes in atrial morphology may be just as relevant or even more pronounced than ventricular remodeling (54). Functional alterations are also present: according to a recent meta-analysis, athletes have lower LA

GLS, which corresponds to lower resting reservoir function of the chamber. The conduit function was comparable between athletes and controls (55). On the other hand, decreased resting contractile strain rate was also noted compared to sedentary individuals (50). Nevertheless, similarly to the changes of LV diastolic properties at rest, significant sinus bradycardia may have a fundamental influence on these measures as well.

1.3.5 Influencing factors of the physiological remodeling

While the effect of the training regime (dynamic and/or static) is classically the most commonly discussed factor regarding the nature of exercise-induced remodeling, other relevant influencing factors are also known. One of the most important ones is gender differences. While females also demonstrate the morphological and functional changes of the athlete's heart, the degree of LV and RV remodeling is significantly less compared to males even when the values are indexed to the body surface area (56). Interestingly, evidence suggests that LA dimensions do not differ between genders; on the other hand, the functional changes seem to be less evident in females (51). The impact of sex hormones was also investigated in experimental studies, generally reporting more pronounced cardiac adaptation in females, raising the possibility that other factors (e.g., different training load, other genetic causes) may also impact the gender differences in exercise-induced cardiac remodeling (56). The absolute training load is another important determinant of the expected changes: athlete's heart may be perceived as a spectrum from the subtle changes of hobby sportsmen to the quite spectacular remodeling of professional athletes (57). Interestingly, while the absolute number of training hours may influence the degree of morphological changes, the cumulative training load may not determine the biventricular functional measures (28). Age also influences the development of athlete's heart: according to previous data, signs of physiological remodeling can be observed even in children (58), while master athletes typically demonstrate higher wall thicknesses (59). Racial differences were also observed: in black athletes, the presence of more concentric-type remodeling with wall thicknesses often exceeding the normal values is not an uncommon finding (60).

1.3.6 The time course of physiological adaptation: development of athlete's heart and the effect of detraining

Exercise cardiology studies are predominantly cross-sectional, and very limited information is available regarding the longitudinal nature of the physiological remodeling. Many consequences of pathological stimuli in cardiovascular diseases typically show only limited reversibility even if the promoting factors have vanished. In opposed to this, athlete's heart is generally thought to have a highly dynamic nature. The first observations regarding the longitudinal changes in athlete's heart reported the effects of deconditioning: in response to suspended athletic activity, a significant reduction of LV wall thicknesses were seen after only a median of 3 months of suspended training (61). A cohort of former professional cyclists showed similar results; however, LV and RV dimensions were considerably higher, while atrial volumes were markedly elevated compared to controls even after a median of 30 years of suspended professional training (62). These results suggest that exercise-induced ventricular, and especially atrial dilation may not be completely reversible, and permanent changes in cardiac morphology may be present as a consequence of previous regular training. On the other hand, functional measures did not differ between the former athlete and sedentary groups.

Development of the athlete's heart shows a more or less similar pattern: LV and RV mass demonstrates a progressive increase as a relatively early response to exercise training. Considerable LV dilation only appears after six months of training; however, RV volume shows a progressive increase from the outset of training (63). LA dilation with lowering LA active emptying function can also be observed (64). Nevertheless, longitudinal studies with professional athletes show that concentric-type LV hypertrophy reoccurs with maintained long-term regular exercise (65). Resting systolic functional measures were found to be unchanged, while diastolic measures were reported to be improved in these studies (66). Still, it is important to mention that the main modifying factors, such as training regime, gender, and age, are proven to impact also the dynamic changes of exercise-induced cardiac remodeling, which limits the generalizability of these observations.

1.3.7 Other cardiovascular properties of the athlete's heart: electrical changes and adaptation of the coronary arteries

Beyond structural and functional remodeling, distinct changes of the ECG are also present in the athlete's heart as a sign of electrical remodeling (67). One of the most characteristic marker of the athlete's heart is the significant resting bradycardia, which is attributable to the increased vagal tone. This markedly increased parasympathetic activity may be associated with atrioventricular (AV) block: cases of atrioventricular dissociation with no apparent underlying heart disease are also known (68).

Several minor alterations on the ECG, such as incomplete right bundle branch block, first-degree AV-block, early repolarization pattern, and voltage criteria of left ventricular hypertrophy, are more common in athletes and considered to be a normal phenomenon. Other ECG changes, such as T-wave inversions, Mobitz I. type AV block may also be present as a normal variant, especially in distinct subpopulations (black athletes, adolescents) (67). Nevertheless, these uncommon patterns usually indicate further examinations to exclude any underlying pathological process.

Another interesting aspect of physiological remodeling is the changes in the coronary arteries. Regular exercise training promotes angiogenesis resulting in an enhanced capillary density of the myocardium and also promotes collateralization of the coronary arteries (69). Moreover, several studies demonstrated the higher basal arterial tone and enhanced coronary artery dilator capacity of athletes, showing the morphological and also functional remodeling of the cardiac vascular bed (70).

1.3.8 The rationale of the physiological remodeling: relationship with exercise capacity

Despite the above discussed marked changes in the athlete's heart, data are scarce regarding the association between cardiac remodeling and exercise capacity. While the success in professional sport is determined by many other factors (e.g., psychological state, precision, or even fortune) cardiopulmonary exercise testing (CPET)-derived peak oxygen uptake (VO_2/kg) may be used as an objective measure of athletic performance, which enables us the quantification of physical status. During CPET, the subject of the examination performs progressively increasing exercise (e.g., running, cycling) until peak workload and exhaustion. Oxygen uptake and also CO_2 removal are measured to quantify

aerobic and anaerobic exercise capacity. Enhanced values presume an increased ability to serve the exercise-induced metabolic demands, which is highly dependent on the cardiopulmonary fitness of the individual. VO_2/kg is an established marker or cardiovascular health with a known strong prognostic role in the general population (71). Previous studies using cMR examinations in athletes observed a strong correlation between cardiac size and VO_2/kg (72). Ventricular and also LA morphological remodeling were associated with better exercise capacity (72,73). A previous study demonstrated an inverse correlation between LV and RV EF and VO_2/kg; however, interestingly, they did not find a relationship between LV deformation parameters and exercise performance (72,74). Another study enrolling older soccer referees found a direct relationship between LV GLS and VO_2/kg (75), which is in line with other studies showing a positive correlation between biventricular EF and GLS and exercise capacity in heart failure patients (76). On the other hand, professional athletes commonly demonstrate low-normal EF and deformation values, which have been in stark contrast with these findings.

1.4. Potential adverse effects of regular exercise, "the athletic heart syndrome"

Physical exercise is generally considered to be beneficial: according to our current knowledge, regular exercise decreases resting blood pressure, lowers blood cholesterol levels, and enhances the expression of anti-atherogenic factors (77). Beyond the cardiovascular system, other organ functions may also improve, moreover, the incidence of various cancer types are also found to be lower in athletic individuals (77). These effects also translate into prognostic consequences: robust evidence shows that regular exercise lengthens life expectancy (78). In contrast to these findings, the overall effects of high-intensity regular training are much more controversial.

1.4.1 Incidence of sudden cardiac death in athletes

Momentous clinical studies confirmed the higher probability of SCD in athletes compared to the age-matched healthy, sedentary population. According to a prospective study enrolling more than 1 million young subjects from the Veneto region, Italy, the incidence of SCD was 2.5 times higher (0.9 vs. 2.3 person/100000 person-years) in athletes (79).

However, a similar study from the United States of America reported a much more alarming 1 person/3100 person-years incidence of SCD in professional basketball players (80). Males have a 3-5 times higher risk, and several studies indicate that in black athletes, SCD has a markedly higher incidence (81). Considering that the events occur in (seemingly) healthy, young individuals, these observations are particularly worrisome. SCD of a famous, renowned athlete also draws significant attention of the media, which may undermine the "athletic idol" and the important role of physical activity in public health.

1.4.2 Etiology of sudden cardiac death in athletes

A handful of studies from different countries examined the most common etiological factors of SCD in athletes, mostly based on post-mortem diagnoses. The findings are fairly consistent over the age of 35 years, reporting ischemic heart disease as the far most prevalent underlying condition in athletes suffering SCD (81). Nevertheless, in athletes under 35 years, the studies have shown well-defined differences across the globe. In Italy, arrhythmogenic right ventricular cardiomyopathy (ARVC) was found to be the most frequent cause of SCD (82). Previous studies suggest that ARVC-related genetic mutations are more prevalent in the South-European countries (83). However, the role of ARVC in exercise-related SCD gains particular importance in the face of novel findings regarding the connection of exercise training and the RV (84). Evidence is growing that chronic, high-intensity training may induce permanent RV damage and/or precipitate subclinical RV diseases due to the disproportionate load of the right side of the heart during intense exercise (41). Experimental studies confirmed that regular training may promote adverse remodeling of the RV in a dose-dependent manner (85). If genetic predisposition (plakophyllin-2 mutation) is present regular training may result in overt ARVC phenotype at molecular level and macroscopically as well, which was not seen in the sedentary group (86). Exercise-induced RV dysfunction was also described in human studies, however, current results refer to it as a transient phenomenon following strenuous training bouts (87).

North American studies reported hypertrophic cardiomyopathy (HCM) as the most prevalent cause of SCD in athletes (88), which may be attributable to the higher frequency of the disease in black populations (60). Moreover, a considerable minority of the autopsy

findings was “idiopathic LV hypertrophy,” which may also correspond to a morphologically mild HCM-variant (81). As previously mentioned, in sport disciplines such as basketball, where a large subset of athletes is African American, a very high incidence of SCD was reported, which may confirm the aforementioned hypothesis. A German prospective registry identified myocarditis as the most frequent cause of SCD, which emphasizes the importance of viral infections in the northern countries (89). Nevertheless, recent autopsy-based studies report the large prevalence of structurally normal hearts after athletic SCD. This population may be comprised of different primary electrical diseases (channelopathies) (81). Beyond these etiological factors, other diseases, such as anomalous coronary arteries, dilated cardiomyopathy (DCM), and aortic dissection, are also not uncommon causes of SCD in this population (81).

1.4.3 Other potential cardiovascular hazards of intense physical exercise

Atrial fibrillation (AF) without the presence of other precipitating factors (e.g., coronary artery disease, cardiomyopathy) is not a well-known potential consequence of long-term intense physical exercise (90). The relationship between competitive sport and AF is controversial. Meta-analyses of this topic concluded that athletes have increased risk of AF compared to the general population, and that is in interaction with age and gender as well: as expected, master athletes and males are consistently reported to be more susceptible to exercise-related AF (91). Furthermore, large studies have shown that exercise intensity has a U-shaped relationship with AF risk (“exercise paradox”): decreases with moderate exercise but increases at both ends of the exercise spectrum (91,92). Moreover, besides anatomical and functional cardiac remodeling, electrical remodeling might be present as well, and there is likely to be a subset of athletes that have high genetic scores for AF risk (93). Nevertheless, we are still lacking prospective studies regarding AF risk in athletes.

While regular exercise is generally considered to be beneficial in structurally normal hearts, several papers reported more advanced coronary artery calcification in master athletes. A few decades earlier, it was hypothesized that anyone who is able to complete a marathon is practically protected from any form of coronary atherosclerosis. This belief was elegantly defeated by a case series of six myocardial infarctions during the New York Marathon of 1976 (94). These results also raised the possibility that vigorous exercise

may accelerate the progression of coronary atherosclerosis and/or precipitate acute coronary syndrome (95). Coronary computed tomography angiography examinations reported higher coronary plaque burden predominantly in male marathon runners who started running at an older age (96). Moreover, a recent small prospective study demonstrated a dramatic increase in non-calcified plaque volume following extreme endurance exercise (97). These results strongly suggest that vigorous physical exercise may have undesirable effects on the coronary arteries. Nevertheless, it is still unclear if these observations actually translate into prognostic consequences.

1.4.4 Distinction of athlete's heart from cardiovascular diseases: the issue of the "grey zone"

The morphological and functional characteristics of manifest pathological hypertrophy are well defined, providing clear cutoffs with acceptable sensitivity and specificity. One of the main issues of sport cardiology is the overlapping features of the athlete's heart and cardiovascular diseases: this diagnostic "grey zone" often complicates the distinction between these two entities. The current consensus statement of the joint branches of the European Society of Cardiology defined findings that warrant further evaluation during pre-participation screening (98).

The diagnosis of ARVC is based on the revised Task Force Criteria; however, it demonstrates only modest specificity in the case of athletes due to significant overlapping of the cutoff values (99). Previous results suggest that RV regional strain values may help to identify athletes with ARVC and also subclinical cases (100). Early detection of the disease is important in this population, considering that the majority of athletes suffer SCD during exercise; however, maintained mild or moderate amount of training may not have adverse effects on clinical outcome (101).

Marked LV wall thickening (≥15 mm in males, ≥13 mm in females) in athletes raises the suspicion of HCM (Figure 5). Examination of further conventional parameters, such as the degree of LV dilation, LA size, or the assessment of LV diastolic function, may give further aid for the distinction between HCM and athlete's heart (102). Surprisingly, previous data suggest that STE-derived resting LV GLS was comparable between athletes with HCM, healthy athletes, and controls; however, LV mechanical dispersion was able to differentiate between HCM and the healthy groups (103). Machine learning-based

phenotypic recognition also demonstrated high efficacy in the distinction between the two entities (104). Nevertheless, in opposed to the traditional viewpoint, a small prospective study suggests that physically active HCM patients have similar event rate compared to those who interrupt regular training (101).

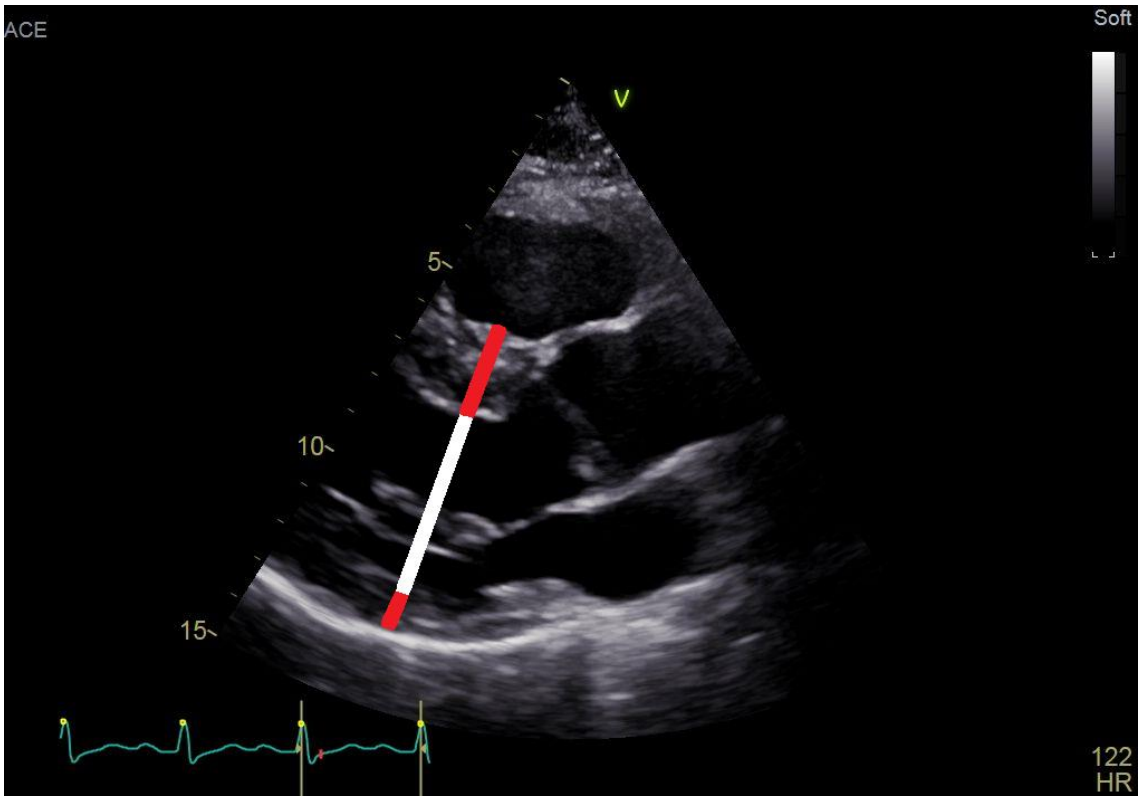

Figure 5: Hypertrophic cardiomyopathy in an athlete. Parasternal long-axis acquisition of a professional soccer player with hypertrophic cardiomyopathy. A screening echocardiography examination found significant left ventricular hypertrophy with a septal predominance (wall thickness: 17 mm, upper red arrow) and high-normal left ventricular end-diastolic diameter (white arrow). Cardiac magnetic resonance showed the absence of cardiac fibrosis; however, suspension of training did not result in regression of the left ventricular hypertrophy confirming the diagnosis of hypertrophic cardiomyopathy.

Echocardiography in the diagnosis of DCM in athletes usually provides a definitive diagnosis. Still, professional athletes often demonstrate significant LV enlargement along with borderline LV systolic function (28). The absence of spherical and/or disproportionate LV remodeling, the presence of functional valvular regurgitation, and

non-specific changes in the ECG support pathological rather than physiological remodeling in these cases.

In dubious cases, the significant reversibility of the athlete's heart offers an effective option for definitive diagnosis: by the interruption of training, a marked regression in chamber volumes and wall thicknesses, and also functional reverse remodeling is expected (105). Nevertheless, it obviously requires the cooperation of the patient, which is markedly limited in several cases.

Overall, conventional examination methods provide the diagnosis in many dubious cases. Still, when several features of pathological and physiological remodeling overlap, an advanced multimodality approach is essential. In order to better characterize the nature of physiological changes and to investigate the continuum of exercise capacity, the examination of healthy, elite athletes is needed.

1.5 Animal models of the athlete's heart

Experimental models of high-intensity exercise training provide important data regarding the athlete's heart. Properly planned and executed experimental research protocols enable us to examine the response of the cardiovascular system to regular exercise in such detailed and controlled fashion, which is not feasible in real-life clinical settings. These protocols may also include measurements and procedures (e.g., cardiac catheterization, autopsy/biopsy), which are technically or ethically, cannot be accomplished in athletes. Therefore, the vast majority of our current molecular understanding in this field is derived from experimental research, and several other important observations are based on experimental data. Nevertheless, an important limitation has to be addressed: animal physiology differs from humans; however, it may also serve as an advantage: the shorter gestation periods, many offsprings, and faster life cycles guarantee faster experimental protocols.

Small rodent models, such as rats and mice, are the most commonly used animal models of athlete's heart (106). Voluntary and mandatory training protocols are also known. In the case of voluntary exercise, wheel running is used: with this setting, the exercise load is limited by the intrinsic willingness of the animal itself. Still, rodents may run 10-15

km/day, and previous studies reported the development of robust cardiac hypertrophy with this approach (107).

Mandatory running protocols use treadmill, which enables to define a more precise workload at the expense of potential stress and injuries of the animals. Different exercise regimes are known: while earlier studies with continuous treadmill velocity demonstrated only modest changes in cardiac morphology and function (108), novel experimental protocols using interval training regimes reported much more pronounced LV and RV remodeling (109).

Swim training in rodents is also commonly used to induce physiological hypertrophy (110). Mouses and rats have the innate ability to swim, and beyond the length and frequency of the training, the workload can also be precisely modified by applying weight or floating devices to the animals. Therefore, a homogeneous training load can be achieved in the study groups (111). As compared to the running protocols, the sedentary control animals should also perform brief swimming sessions as a form of "sham training," to exclude the effect of the water itself. It is important to note that water tank depth, animal density in the tank, and water movement may also affect the results, which limit the comparability of different trials (106).

It is worth to mention that these aforementioned experimental training protocols are predominantly dynamic exercise models. Animal models of resistance exercise are also known in the literature (112); however, they are applied mainly in neurophysiological studies, and data are scarce regarding the cardiovascular adaptation in such experimental settings.

2. OBJECTIVES

As sports cardiology evolves, exercise-induced cardiac changes are gaining more and more clinical significance. Nevertheless, the vast majority of available studies are cross-sectional and focus only on the LV remodeling omitting functional changes and the accompanying alterations of other cardiac chambers. Therefore, data regarding the longitudinal nature of exercise-induced cardiac remodeling and assessment of RV and LA adaptation to intense exercise would be of high importance.

1. Characterization of the dynamic changes in left ventricular morphology and function induced by exercise training and detraining in a rat model of athlete's heart

Although exercise-induced cardiac hypertrophy has been intensively investigated, the dynamics of its development and regression and subsequent functional changes have not been comprehensively described. Therefore, we aimed to characterize the effects of regular exercise training and detraining on LV morphology and function in a rat model of exercise-induced cardiac hypertrophy.

2. Assessment of the exercise-induced shift in right ventricular contraction pattern

Despite the growing attention concerning RV morphology and function in health and disease, data are limited to the functional adaptation of the RV to intense exercise. Our aim was to characterize the RV mechanical pattern in top-level athletes using 3D echocardiography and also to determine the relationship of RV mechanics to CPET-derived VO_2/kg.

3. Unfolding the relationship between left atrial morphology and function and exercise capacity in elite athletes

Data are scarce regarding LA adaptation to regular physical exercise. We aimed to examine LV and also LA morphological and functional remodeling in a large cohort of elite athletes using 3D echocardiography. Beyond the comprehensive assessment of exercise-induced changes in the LA and LV, we also aimed at examining their relationship with CPET-derived exercise capacity.

3. METHODS

3.1 Experimental groups and study design in the rat model of athlete's heart

In our first study, all experimental procedures were reviewed and approved by the Ethical Committee of Hungary for Animal Experimentation (permission no. 22.1/1162/3/2010). This investigation conformed to the Guide for the Care and Use of Laboratory Animals provided by the National Institute of Health (NIH Publication No. 86–23, revised 1996.) and to the EU Directive 2010/63/EU. All animals received humane care.

Young adult, male Wistar rats (n=48, weight=275–325 g) were housed in standard rat cages at constant room temperature (22±2 °C) and humidity with a 12:12-hours light-dark cycle. Rats were fed standard laboratory rodent chow and water ad libitum.

After acclimation, twenty-four rats were randomly divided into control (Co, n=12) and exercised groups (Ex, n=12). These rats completed a 12-week-long training and also an 8-week-long detraining period, and during this period, they underwent regular echocardiographic measurements at weeks 0, 4, 8, 12, 14, 16, 18 and 20. At week 20, these animals underwent LV pressure-volume (PV) analysis.

Additionally, to obtain hemodynamic data at weeks 0 (baseline) and 12 (end of training period), twelve rats were assigned to groups (Co0, n=6, and Ex0, n=6), and pressure-volume analysis was performed at week 0. Further, twelve rats were used to perform invasive hemodynamic measurements (Co12, n=6, and Ex12, n=6) after completion of the training protocol.

Body weight (BW) was measured three times a week during the 20-week-long period. The rats were euthanized after completion of in vivo experiments (PV analysis); the heart was excised, and heart weight (HW) was measured immediately and was indexed to BW values.

3.1.1 Training and detraining protocol

Swim training was performed in a container divided into six lanes filled with tap water (45 cm deep) maintained at 30–32 °C. Rats of exercised groups were exposed to

200 min/day swimming 5 days/week for 12 weeks to induce physiological LV hypertrophy, as described previously (110).

Thereafter, during the detraining period, animals from both groups remained sedentary for 8 weeks. The duration of the detraining period was chosen according to a pilot study and corresponding literature data.

3.1.2 Echocardiography

Rats were anesthetized with pentobarbital sodium (60mg/kg ip.). Animals were placed on controlled heating pads, and the core temperature was maintained at 37°C. After shaving the anterior chest, transthoracic echocardiography was performed in the supine position by one investigator blinded to the experimental groups. Standard two-dimensional long- and short-axis (at the midpapillary level), as well as M-mode images, were acquired using a 13-MHz linear transducer (12L-RS; GE Healthcare, Horten, Norway) connected to a commercially available system (Vivid i; GE Healthcare). Archived recordings were analyzed by a blinded investigator using dedicated software (EchoPac v113; GE Healthcare). On 2D recordings of long-axis and short-axis (at the midpapillary level), LV anterior (AWT) and posterior (PWT) wall thickness in diastole (index: d) and systole (index: s) as well as LV end-diastolic (LVEDD) and end-systolic diameter (LVESD) were measured. End-systole and end-diastole were defined as the time point of minimal and maximal LV dimensions, respectively. All values were averaged over three consecutive cycles. Relative wall thickness (RWT) was calculated as (AWTd+PWTd)/LVEDD. Fractional shortening (FS) was determined from the measurements of LV chamber diameters: $FS = [(LVEDD - LVESD)/LVEDD] \times 100$. LV mass (M) was calculated according to the following formula: $LVM = [(LVEDD + AWTd + PWTd)^3 - LVEDD^3] \times 1.04 \times 0.8 + 0.14$. To calculate LV mass index (LVMi), we normalized LV mass values to the body weight of the animal. The Teichholz formula ($LVEDV=[7.0/(2.4+LVEDD)] \times LVEDD^3$) was utilized to calculate LV volume values. SV, EF, and CO were determined using standard formulas.

3.1.3 Speckle-tracking echocardiography

Strain analysis was carried out in accordance with our internal protocol (113). Briefly, two-dimensional acquisitions of long- and short-axis views of the LV dedicated for

speckle-tracking analysis were recorded at least three times by a constant frame rate of 218 Hz. Speckle-tracking analysis was performed by a blinded operator with expertise in the software environment (EchoPAC v113). To quantify GLS and longitudinal systolic strain rate (LSr), three different long-axis recordings from each animal, and three cardiac cycles from each recording were analyzed. To measure global circumferential strain (GCS) and circumferential systolic strain rate (CSr), the same sequence was performed using short-axis loops. After manual contouring of the endocardial border, the software automatically separated the region of interest into six segments and calculated strain and strain rate values, correspondingly. In the case of low tracking fidelity, the contour was further corrected manually, and the analysis was repeated. Acceptance of a segment to be included in the further analysis was guided by the recommendation of the software. Ideally, for each parameter (3 × 3 × 6), 54 segmental values were available. Based on our protocol, animals with <36 values did not enter into statistical analysis (none).

3.1.4 Hemodynamic measurements – left ventricular pressure-volume analysis

After completion of the training and detraining protocol (at week 20) and in the additional groups (at week 0 and 12), in vivo hemodynamic measurements under ketamine (100mg/kg ip.) and xylazine (3mg/kg ip.) anesthesia were performed as described earlier (110). Shortly, after proper surgical preparation of the animal, a 2-Fr pressure-conductance microcatheter (SPR-838, Millar Instruments, Houston, TX, USA) was inserted into the right carotid artery and advanced into the ascending aorta where aortic pressure curves were recorded to calculate mean arterial blood pressure (MAP). The catheter was thereafter advanced into the LV. After stabilization HR, LV end-systolic pressure (LVESP), LV end-diastolic pressure (LVEDP), the maximal slope of LV systolic pressure increment (dP/dtmax) and diastolic pressure decrement (dP/dtmin), LV end-diastolic volume (LVEDV), LV end-systolic volume (LVESV), SV, EF and stroke work (SW) were calculated and corrected according to in vitro and in vivo volume calibrations. To exclude the influence of body weight differences, CO was normalized to BW [cardiac index (CI)]. The volume calibration of the conductance system was performed, as previously described (110).

In addition to the above parameters, PV loops recorded at different preloads can be used to derive useful indices of LV contractility that are less influenced by loading conditions

and cardiac mass. Therefore, LV PV relations were measured by transiently compressing the inferior vena cava (reducing preload) under the diaphragm with a cotton-tipped applicator. The slope of the LV end-systolic PV relationship (ESPVR; according to the parabolic curvilinear model), preload recruitable stroke work (PRSW), and the slope of the dP/dtmax - end-diastolic volume relationship (dP/dtmax-EDV) were calculated as load-independent indices of LV contractility.

All animals were euthanized by exsanguination. Thereafter the heart was quickly removed, and HW was measured.

3.1.5 Histology

The hearts were removed and were fixed in buffered paraformaldehyde solution (4%) and embedded in paraffin. Transverse, transmural, ~5 μm thick slices of the ventricles were cut and placed on adhesive slides.

Hematoxylin and eosin staining was performed to measure cardiomyocyte diameter as a cellular marker of myocardial hypertrophy. In each sample, 100 longitudinally oriented cardiomyocytes from the LV were examined, and the diameters at transnuclear position were defined. The mean value of 100 measurements represented one sample.

The extent of myocardial fibrosis was assessed on picrosirius-stained sections. ImageJ software (National Institutes of Health, Bethesda, MD) was used to identify the picrosirius-red positive area. Three transmural images (magnification 50×) were randomly taken from the free LV wall on each section. The fibrosis area (picrosirius red positive area-to-total area ratio) was determined on each image, and the mean value of three images represents each animal.

3.1.6 Statistical analysis

Results are expressed as mean ± SEM. The normal distribution of our data was confirmed by Shapiro-Wilk test. StatSoft Statistica 12.0 (StatSoft Inc., Tulsa OK, USA) was used in order to perform the statistical analyses.

To compare differences regarding hemodynamic parameters and heart weight data during the 12 weeks of training, two-way analysis of variance (ANOVA) was performed with time and training as factors on data of independent animals in Co0, Ex0, Co12, and Ex12 groups. p values for time x training interaction (piT) were calculated. During the 8-week-

long detraining period, two-way analysis of variance (ANOVA) was carried out with time and trained state as factors on data of independent animals in Co12, Ex12, Co, and Ex groups. p values for time x trained state interaction (piD) were calculated.

For the statistical analysis of consecutive echocardiographic data of animals in Co and Ex groups, during the 12 weeks of training, mixed ANOVA was performed with time as within-subject factor and training as between-subject factor. p values for time x training interaction (piT) were calculated. During the 8-week-long detraining period, mixed ANOVA was carried out with time as within-subject factor and trained state as a between-subject factor. p values for time x trained state interaction (piD) were calculated.

Post hoc pairwise comparisons with Bonferroni method were performed to determine differences between Co and Ex groups at the given time points.

To assess the reproducibility of STE measurements, four animals from each group were randomly selected. STE analysis was performed again using the aforementioned protocol by the first and second operator blinded to grouping and to previous results. Lin's concordance correlation coefficient was calculated, respectively. A p value <0.05 was the criterion of significance (Table 13).

3.2 Study groups and methods of the right ventricular and the left atrial assessment in athletes

Between March 2017 and May 2018, we have consecutively examined elite athletes enrolled through our Center's complex sports cardiology screening programme (approved by the Medical Research Council ETT-TUKEB No. 13687-0/2011-EKU). The participants gave written informed consent to every procedure of our study. In our second study, sixty (30 female and 30 male) healthy, young top-level water polo athletes, all of them members of the national teams in the corresponding age group were enrolled). In our third study, inclusion criteria were elite athletes defined by being a member of the national team in the corresponding age group and with a mixed-type exercise regimen (waterpolo [n=113], swimming, [n=11], kayaking [n=14]; n=138). All of the

measurements were performed during the in-season competition phase and at least 24 hours after the last athletic training. Detailed medical history and training regime were obtained along with the standard physical examination and 12-lead ECG. Echocardiography, then CPET were performed. Subjects with uncommon echocardiographic and/or ECG features, suboptimal echocardiographic image quality, or athletes who suspended regular training in the last 6 months were excluded. In our second study 40, while in our third study 50 healthy, sedentary volunteers from our existing database (no previous participation in intensive training, <3 hours of exercise/week) with no relevant medical history, no signs or symptoms of cardiovascular disease and normal ECG and echocardiogram served as the control group with similar age and gender distribution.

3.2.1 Echocardiography

Echocardiographic examinations were performed on commercially available ultrasound systems (Philips EPIQ 7G, X5-1 transducer, Best, The Netherlands; or GE Vivid E95, 4V-D transducer, GE Vingmed Ultrasound, Horten, Norway). Standard acquisition protocol consisting of loops from parasternal, apical, and subxyphoid views was used according to current guidelines (13). LV wall thicknesses and diameters were evaluated in parasternal long-axis (PLAX) view at the level of mitral valve coaptation. LA anteroposterior diameter was measured in PLAX view perpendicular to the aortic root at the level of sinuses. LA and RA areas were calculated by contouring atrial endocardial borders in apical 4 chamber view, and LA and RA volumes were estimated by the Simpson method indexed to BSA. RV basal short-axis diameter, RV length, tricuspid annular plane systolic excursion (TAPSE), fractional area change (FAC) were measured from apical four-chamber view. LV inflow by pulsed-wave Doppler at the level of the mitral valve coaptation was obtained to measure E and late A wave peak velocities, their ratio, and E-wave deceleration time. Pulsed wave Tissue Doppler Imaging was used to measure systolic (s’), early (e’), and late diastolic (a’) velocities at the mitral lateral and medial annulus and also on the tricuspid annulus. The ratio of E-wave velocity to averaged e’ velocities of the mitral medial and lateral annulus was calculated as an estimate of LV filling pressures.

DOI:10.14753/SE.2021.2460

Beyond routine echocardiographic protocol, ECG gated full-volume 3D datasets reconstructed from 4 or 6 cardiac cycles optimized for the LV, LA, and RV were obtained from apical view with a minimum volume rate of 25 volumes/sec for off-line analysis. Image quality was verified bedside to avoid "stitching" and "drop-out" artifacts of the 3D data. Further measurements were performed on a separate workstation using dedicated softwares (4D LALV Function and 4D RV Function 2, TomTec Imaging GmbH, Unterschleissheim, Germany). Concerning the LV and the LA, the software detects endocardial surfaces of the chambers, and following manual correction, it traces its motion throughout the cardiac cycle (Figure 6). In the case of the LV, we determined EDVi, ESVi, SVi, and LVMi indexed to BSA, and to characterize global LV function EF and deformation parameters such as GLS and GCS were also assessed. We have also determined RVEDVi and RVESVi to quantify RV 3D morphology, and for the assessment of RV function, we have measured RVSVi, RVEF, and RV free wall longitudinal strain (RVFWLS). Parameters were normalized to body surface area (BSA) calculated by the Mosteller formula (114).

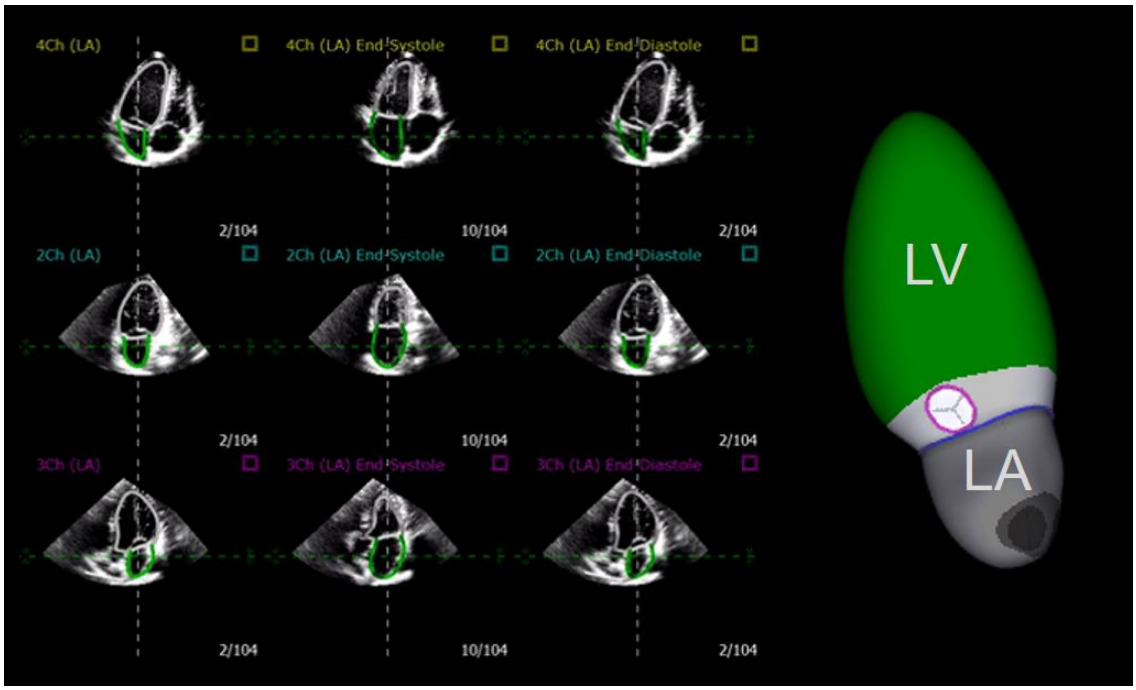

Figure 6: Three-dimensional echocardiographic analysis of the left atrium (LA) and the left ventricle (LV). Following the correction of the LV and LA long axis, the algorithm detects the endocardial borders and traces their motion throughout the cardiac cycle in multiple planes, also allowing manual editing if needed. Therefore, 3D models of the LA

and LV are generated, and changes in chamber volumes and global longitudinal strain can be calculated. 4ch = four-chamber view; 3ch = three-chamber view; 2ch = two-chamber view

To examine LA 3D morphology and function, the timing of the late diastolic atrial contraction was confirmed by mitral annular motion to measure LA maximal volume (LAVi), minimal volume (Vmin), and pre A-wave volume (preAV) indexed to BSA. Total emptying volume was defined as LAVi-Vmin. Using these volumetric data, we calculated LA total emptying fraction (EF) as 100*(LAVi-Vmin)/LAVi, LA passive EF as 100*(LAVi-VpreA)/LAVi, and LA active EF as 100*(VpreA-Vmin)/VpreA, as parameters of the LA reservoir, conduit and contractile function, respectively (Figure 1). We have also quantified true conduit volume as LVSVi-(LAVi-Vmin). The software also automatically calculates 3D LAGLS.

3.2.2 Detailed assessment of right ventricular deformation

For the detailed assessment of RV mechanics, the 3D model of the RV was exported frame-by-frame throughout the cardiac cycle for further analysis using our custom made software (Right VentrIcular Separate wall motIon quantificatiON – ReVISION). Briefly, the wall motions of the 3D RV model are decomposed in a vertex-based manner. The volumes of the models accounting for only one motion direction were calculated at each time frame using the signed tetrahedron method. By the decomposition of the model's motion along the three orthogonal, anatomically relevant axes, volume loss attributable to either longitudinal, radial, or anteroposterior wall motions could be separately quantified (115). Thus, longitudinal (LEF), radial (REF), and anteroposterior (AEF) ejection fraction and their ratio to global RV EF (LEF/RVEF, REF/RVEF, AEF/RVEF, respectively) could be expressed as a measure of the relative contribution of the given wall motion direction to a global function. To assess longitudinal and circumferential myocardial deformation, we computed 3D GLS and GCS as well. On the end-diastolic frame, a plane was rotated around the longitudinal axis of the 3D RV model 20 times by 18 degrees (Figure 7). At each position, the length of each longitude defined by the intersections of the endocardial contour and the plane was calculated. Each longitude was composed of an infinite number of vertices, which coordinates could be interpolated

based on their barycentric coordinates in each frame throughout the cardiac cycle. Only accounting for the motion along the longitudinal axis, the changes in the length of each longitude can be measured, and GLS can be computed (Figure 7). To calculate GCS, the 3D model was sliced with 20 horizontal planes (Figure 7). Similarly to GLS, the vertices of the horizontal contours were interpolated using barycentric coordinates on each frame. By averaging the length changes of each contour referenced to their end-diastolic length, GCS could be evaluated (Figure 7). In order to examine the regional differences in RV LS and CS, the free wall and the septal surface of the 3D model was separated, and the free wall was divided into three regions (basal, mid and apical parts) by trisection along the vertical axis. The tricuspid and pulmonary annulus were omitted from all analyses.

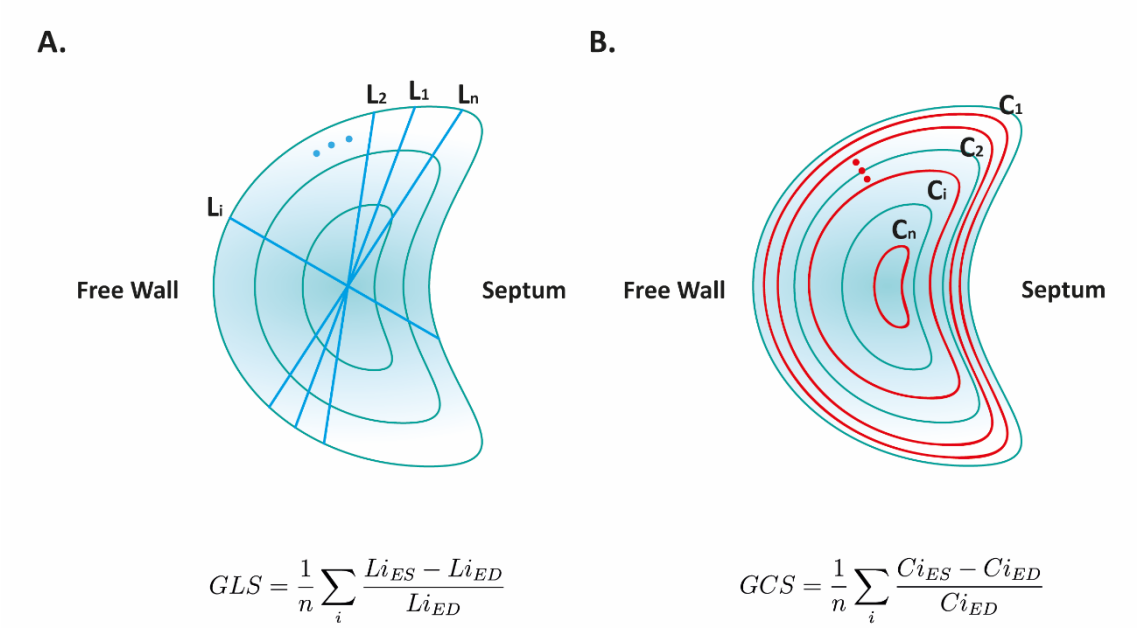

Figure 7: Determination of right ventricular global longitudinal strain (GLS; A) and global circumferential strain (GCS; B). ED, end-diastolic; ES, end-systolic.

3.2.3 Cardiopulmonary exercise testing

CPET for peak oxygen uptake quantification was performed on a treadmill using an incremental protocol commencing at a 2 minutes 6 km/h flat race followed by 8 km/h uphill running with an increasing slope of 1.5% every minute until exhaustion. The volume and composition of the expired gases were analyzed breath-by-breath using an

automated cardiopulmonary exercise system (Respiratory Ergostik, Geratherm, Bad Kissingen, Germany). Subjects were encouraged to achieve maximal effort, which was confirmed by respiratory exchange ratio and also by reaching the predicted maximal HR and a plateau in oxygen uptake.

3.2.4 Statistical analysis

Statistical analysis was performed using dedicated software (Statsoft Statistica v12, Tulsa, OK, USA). Data are presented as mean ± SD. Shapiro-Wilk test was used to test normal distribution. In the RV study, two-way ANOVA with two factors (gender and sport activity) and their interactions (gender*sport) was used to compare groups, and in the case of significant interaction, Tukey's post-hoc analysis was performed to compare the four study groups. In the LA study, the gender-based matching of the two study groups was confirmed by Chi-square test, and unpaired Student's t-test was used to compare groups. Pearson or Spearman test was applied for correlation analysis as appropriate. Multiple linear regression analysis was applied to find independent predictors that determine VO_2/kg. To avoid multicollinearity issues, tolerance was set as > 0.5. p values <0.05 were considered significant. The intra- and interobserver variability were evaluated using Lin's concordance correlation. To assess the intraobserver reproducibility of the presented key parameters, the operator of the off-line measurements (blinded to previous results) repeated the 3D analysis: in both studies, a randomly chosen subset of 10 athletes and 5 controls were used (Table 13). The interobserver variability was determined by 3D analysis of the same subjects by a second experienced operator in a blinded fashion (Table 13).

DOI:10.14753/SE.2021.2460

4. RESULTS

4.1 Characterization of the dynamic changes in left ventricular morphology and function induced by exercise training and detraining in a rat model of athlete's heart

4.1.1 Heart weight data

HW/BW ratio did not differ between our baseline groups (3.42 ±0.06 g/kg Ex0 vs. 3.39 ± 0.03 g/kg Co0). A marked increase in the HW/BW ratio confirmed cardiac hypertrophy in trained animals (piT= 0.0051; Ex12 vs. Co12: 3.67 ± 0.14 g/kg vs. 2.96 ± 0.16 g/kg), which regressed to control values after the detraining period (piD=0.0012; Ex vs. Co: 2.72 ± 0.04 g/kg vs. 2.73 ± 0.10 g/kg).

4.1.2 Data from LV pressure-volume analysis

HR and pressure values did not differ between control and exercised animals, either after completing the training plan (at week 12) or after the detraining period (at week 20) (Table 1). The volume values corresponded to the echocardiographic data: as a result of 12-week-long swim training, unaltered LVEDV was associated with decreased LVESV, resulting in increased SV, EF, CI, and SW compared to control animals. Load-independent indices of myocardial contractility (PRSW; ESPVRq and dP/dtmax-EDV) were increased as a result of long-term exercise training (Table 1, Figure 8). Both conventional and load-independent parameters of systolic function and contractility did not show any difference in week 20, confirming the complete morphological and functional reversibility of exercise-induced alterations (Figure 8).

DOI:10.14753/SE.2021.2460

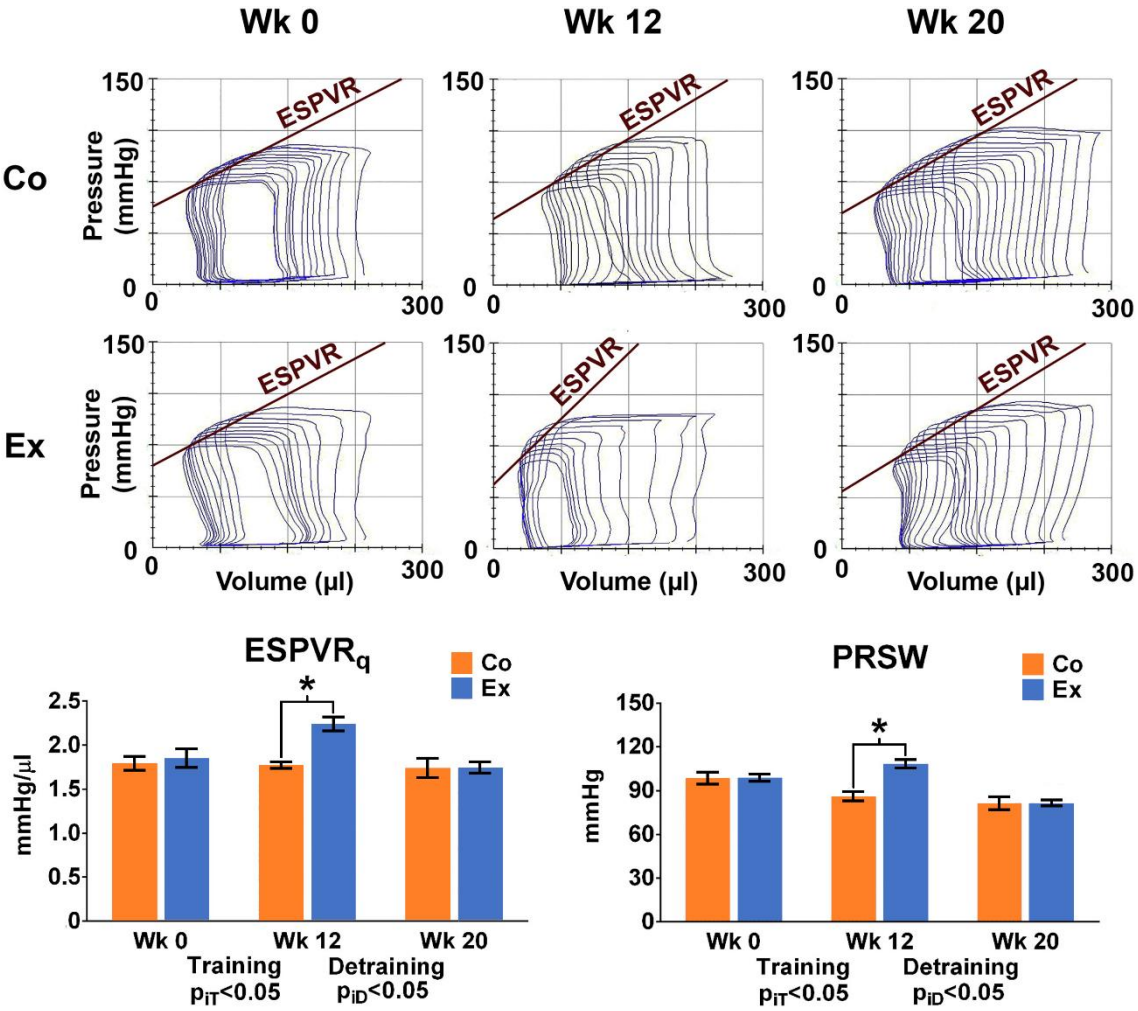

*Figure 8: Load-independent contractility parameters measured by left ventricular pressure-volume analysis. Upper panel: representative original recordings of one control (Co) and exercised (Ex) rat during transient occlusion of the inferior vena cava at weeks (Wk) 0, 12, and 20. The slope of the end-systolic pressure-volume relationship (ESPVR) reflects alterations of cardiac contractility. Lower panel: alterations of sensitive contractility parameters [ESPVR and preload recruitable stroke work (PRSW)] during training and detraining. *p < 0.05 vs. Co. piT and piD: interaction value of two-way analysis of variance (ANOVA) during training and detraining, respectively. Co0 n=6; Ex0 n=6; Co12 n=6; Ex12 n=6; Co20 n=12; Ex20 n=12.*

DOI:10.14753/SE.2021.2460

Table 1: Haemodynamic data of the study groups.

	Week 0		Week 12		piT	Week 20		piD
	Co0 (n=6)	**Exo (n=6)**	**Co12 (n=6)**	**Ex12 (n=6)**		**Co (n=12)**	**Ex (n=12)**	
HR (1/min)	272±11	273±5	224±6	243±14	0.38	244.±8	239±10	0.23
MAP (mmHg)	77.4±1.4	77.0±1.8	81.6±3.8	85.3±2.8	0.44	85.9±3.9	80.9±2.3	0.61
LVESP (mmHg)	85±.4.1	85.5±1.1	100.4±2.8	96.3±2.6	0.44	101.1±4.2	100.5±3.4	0.67
LVEDP (mmHg)	5.0±0.2	4.5±0.3	4.9±0.4	5.6±0.5	0.12	4.3±0.2	4.2±0.2	0.20
dP/dt_{max}(mmHg/s)	6453±429	5880±309	7305±345	7585±227	0.21	6979±284	6775±304	0.45
dP/dt_{min}(mmHg/s)	-6570±441	-6167±228	-7509±583	-7552±298	0.61	-7539±365	-7176±239	0.61
LVEDV (µL)	212.8±8.3	224.4±7.9	261.6±7.6	258.3±8.3	0.36	276.4±8.5	269.0±7.4	0.82
LVESV (µL)	65.8±5.0	69.1±6.1	110.4±8.2	85.3±3.4*	**0.02**	123.4±4.3	118.2±3.7	0.054
SV (µL)	147.0±4.0	155.3±3.0	151.3±6.3	173.0±7.3*	**0.02**	153.0±5.2	150.8±5.8	**0.049**
EF (%)	69.3±1.3	69.5±1.8	58.8±2.4	66.9±1.1*	**0.02**	55.4±0.7	56.0±1.1	**<0.01**
CI (mL/min)/100 g	127.4±4.7	136.2±4.9	72.9±3.3	98.2±9.7*	0.19	64.7±2.7	67.4±3.6	**0.02**
SW (mmHg*mL)	11798±536	11735±253	12612±844	15012±649*	0.06	12615±594	12226±360	**0.03**
ESPVR	1.78±0.09	1.84±0.12	1.76±0.05	2.23±0.10*	**0.04**	1.73±0.13	1.74±0.08	**0.03**
PRSW	97.9±4.9	98.3±2.8	85.2±4.1	107.4±3.9*	**0.01**	80.7±5.2	80.8±3.1	**0.01**
dP/dt_{max}-EDV	35.4±1.0	33.6±1.1	35.2±1.5	44.4±1.1*	**<0.001**	34.6±1.6	34.5±1.7	**0.01**

*Abbreviations: HR = heart rate; MAP = mean arterial pressure; LVESP =left ventricular (LV) end-systolic pressure; LVEDP = LV end-diastolic pressure; dP/dtmax and dP/dtmin = maximal slope of the systolic pressure increment and the diastolic pressure decrement,respectively; LVEDV = LV end-diastolic volume; LVESV = LV end-systolic volume; SV = stroke volume; EF = ejection fraction; CI = cardiac index; BW = bodyweight; SW = stroke work; ESPVR = slope of end-systolic pressure-volume relationship; PRSW = preload recruitable stroke work; dP/dtmax-EDV = slope of dP/dtmax–end-diastolic volume relationship. *p<0.05 vs. Co at week 12. p_{iT} and p_{iD}: interaction value of two-way analysis of variance (ANOVA) during training and detraining, respectively*

4.1.3 Echocardiography

Our results during the training period indicate that LV wall thickness values and calculated LV mass index were significantly increased after one month of swim training (Figure 9, Table 2). While end-diastolic dimensions (LVEDD, LVEDV) remained unaltered compared to control animals, end-systolic dimensions (LVESD, LVESV) significantly decreased in swimming animals, resulting in increased SV and CO as well as improved FS and EF (Table 2). RWT clearly increased in the training period, suggesting the appearance of a concentric hypertrophy in our trained rats (Figure 9). HR did not differ between groups at any time points (Table 2). Cessation of swim training resulted in a rapid, complete regression of wall thickness, LV mass index, and RWT values (Table 2): just two weeks after discontinuation of swim training (at week 14), there was no difference between control and exercised groups. This morphological regression was followed by reversion of alterations in cavital dimensions and systolic parameters (FS and EF), which did not differ after 4 weeks of detraining. The values between these two groups did not differ in the remaining six weeks of our protocol, suggesting complete rapid regression of exercise-induced hypertrophy.

DOI:10.14753/SE.2021.2460

Table 2: Echocardiographic assessment of the study groups (Control [Co]: n=12; Exercised [Ex]: n=12)

	Week 0		Week 4		Week 8		Week 12		p_{iT}	Week 14		Week 16		Week 18		Week 20		p_{iD}
	Co	Ex	Co	Ex	Co	Ex	Co	Ex		Co	Ex	Co	Ex	Co	Ex	Co	Ex	
HR (beats/min)	406±13	428±10	350±7	353±7	342±8	335±9	319±7	330±8	0.1623	353±11	365±13	357±10	374±11	350±9	369±12	365±8	376±9	0.8928
LVAWd (mm)	1.75±0.04	1.81±0.02	1.89±0.05	2.10±0.04[1]	1.97±0.03	2.26±0.03[2]	2.06±0.04	2.36±0.04[3]	<0.0001	2.08±0.03	2.13±0.02	2.12±0.03	2.14±0.02	2.14±0.04	2.12±0.01	2.18±0.05	2.15±0.01	<0.0001
LVAWs (mm)	2.84±0.06	2.84±0.05	2.96±0.05	3.2±0.05[1]	2.99±0.07	3.40±0.03[2]	3.21±0.08	3.48±0.05[3]	<0.0001	3.12±0.08	3.09±0.03	3.16±0.07	3.07±0.03	3.21±0.07	3.12±0.03	3.23±0.06	3.16±0.02	<0.0001
LVPWd (mm)	1.59±0.03	1.58±0.02	1.68±0.03	1.84±0.04[1]	1.73±0.03	1.93±0.03[2]	1.84±0.02	1.98±0.03[3]	<0.0001	1.88±0.03	1.90±0.03	1.88±0.02	1.85±0.02	1.89±0.03	1.86±0.02	1.91±0.04	1.90±0.02	0.0001
LVPWs (mm)	2.56±0.03	2.64±0.05	2.73±0.0	3.04±0.04[1]	2.74±0.05	3.28±0.06[2]	2.82±0.05	3.20±0.05[3]	<0.0001	2.89±0.06	2.97±0.06	2.83±0.06	2.86±0.06	2.87±0.07	2.86±0.05	2.85±0.07	2.89±0.05	<0.0001
LVEDD (mm)	6.46±0.08	6.32±0.07	6.83±0.06	6.66±0.11	6.91±0.07	6.66±0.05	6.93±0.07	6.85±0.06	0.3941	6.93±0.10	6.91±0.07	7.04±0.05	7.00±0.05	7.15±0.05	7.12±0.04	7.17±0.07	7.14±0.08	0.9080
LVESD (mm)	3.56±0.05	3.47±0.08	3.87±0.10	3.46±0.12[1]	4.20±0.05	3.27±0.09[2]	4.28±0.06	3.53±0.11[3]	<0.0001	4.29±0.09	3.88±0.10[4]	4.34±0.05	4.19±0.09	4.37±0.08	4.27±0.09	4.45±0.08	4.36±0.09	<0.0001
RWT	0.52±0.01	0.54±0.01	0.52±0.01	0.59±0.01[1]	0.54±0.01	0.63±0.01[2]	0.56±0.01	0.63±0.01[3]	<0.0001	0.57±0.01	0.58±0.01	0.57±0.01	0.57±0.01	0.56±0.01	0.56±0.01	0.57±0.01	0.57±0.01	<0.0001
LVM (g)	0.70±0.02	0.69±0.01	0.81±0.02	0.89±0.03[1]	0.86±0.02	0.96±0.02[2]	0.92±0.02	1.04±0.04[3]	<0.0001	0.94±0.03	0.96±0.02	0.97±0.01	0.96±0.01	1.00±0.03	0.98±0.04	1.02±0.02	1.00±0.01	<0.0001
LVMi (g/kg)	2.32±0.07	2.28±0.06	2.10±0.05	2.53±0.09[1]	2.00±0.04	2.60±0.05[2]	2.01±0.03	2.66±0.07[3]	<0.0001	1.95±0.06	2.16±0.06[4]	1.95±0.05	2.05±0.05	1.97±0.03	2.06±0.04	1.96±0.04	2.01±0.04	<0.0001
FS (%)	44.8±0.8	45.1±0.9	43.3±1.2	48.1±1.0[1]	39.2±0.6	51.0±1.0[2]	38.3±0.5	48.4±1.3[3]	<0.0001	38.1±1.1	43.9±1.2[4]	38.3±0.7	40.1±1.0	38.8±0.9	40.1±1.1	37.9±1.0	38.8±1.2	<0.0001
LVEDV (µl)	213.5±6.0	203.3±5.3	241.5±5.0	229.2±8.5	248.7±5.6	228.7±4.2	249.9±5.6	243.2±5.2	0.3757	250.5±8.1	248.3±5.6	259.1±4.4	255.7±4.4	267.7±4.2	265.9±3.8	270.0±5.7	267.2±6.4	0.9156
LVESV (µl)	53.2±2.0	50.4±3.0	65.6±4.2	50.6±4.2[1]	79.0±2.5	43.8±2.9[2]	82.2±2.7	52.9±3.9[3]	<0.0001	83.3±4.5	65.7±3.9[4]	85.3±2.4	78.8±4.0	86.9±3.9	82.1±4.2	90.7±3.9	86.6±4.4	<0.0001
SV (µl)	160.3±5.2	152.9±3.8	175.9±4.3	178.6±4.8	169.8±4.1	184.9±2.2[2]	167.6±3.8	190.3±4.2[3]	0.0002	167.2±6.5	182.5±4.7	173.8±4.1	177.0±3.9	180.8±3.5	183.8±4.2	179.3±5.0	180.6±6.2	0.0087
EF (%)	75.0±0.8	75.3±1.1	72.9±1.5	78.3±1.1[1]	68.2±0.7	81.0±1.0[2]	67.1±0.7	78.4±1.4[3]	<0.0001	66.7±1.4	73.6±1.4	67.0±0.9	69.3±1.3	67.6±1.2	69.2±1.4	66.4±1.2	67.5±1.5	<0.0001
CO (ml/min)	64.6±2.1	65.5±2.5	61.6±1.8	63.0±2.2	58.0±1.9	61.9±1.6	53.4±1.6	63.0±2.2[3]	0.0253	58.6±2.6	66.5±2.9	61.8±1.9	66.1±2.3	63.3±1.9	67.6±2.0	65.3±1.9	67.8±2.7	0.2031
GLS (%)	-17.1±0.8	-16.5±0.5	-14.9±0.3	-13.9±0.6	-14.2±0.7	-16.8±0.7[2]	-15.5±0.6	-17.1±0.4	0.0006	-15.0±1.0	-15.4±0.7	-15.3±0.7	-16.0±0.9	-15.2±0.6	-15.2±0.5	-13.6±0.6	-13.8±0.4	0.0457
LSr (Hz)	-4.35±0.16	-4.29±0.12	-3.73±0.09	-3.79±0.15	-3.51±0.13	-4.29±0.21[2]	-3.72±0.18	-4.51±0.12[3]	0.0032	-3.63±0.20	-3.94±0.21	-3.47±0.16	-3.74±0.19	-3.69±0.14	-3.71±0.13	-3.33±0.13	-3.49±0.11	0.0244
GCS (%)	-13.9±0.3	-12.7±0.6	-12.5±0.2	-12.3±0.6	-13.0±0.7	-18.1±1.5[2]	-14.2±0.4	-19.1±1.0[3]	<0.0001	-13.6±0.8	-13.6±0.4	-11.9±0.4	-12.6±0.3	-13.5±0.9	-13.4±0.5	-12.9±0.7	-13.3±0.6	<0.0001
CSr (Hz)	-3.79±0.12	-3.49±0.19	-3.21±0.05	-3.19±0.18	-3.34±0.19	-4.83±0.42[2]	-3.46±0.11	-5.14±0.23[3]	<0.0001	-3.47±0.25	-3.56±0.11	-3.03±0.08	-3.38±0.08	-3.34±0.21	-3.48±0.12	-3.17±0.18	-3.44±0.15	<0.0001

Abbreviations: Co = control group, Ex = exercise group, HR = heart rate, LVAWd = left ventricular anterior wall end-diastolic thickness, LVAWs = left ventricular anterior end-systolic thickness, LVPWd = left ventricular posterior wall end-diastolic thickness, LVPWs = left ventricular posterior wall end-systolic thickness, LVEDD = left ventricular end-diastolic diameter, LVESD = left ventricular end-systolic diameter, RWT = relative wall thickness, LVM = left ventricular mass, LVMi = left ventricular mass index, FS = fractional shortening, LVEDV = left ventricular end-diastolic volume, LVESV = left ventricular end-systolic volume, SV = stroke volume, EF = ejection fraction, CO = cardiac output, GLS = global longitudinal strain, LSr = longitudinal strain rate, GCS = global circumferential strain, CSr = circumferential strain rate, p_{iT} and p_{iD}: interaction value of two-way analysis of variance (ANOVA) during training and detraining, respectively, [1]:p<0.05 vs. Co at week (Wk) 4; [2]:p<0.05 vs. Co at Wk 8; [3]:p<0.05 vs. Co at Wk 12; [4]:p<0.05 vs. Co at Wk 14.

DOI:10.14753/SE.2021.2460

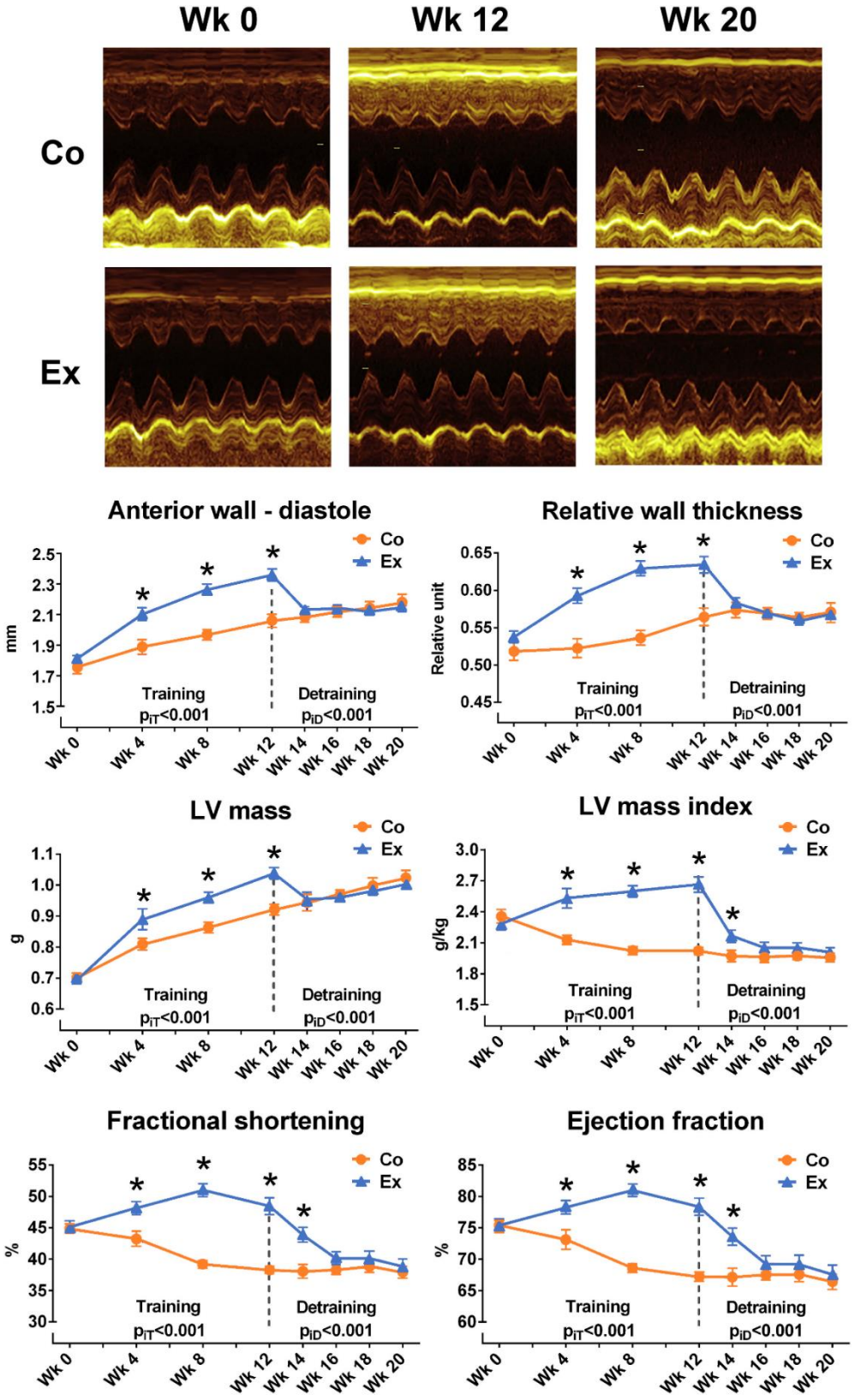

Figure 9: Consecutive standard echocardiographic measurements. Upper panel: representative left ventricular (LV) M-mode images from one control (Co) and exercised (Ex) rat at weeks (Wk) 0, 12, and 20. Note the increased wall thickness and decreased

*end-systolic dimensions in Ex rats compared to Co rats after completion of the training programme (Wk 12) and the reversibility of the observed structural alterations (Wk 20). Lower panel: Echocardiographic data of consecutive LV measurements: end-diastolic anterior wall thickness, relative wall thickness, and LV mass values showed rapid development and regression of exercise-induced morphological alterations, which were followed by changes in fractional shortening and ejection fraction. Data: the mean ± SEM. *p < 0.05 Co vs. Ex. piT and piD: interaction value of mixed analysis of variance (ANOVA) during training and detraining, respectively. Co0 n=6; Ex0 n=6; Co12 n=6; Ex12 n=6; Co20 n=12; Ex20 n=12.*

4.1.4 Speckle-tracking echocardiography

After the initiation of the training period, a slight, non-significant decrease could be observed regarding longitudinal and circumferential strain and strain rate parameters in both control and exercise groups (Figure 10). This finding could be a consequence of body mass gain, while the continuous increase in EDV refers to this phenomenon. At week 8, and even more prominently at week 12, in the trained group, both longitudinal and circumferential strain and strain rate parameters showed a significant increase in systolic function compared to control animals. Consistently with morphological data, an immediate drop in STE-derived parameters could be observed in the trained group after cessation of training. There was no difference between the two groups from week 14 to week 20. The assessment of intra- and interobserver variability demonstrated good reproducibility of GLS and GCS (Table 15).

DOI:10.14753/SE.2021.2460

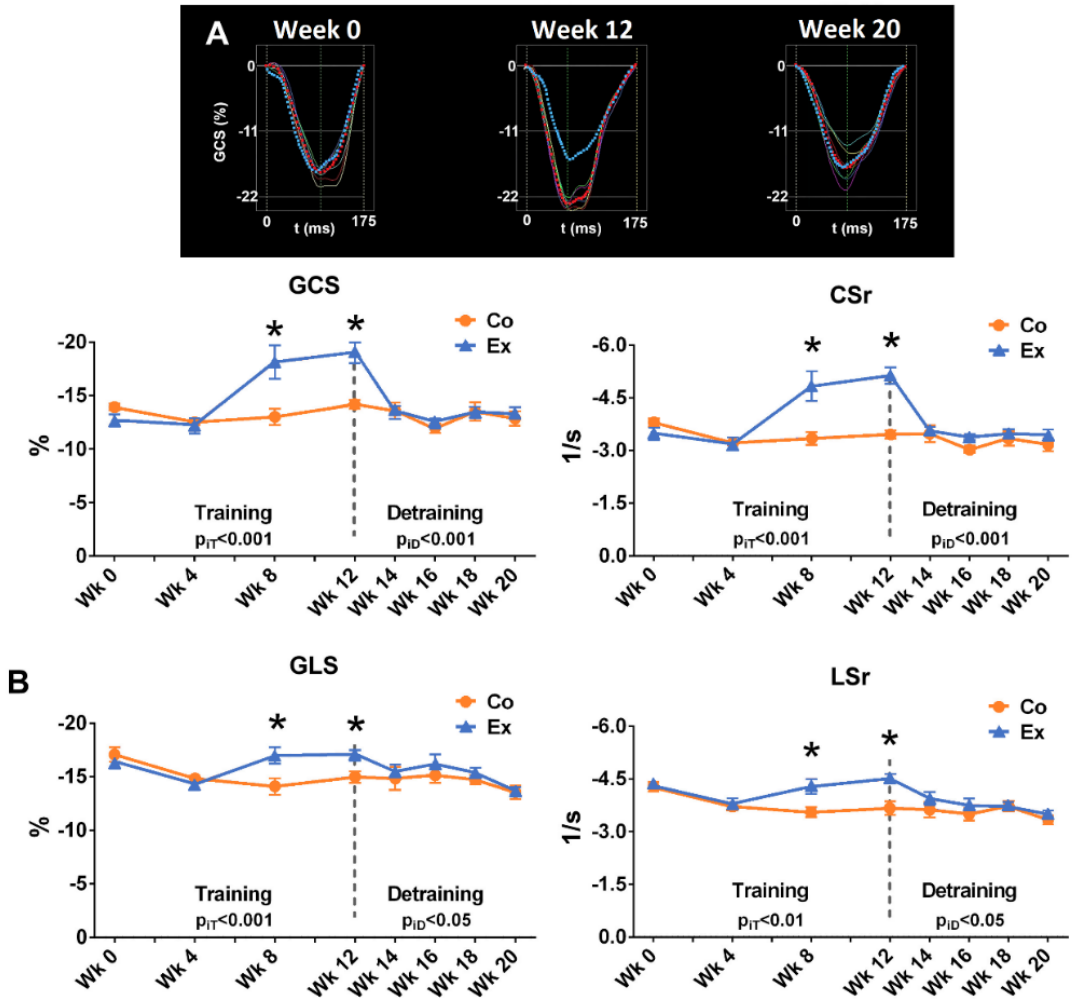

*Figure 10: Layout and results of the speckle-tracking analysis. A: Representative speckle-tracking analysis images to determine global circumferential strain (GCS) and circumferential strain rate (CSr) on left ventricular mid-papillary short-axis original recordings of an exercised (Ex) rat at weeks (Wk) 0, 12 and 20. Each continuous curve represents a given segment of the echocardiographic image. Average values of the 6 segments are delineated with the red dotted line and compared to an original recording from a control (Co) rat (blue dotted line). Results of consecutively measured GCS and CSr during training and detraining periods are depicted below. B: Results of consecutively measured global longitudinal strain (GLS) and longitudinal strain rate (LSr) during training and detraining periods *p < 0.05 Co vs. Ex. piT and piD: interaction value of mixed analysis of variance (ANOVA) during training and detraining, respectively. Co0 n=6; Ex0 n=6; Co12 n=6; Ex12 n=6; Co20 n=12; Ex20 n=12.*

DOI:10.14753/SE.2021.2460

4.1.5 Histology

Increased cardiomyocyte width values were observed in exercised rats compared to control ones after completion of the training program (Figure 11/A). This exercise-induced alteration showed complete regression after the 8-week long resting period. Picrosirius staining revealed no collagen deposition in the myocardium of exercise-trained rats, that confirms the physiological nature of the observed hypertrophy (Figure 11/B).

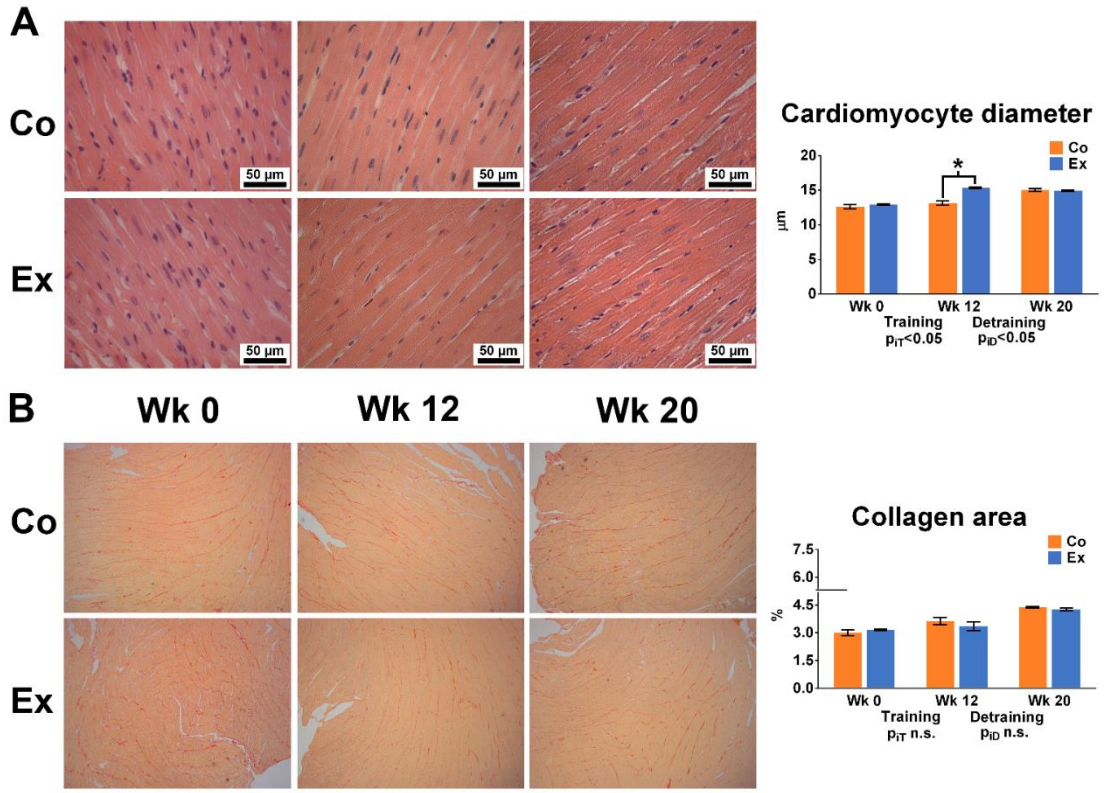

*Figure 11: A: Representative hematoxylin-eosin stained sections (magnification 400x) from control (Co) and exercised (Ex) groups at different stages, that were used to measure transnuclear cardiomyocyte width. Mean LV cardiomyocyte diameter was increased after swim training, which confirmed myocardial hypertrophy at cellular level. Our histological data also confirmed the regression of exercise-induced alteration. B: Representative picrosirius-stained sections (magnification 50x) from each group. Red color shows collagen fibers in the myocardium. The analysis of picrosirius-staining showed unaltered collagen density between exercised and control rats during training and detraining program. Values are means ± SEM. *p<0.05 vs. Co. piT and piD:*

interaction value of two-way analysis of variance (ANOVA) during training and detraining, respectively. Co0 n=6; Ex0 n=6; Co12 n=6; Ex12 n=6; Co20 n=12; Ex20 n=12.

4.2 Assessment of the exercise-induced shift in right ventricular contraction pattern

4.2.1 Basic demographic and anthropometric data

The mean age of the athletes was 19 years. They were participating in competitive sport for 10±5 years with a training time of 17±6 hours per week. Both control groups were age-matched. Athletes demonstrated higher height, weight, and BSA compared to the control groups, and also males had higher values compared to females. Athletes had higher systolic but similar diastolic blood pressure compared to the control groups. Males had lower HR compared to females, while athletes also demonstrated lower HR values. Peak oxygen uptake was higher in male athletes compared to female athletes (Table 3).

Table 3: Baseline characteristics of athlete and control groups

	MA (n=30)	**FA (n=30)**	**MC (n=20)**	**FC (n=20)**	**p for gender**	**p for sport**	**p for interaction**
Age (years)	18.9±4.0	19.0±3.7	19.9±3.8	19.5±2.3	0.81	0.27	0.71
Height (cm)	191.3±6.4	174.5±5.8	180.0±8.3	165.7±4.9	**<0.001**	**<0.001**	0.40
Weight (kg)	90.0±10.6	67.8±6.6	74.8±13.8	56.5±5.9	**<0.001**	**<0.001**	0.36
BMI (kg/m²)	25.5±2.0	22.3±2.2	23.1±3.9	20.6±2.0	**<0.001**	**<0.01**	0.86
BSA (m²)	2.2±0.2	1.8±0.1	1.9±0.2	1.6±0.1	**<0.001**	**<0.001**	0.37
SBP (mmHg)	138.2±19.7	134.1±13.2	118.4±17.8	114.4±13.1	0.33	**<0.001**	0.98
DBP (mmHg)	70.2±11.0	71.6±9.9	71.3±8.2	73.9±12.0	0.45	0.53	0.81
HR (1/min)	67.2±11.5	71.1±12.1	68.4±9.1	84.2±19.2	**<0.01**	**<0.05**	0.10
VO_2/kg (mL/kg/min)	51.9±6.7	47.6±4.2			**<0.05**		

Abbreviations: MA = male athlete; FA = female athlete; MC = male control; FC = female control; BMI = body mass index; BSA = body surface area; SBP = systolic blood pressure; DBP = diastolic blood pressure, HR = heart rate, VO_2/kg = peak oxygen uptake

4.2.2 Conventional 2D and Doppler echocardiographic data

Linear LV wall thickness and internal diameter measurements showed higher values in athletes with a trivial gender difference as well. The ratio of mitral inflow velocities, deceleration time, and E/e' did not differ between groups. Mitral annular systolic velocities were also similar. Left and right atrial volume indices were higher in athletes, while the LA volume index was similar between genders. RV linear measurements showed enlargement of the chamber in athletes compared to controls. Athletes had higher TAPSE values than controls; on the other hand, FAC was significantly lower in athletes. Tricuspid annular velocities did not differ between groups. RV myocardial performance index values were higher in the athlete groups. RVFWLS was higher in females (Table 4).

Table 4: Conventional echocardiographic parameters of athlete and control groups

	MA (n=30)	FA (n=30)	MC (n=20)	FC (n=20)	p for gender	p for sport	p for interaction
LVIDd (mm)	54.0±3.5	48.3±3.9	47.8±4.5	43.4±3.5	**<0.001**	**<0.001**	0.47
IVSd (mm)	11.6±1.3	9.3±1.1	9.3±1.4	7.6±0.8	**<0.001**	**<0.001**	0.24
PWd (mm)	10.3±1.0	8.6±1.9	8.2±0.6	7.3±1.0	**<0.001**	**<0.001**	0.10
RWT (%)	0.41±0.05	0.37±0.05	0.36±0.08	0.34±0.05	0.08	**<0.01**	0.34
E/A	1.6±0.5	1.81±0.5	1.6±0.4	1.7±0.5	0.14	0.59	0.80
DT (ms)	182.3±59.5	172.9±41.0	155.0±20.9	171.2±29.6	0.62	0.18	0.24
E/e' average	5.7±0.9	5.5±0.9	5.7±1.0	5.3±0.8	0.08	0.99	0.58
Mitral lateral annulus s' (cm/s)	10.1±1.2	11.1±1.6	11.6±1.0	11.1±2.6	0.85	0.35	0.33
Mitral medial annulus s' (cm/s)	8.9±1.1	9.1±1.0	8.6±1.1	8.6±1.1	0.78	0.07	0.65
LAVi (ml/m^2)	29.0±7.9	30.4±9.8	19.1±7.7	16.5±5.0	0.74	**<0.001**	0.31
RAVi (ml/m^2)	31.2±6.6	25.8±7.6	21.1±9.0	15.2±5.2	**<0.01**	**<0.001**	0.88
RV basal diameter (mm)	36.3±4.6	31.4±3.8	32.7±2.3	27.6±2.5	**<0.001**	**<0.001**	0.93
RV length (mm)	104.6±6.7	94.7±8.2	90.8±4.9	87.4±8.7	**<0.001**	**<0.001**	**<0.05**
TAPSE (mm)	24.7±3.7	25.6±2.7	23.9±3.5	23.0±4.1	0.95	0.03	0.26
FAC (%)	44.7±4.9	47.0±6.3	50.4±6.1	54.6±5.8	**<0.01**	**<0.001**	0.41
Tricuspid annulus s' (cm/s)	12.1±1.7	12.7±2.1	12.7±2.2	12.9±2.3	0.18	0.20	0.68
Tricuspid annulus e' (cm/s)	14.1±2.5	14.2±2.8	14.2±3.1	16.3±3.1	0.08	0.08	0.11
RIMP	0.42±0.08	0.39±0.08	0.36±0.08	0.33±0.06	0.13	**<0.001**	0.85
RV septal LS (%)	-24.3±4.4	-25.5±4.5	-24.0±4.7	-26.2±4.4	0.07	0.82	0.59
RVFWLS (%)	-31.1±4.3	-30.5±3.8	-30.5±4.1	-33.4±3.9	**<0.05**	0.06	0.15

Abbreviations: MA = male athlete; FA = female athlete; MC = male control; FC = female control; LVIDd = left ventricular diastolic internal diameter; IVSd = interventricular septum diastolic thickness; PWd = posterior wall diastolic thickness; RWT = relative wall thickness; DT: deceleration time; LAVi = left atrial volume index; RAVi = right atrial volume index; TAPSE = tricuspid annular plane systolic excursion; FAC = fractional area change; RIMP = right ventricular myocardial performance index; LS: longitudinal strain; RVFWLS = right ventricular free wall longitudinal strain

4.2.3 3D echocardiographic data

As expected, athletes demonstrated increased LV and RV end-diastolic, end-systolic, and stroke volume indices along with significantly higher LVMi. There was a significant interaction between gender and athletic activity in the case of various LV and RV morphological parameters (LVEDVi, LVESVi, LVSVi, RVEDVi, RVSVi). Post-hoc analysis showed that gender has a significant impact on the degree of geometrical remodeling: while there was no significant difference in ventricular volume indices between the male and female control groups, male athletes demonstrated significantly higher LV and RV volume indices compared to female athletes (all $p<0.01$). LV and also RV EF were significantly lower compared to controls; however, it remained in the normal range in every athlete. Males had significantly lower LV and RV EF, while SVi did not differ between genders. Similarly, LV GLS and GCS were lower in athletes, and also in males (Table 5).

Table 5: Basic 3D echocardiographic data of athlete and control groups

	MA (n=30)	FA (n=30)	MC (n=20)	FC (n=20)	p for gender	p for sport	p for interaction
LVEDVi (ml/m^2)	93.5±11.1	79.9±6.5	62.9±7.4	64.4±8.9	**<0.01**	**<0.001**	**<0.001**
LVESVi (ml/m^2)	39.5±9.0	33.5±5.1	24.1±3.6	23.1±4.4	**<0.001**	**<0.001**	**<0.01**
LVSVi (ml/m^2)	50.9±10.4	46.4±5.7	38.8±5.1	41.3±5.4	0.55	**<0.001**	**<0.05**
LVMi (g/m^2)	103.2±14.9	89.7±8.4	62.1±6.7	64.8±12.9	**<0.05**	**<0.001**	**<0.01**
LVEF (%)	56.3±3.0	58.1±5.5	61.7±3.3	64.0±2.9	**<0.05**	**<0.001**	0.77
LV GLS (%)	-18.9±1.7	-19.6±1.9	-21.1±1.6	-22.5±1.5	**<0.01**	**<0.001**	0.28
LV GCS (%)	-27.2±2.3	-28.4±3.9	-30.6±2.8	-32.0±2.6	**<0.05**	**<0.001**	0.89
RVEDVi (ml/m^2)	94.3±9.8	81.1±8.9	65.8±8.3	64.2±10.9	**<0.001**	**<0.001**	**<0.01**
RVESVi (ml/m^2)	42.9±6.3	35.2±6.6	26.5±5.2	24.0±6.8	**<0.001**	**<0.001**	0.07
RVSVi (ml/m^2)	51.4±5.6	46.0±4.6	39.4±4.9	40.2±5.5	0.05	**<0.001**	**<0.01**
RVEF (%)	54.6±3.6	56.9±4.9	59.6±4.4	62.5±4.9	**<0.01**	**<0.001**	0.75

Abbreviations: MA = male athlete; FA = female athlete; MC = male control; FC = female control; LVEDVi = left ventricular end-diastolic index; LVESVi = left ventricular end-systolic volume index; LVSVi = left ventricular stroke volume index; LVMi = left ventricular mass index; LVEF = left ventricular ejection fraction; LV GLS = left ventricular global longitudinal strain; LV GCS = left ventricular global circumferential strain; RVEDVi = right ventricular end-diastolic volume index; RVESVi = right ventricular end-systolic volume index; RVSVi = right ventricular stroke volume index; RVEF = right ventricular ejection fraction

DOI:10.14753/SE.2021.2460

3D echocardiographic parameters of RV mechanics revealed significant differences between the groups (Table 6). RV GLS was comparable between the pooled athlete population and controls (-22±5 vs. -23±5 %, p=0.24). On the other hand, RV GCS was significantly lower in athletes (-21±4 vs. -26±7 %, p<0.0001; Table 6). This functional shift was even more prominent by examining the relative contribution of longitudinal and radial motion to global function: LEF/RVEF was significantly higher, while REF/RVEF was significantly lower in both athlete groups (Figure 12 and 13). REF/RVEF found to be significantly lower in males compared to females.

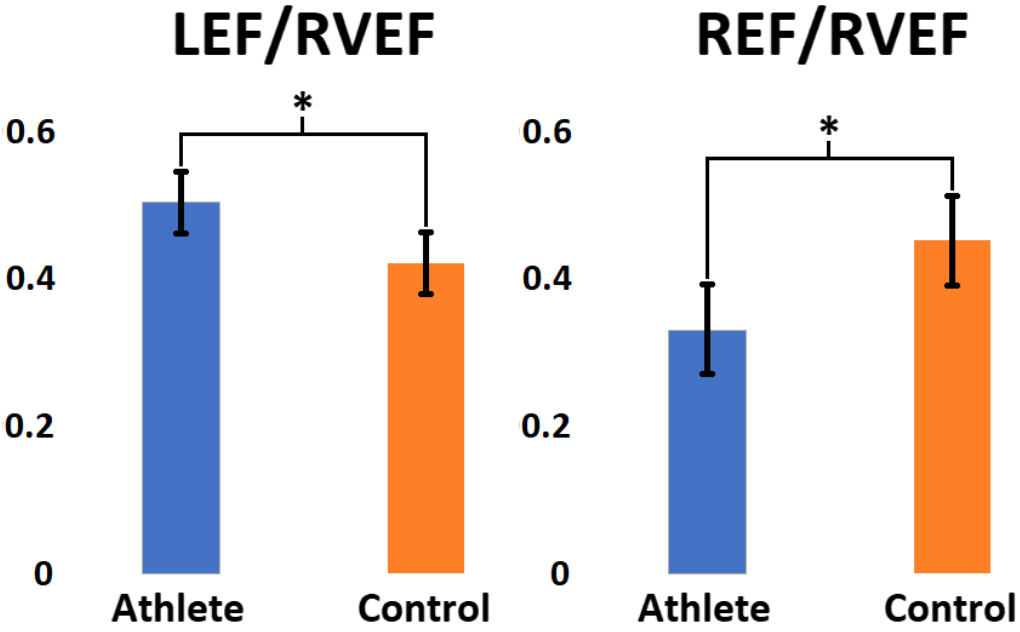

*Figure 12: The relative contribution of longitudinal (LEF/RVEF) and radial motion (REF/RVEF) to global right ventricular function in the two study groups. In athletes, an increased longitudinal contribution can be seen. On the other hand, the radial contribution is significantly decreased compared to controls. Athletes n=60, controls n=40; *p<0.05*

DOI:10.14753/SE.2021.2460

Table 6: 3D global and regional right ventricular deformation data of athlete and control groups

	MA (n=30)	FA (n=30)	MC (n=20)	FC (n=20)	p for gender	p for sport	p for interaction
RV GLS (%)	-21.7±4.4	-21.8±4.7	-20.9±4.1	-24.8±4.9	**<0.05**	0.25	0.06
RV free wall LS (%)	-22.2±4.7	-22.4±4.0	-21.4±4.5	-26.2±5.0	**<0.01**	0.11	**<0.05**
RV septal LS (%)	-22.2±4.8	-21.4±5.5	-20.2±4.7	-23.5±6.5	0.25	0.98	0.07
RV free wall basal LS (%)	-16.5±6.7	-16.3±5.7	-18.4±4.2	-24.0±8.1	**<0.001**	**<0.05**	**<0.05**
RV free wall mid LS (%)	-30.9±7.6	-31.2±5.4	-29.6±6.8	-36.9±7.8	**<0.01**	0.16	**<0.05**
RV free wall apical LS (%)	-19.4±6.9	-19.4±6.3	-16.4±5.5	-17.8±7.3	0.58	0.09	0.62
RV GCS (%)	-20.6±4.4	-21.6±4.2	-24.7±4.0	-27.5±8.4	0.10	**<0.001**	0.41
RV free wall CS (%)	-22.5±4.7	-25.0±5.6	-29.3±5.2	-33.4±8.0	**<0.01**	**<0.001**	0.49
RV septal CS (%)	-20.1±5.9	-21.1±4.6	-21.0±4.8	-23.1±9.6	0.36	0.41	0.49
RV free wall basal CS (%)	-21.7±6.6	-24.0±8.4	-29.7±6.0	-32.6±8.7	0.09	**<0.001**	0.85
RV free wall mid CS (%)	-23.6±4.4	-26.4±5.4	-30.3±5.2	-35.0±7.5	**<0.01**	**<0.001**	0.41
RV free wall apical CS (%)	-22.2±4.6	-24.4±5.3	-27.8±6.0	-32.4±8.7	**<0.01**	**<0.001**	0.32
RV early diastolic SR (1/s)	0.29±0.07	0.28±0.06	0.24±0.04	0.30±0.08	0.47	0.10	**<0.05**
RV LEF (%)	27.5±4.9	27.3±4.9	25.8±5.3	25.9±6.6	0.94	0.17	0.88
RV REF (%)	16.7±3.7	19.2±5.7	25.8±5.2	29.8±7.6	**<0.01**	**<0.001**	0.49
RV AEF (%)	24.7±4.4	25.6±4.5	25.0±5.1	27.9±5.1	0.05	0.19	0.31
LEF/RVEF	0.52±0.07	0.49±0.07	0.43±0.07	0.41±0.08	0.16	**<0.001**	0.98
REF/RVEF	0.31±0.06	0.34±0.09	0.43±0.07	0.47±0.09	**<0.05**	**<0.001**	0.72
AEF/RVEF	0.46±0.07	0.46±0.07	0.42±0.08	0.45±0.08	0.28	0.05	0.36

Abbreviations: MA = male athlete; FA = female athlete; MC = male control; FC = female control; RV GLS = right ventricular global longitudinal strain; RV free wall LS = right ventricular free wall longitudinal strain; RV septal LS = right ventricular septal longitudinal strain; RV free wall basal LS = Right ventricular free wall basal longitudinal strain; RV free wall mid LS = Right ventricular free wall mid longitudinal strain; RV free wall apical LS = Right ventricular free wall apical longitudinal strain; GCS = global circumferential strain; RV free wall CS = right ventricular free wall circumferential strain; RV septal CS = right ventricular septal circumferential strain; RV free wall basal CS = Right ventricular free wall basal circumferential strain; RV free wall mid CS = Right ventricular free wall mid circumferential strain; RV free wall apical CS = Right ventricular free wall apical circumferential strain; RV early diastolic SR = right ventricular early diastolic global longitudinal strain rate; LEF = longitudinal ejection fraction; REF = radial ejection fraction; AEF = anteroposterior ejection fraction

DOI:10.14753/SE.2021.2460

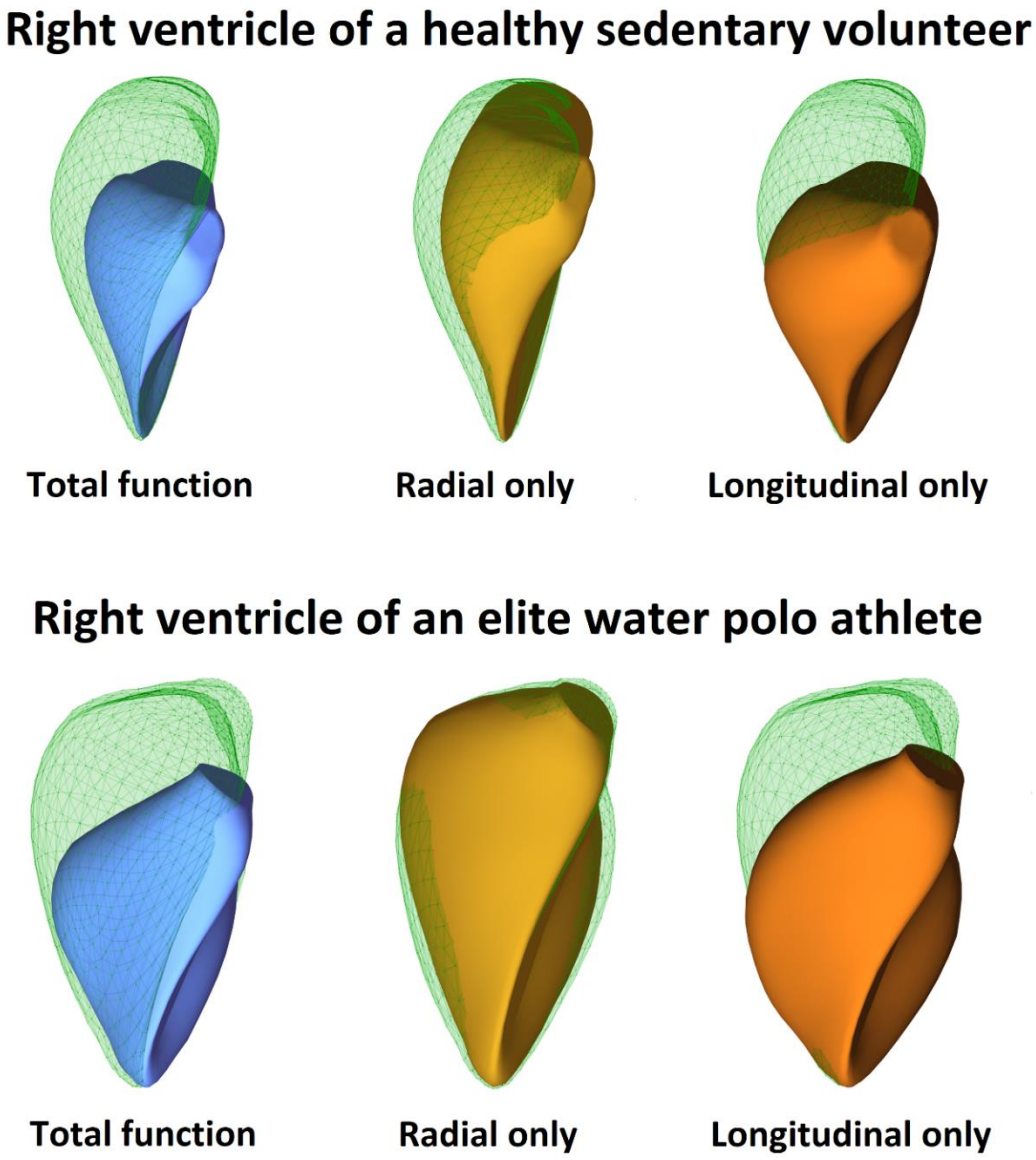

Figure 13: Representative cases of a healthy sedentary volunteer and a water polo athlete. Green mesh represents end-diastolic volume, and the blue surface is the end-systolic volume with all motion directions enabled. By decomposing the motion of the three-dimensional right ventricular model, the different anatomically relevant wall motion directions can be separately quantified. The yellow surface represents the volume loss at end-systole generated by only the radial motion. The orange surface represents the volume loss at end-systole generated by only the longitudinal motion. In the healthy subject, the longitudinal and radial motion roughly equally contributes to global RV function (LEF/RVEF: 0.46; REF/RVEF: 0.48; RVEF: 63%). In the athlete, the relative contribution of right ventricular longitudinal motion is higher; however, a decreased radial motion is also present (LEF/RVEF: 0.54; REF/RVEF: 0.25; RVEF: 57%).

Moreover, the degree of this functional shift showed correlation with VO_2/kg (Table 7). Morphological parameters, such as LVEDVi and RVEDVi, also correlated with CPET-derived VO_2/kg, while no other LV or RV parameter showed a relationship with exercise capacity (Table 7).

Table 7: Correlations between VO_2/kg and LV and RV morphological and functional parameters. Pearson or Spearman correlation test, n=60.

	r value	p value
LVEDVi	**0.32**	**0.02**
LVEF	-0.09	0.51
LV GLS	-0.01	0.93
LV GCS	-0.11	0.43
RVEDVi	**0.37**	**<0.01**
RVEF	-0.11	0.43
RV GLS	0.11	0.43
RV GCS	-0.19	0.17
LEF	0.20	0.13
REF	**-0.26**	**0.04**
LEF/RVEF	**0.30**	**0.02**
REF/RVEF	**-0.27**	**0.04**

Abbreviations: LVEDVi = left ventricular end-diastolic volume index; LVEF = left ventricular ejection fraction; LV GLS = left ventricular global longitudinal strain; LV GCS = left ventricular global circumferential strain; RVEDVi = right ventricular end-diastolic volume index; RVEF = right ventricular ejection fraction; RV GLS = right ventricular global longitudinal strain; RV GCS = right ventricular global circumferential strain; LEF = longitudinal ejection fraction; REF = radial ejection fraction

3D regional analysis of RV deformation parameters was also applied. In female athletes, free wall LS was significantly lower compared to the corresponding control group ($p<0.01$). RV free wall CS was lower in athletes and in males as well (Table 6). Septal LS and CS were not significantly different among groups. On the other hand, LS of the free wall basal region showed a significant decrease, predominantly in female athletes ($p<0.001$), while there was no difference in the apical region. Free wall basal, mid and apical CS were all lower in athletes, without significant interaction between gender and sport. There was a significant interaction between gender and athletic activity in terms of early diastolic SR showing significantly better diastolic function in male athletes

compared to male controls ($p<0.05$). No regional or diastolic parameters showed a correlation with exercise capacity.

Intra- and interobserver variability demonstrated good reproducibility of the key RV deformation parameters (Table 15).

4.3 Unfolding the relationship between left atrial morphology and function and exercise capacity in elite athletes

4.3.1 Basic demographic and morphometric data

The mean age of our athletes was 20 years. They have been participating in competitive sport for 11±5 years, with a current average training of 18±7 hours per week. Athletes had significantly higher BSA and lower resting diastolic blood pressure and resting HR compared to controls (Table 8).

Table 8: Baseline characteristics of athlete and control groups

	Athlete (n=138)	Control (n=50)	p value
Age (years)	19.6±4.3	19.9±2.8	0.66
Female (n)	53	20	0.84
BSA (m^2)	2.00±0.20	1.78±0.24	**<0.001**
SBP (mmHg)	136.1±16.7	128.4±13.7	0.29
DBP (mmHg)	73.5±10.1	79.6±12.4	**<0.001**
HR (1/min)	68.0±11.7	83.2±16.2	**<0.001**
VO_2/kg (mL/kg/min)	52.2±6.7		

Abbreviations: BSA = body surface area; SBP = systolic blood pressure; DBP = diastolic blood pressure; HR = heart rate; VO_2/kg = peak oxygen uptake

4.3.2 Basic 2D echocardiographic data

Left ventricular end-diastolic diameter, wall thicknesses, and relative wall thickness were significantly higher in athletes compared to controls. Conventional measures of LA morphology, such as anteroposterior diameter, LA area, and 2D LA volume index, were significantly higher in athletes, and similar changes were observed in right atrial area and volume index as well. 25% of our athletes exceeded the upper limit of 2D LAVi (>34 mL/m2), as suggested by most recent guidelines. Athletes demonstrated lower transmitral E and A wave velocities along with significantly higher E/A ratio and also longer deceleration time. The control group demonstrated significantly higher tissue Doppler

DOI:10.14753/SE.2021.2460

imaging-derived mitral lateral, and also medial e' and a' velocities, however, E/e' ratio did not differ between the two groups (Table 9).

Table 9: Conventional echocardiographic parameters of athlete and control groups

	Athlete (n=138)	Control (n=50)	p value
LVIDd (mm)	51.9±4.2	46.7±4.2	**<0.001**
IVSd (mm)	10.3±1.6	8.7±1.2	**<0.001**
PWd (mm)	9.2±1.2	7.6±1.2	**<0.001**
RWT (%)	0.38±0.05	0.35±0.05	**<0.001**
LA diameter (mm)	37.2±4.4	31.5±4.5	**<0.001**
LA area (cm²)	19.3±4.0	14.9±3.4	**<0.001**
2D LAVi (ml/m²)	29.4±8.6	23.0±9.3	**<0.001**
RA area (cm²)	18.1±3.8	14.2±3.5	**<0.001**
2D RAVmax (ml/m²)	27.9±7.6	21.5±8.1	**<0.001**
Transmitral E wave (cm/s)	82.5±15.5	92.8±20.1	**<0.001**
Transmitral A wave (cm/s)	51.7±12.6	64.7±14.9	**<0.001**
E/A	1.67±0.47	1.51±0.45	**<0.05**
DT (ms)	179.6±42.4	163.9±29.7	**<0.05**
E/e' average	5.70±1.20	5.61±1.57	0.98
Mitral lateral annulus s' (cm/s)	11.2±2.3	11.8±2.1	**<0.05**
Mitral lateral annulus e' (cm/s)	17.2±3.1	18.6±3.5	**<0.01**
Mitral lateral annulus a' (cm/s)	6.7±2.1	7.6±1.7	**<0.01**
Mitral medial annulus s' (cm/s)	8.9±1.3	9.1±1.3	0.34
Mitral medial annulus e' (cm/s)	12.5±2.2	14.2±2.4	**<0.001**
Mitral medial annulus a' (cm/s)	6.9±1.6	7.3±1.6	**<0.05**

Abbreviations: LVIDd = left ventricular end-diastolic diameter; IVSd = interventricular septal thickness; PWd = posterior wall thickness; RWT = relative wall thickness; LA diameter: left atrial diameter; LA area: left atrial area; LAVi = left atrial volume index; RA area: right atrial volume index; RAVmax = right atrial volume index DT: deceleration time

DOI:10.14753/SE.2021.2460

4.3.3 3D echocardiographic data

Athletes demonstrated significantly higher 3D LV volumes and LVMi compared to controls. Functional measures of the LV, such as LV EF, GLS, and GCS, were significantly lower in athletes. Similarly to the morphological changes of the LV, LA dilation was seen in athletes with significantly higher 3D LAVi, Vmin, preAV, total emptying volume index, and true conduit volume. LAEF and LA active EF was significantly lower in the athlete group. LA passive EF did not differ between groups; however, it showed a tendency towards lower values in athletes (Figure 14, Table 10). Athletes demonstrated lower 3D LAGLS as well. Similarly to the LV, 3D RV volumes were significantly higher in athletes along with lower RVEF; however, RVFWLS was comparable between the athletes and controls (Table 10).

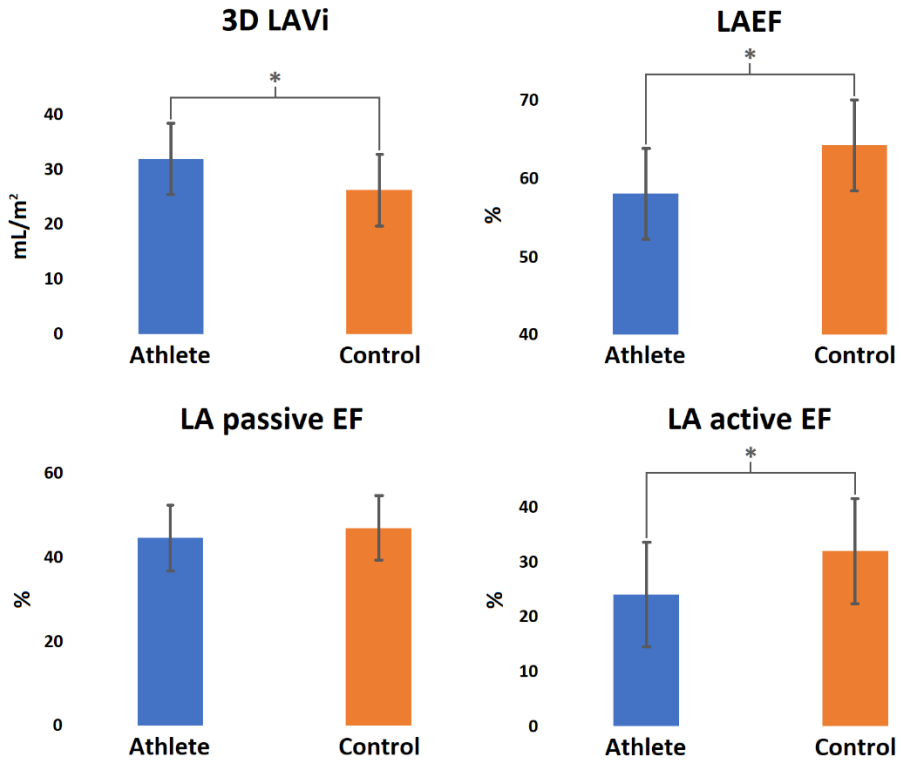

*Figure 14: Comparison of left atrial (LA) morphology and function in athletes and controls. *: p<0.05; LAVi = left atrial maximal volume index; LAEF = left atrial total emptying fraction; LA passive EF = left atrial passive emptying fraction; LA active EF = left atrial active emptying fraction*

DOI:10.14753/SE.2021.2460

Table 10: 3D echocardiographic data of athlete and control groups

	Athlete (n=138)	Control (n=50)	p value
LVEDVi (mL/m^2)	85.4±12.4	62.0±10.3	**<0.001**
LVESVi (mL/m^2)	37.3±6.9	23.9±5.3	**<0.001**
LVSVi (mL/m^2)	48.0±7.3	38.1±6.3	**<0.001**
LVMi (g/m^2)	94.9±14.4	68.9±11.7	**<0.001**
LVEF (%)	56.3±4.2	61.6±4.3	**<0.001**
LVGLS (%)	-18.8±1.9	-21.5±1.6	**<0.001**
LVGCS (%)	-27.4±2.9	-29.9±9.0	**<0.01**
LAVi (mL/m^2)	32.0±5.8	26.3±7.7	**<0.001**
LAVmin (mL/m^2)	13.5±3.2	9.6±3.6	**<0.001**
LA total emptying volume index	18.6±3.7	16.8±4.9	**<0.05**
LApreAV (ml/m^2)	17.8±4.3	14.0±4.9	**<0.001**
LAEF (%)	58.1±6.2	64.2±5.7	**<0.001**
LA active EF (%)	24.1±9.5	32.0±9.6	**<0.001**
LA passive EF (%)	44.6±7.6	46.9±8.0	0.07
LA true conduit volume (mL/m^2)	29.4±6.3	21.3±8.7	**<0.01**
LAGLS (%)	32.2±7.3	38.5±7.4	**<0.001**
RVEDVi (ml/m^2)	88.2±13.8	63.5±11.9	**<0.001**
RVESVi (ml/m^2)	40.6±9.1	26.1±6.4	**<0.001**
RVSVi (ml/m^2)	47.7±6.4	37.7±6.9	**<0.001**
RVEF (%)	54.3±4.8	56.2±6.9	**<0.001**
RVFWLS (%)	-29.1±7.4	-30.6±4.6	0.22

Abbreviations: LVEDVi = left ventricular end-diastolic index; LVESVi = left ventricular end-systolic volume index; LVSVi = left ventricular stroke volume index; LVMi = left ventricular mass index; LVEF = left ventricular ejection fraction; LVGLS = left ventricular global longitudinal strain; LVGCS = left ventricular global circumferential strain; LAVi: left atrial maximal volume index; LAVmin: left atrial minimal volume index; LApreAV: left atrial pre-A wave volume index; LAEF: left atrial total emptying fraction; LA active EF = left atrial active emptying fraction; LA passive EF = left atrial passive emptying fraction; LA true conduit volume: left atrial true conduit volume; LAGLS: left atrial global longitudinal strain; RVEDVi = right ventricular end-diastolic volume index; RVESVi = right ventricular end-systolic volume index; RVSVi = right ventricular stroke volume index; RVEF = right ventricular ejection fraction; RVFWLS: right ventricular free wall longitudinal strain

Comparison of 3D echocardiographic data in female and male athletes are shown in Table 11. Male athletes had significantly higher 3D LV volume indices and LVMi. On the other hand, LV EF was significantly lower in male athletes, and LV GLS and GCS were also lower compared to female athletes. In contrast with the LV volumetric adaptation, 3D LAVi and Vmin did not differ between genders. Interestingly, however, LA functional differences were present with significantly higher 3D LAEF and LAGLS in females, resulting in a higher total emptying volume index as well. Male athletes demonstrated significantly higher RV volumes along with lower RVEF compared to females, while RVFWLS did not differ between genders (Table 11).

DOI:10.14753/SE.2021.2460

Table 11: Comparison of 3D echocardiographic data in female and male athletes

	Male athlete (n=85)	Female athlete (n=53)	p value
LVEDVi (mL/m^2)	89.0±13.1	79.7±8.3	**<0.001**
LVESVi (mL/m^2)	39.7±6.8	33.6±5.3	**<0.001**
LVSVi (mL/m^2)	49.3±7.8	46.1±5.9	**<0.05**
LVMi (g/m^2)	98.7±15.6	88.9±9.5	**<0.001**
LVEF (%)	55.4±3.5	57.9±4.7	**<0.01**
LVGLS (%)	-18.3±1.8	-19.4±1.9	**<0.001**
LVGCS (%)	-26.9±2.4	-28.1±3.4	**<0.05**
LAVi (mL/m^2)	31.5±5.9	32.9±5.4	0.18
LAVmin (mL/m^2)	13.5±3.3	13.3±3.2	0.73
LA total emptying volume index (mL/m^2)	18.0±3.6	19.5±3.7	**<0.05**
LApreAV (ml/m^2)	17.8±4.6	17.8±3.8	0.91
LAEF (%)	57.2±5.7	59.5±6.7	**<0.05**
LA active EF (%)	23.2±9.9	25.4±8.7	0.20
LA true conduit volume (mL/m^2)	31.2±6.3	26.6±5.4	**<0.001**
LA passive EF (%)	44.0±7.4	45.6±7.8	0.24
LAGLS (%)	31.0±6.6	34.3±7.8	**<0.01**
RVEDVi (ml/m^2)	92.9±13.7	80.8±10.2	**<0.001**
RVESVi (ml/m^2)	43.8±9.0	35.5±6.8	**<0.001**
RVSVi (ml/m^2)	49.1±6.6	45.5±5.6	**<0.01**
RVEF (%)	53.1±4.2	56.3±5.0	**<0.001**
RVFWLS (%)	-28.1±6.9	-30.6±4.0	0.07

Abbreviations: LVEDVi = left ventricular end-diastolic index; LVESVi = left ventricular end-systolic volume index; LVSVi = left ventricular stroke volume index; LVMi = left ventricular mass index; LVEF = left ventricular ejection fraction; LVGLS = left ventricular global longitudinal strain; LVGCS = left ventricular global circumferential strain; LAVi: left atrial maximal volume index; LAVmin: left atrial minimal volume index; LApreAV: left atrial pre-A wave volume index; LAEF: left atrial total emptying fraction; LA active EF = left atrial active emptying fraction; LA passive EF = left atrial passive emptying fraction; LAGLS: left atrial global longitudinal strain; RVEDVi = right ventricular end-diastolic volume index; RVESVi = right ventricular end-systolic volume index; RVSVi = right ventricular stroke volume index; RVEF = right ventricular ejection fraction; RVFWLS: right ventricular free wall longitudinal strain

Univariate correlations between 3D echocardiography-derived parameters and VO_2/kg in athletes are summarized in Table 10. 3D LAVi showed weak, but significant positive correlation with age, LVEDVi, LVMi, and RVEDVi. Higher LAEF and LA active EF were weakly associated with higher LV GLS (higher deformation), higher RVEF, and also with higher RVFWLS (better deformation), while LA active EF showed a weak, but significant relationship with LVEF. LA passive EF showed a weak inverse correlation with age. While 2D LA measurements did not show any relationship with VO_2/kg, several 3D LA, LV and RV parameters had weak, but significant correlation with exercise performance: higher LVEDVi, LVMi, LAVi, and RVEDVi were associated with better VO_2/kg, as were lower resting functional parameters, such as LVEF, LVGLS, LAEF, LA

passive EF and RVEF (Table 12). We found no correlation between LA size and LA functional parameters in athletes.

Table 12: Univariate correlation analysis in athletes

	LAVi	LAEF	LA active EF	LA passive EF	VO_2/kg
Age	***r=0.25***	r=-0.13	r=0.06	**r=-0.22**	r=-0.02
	p<0.01	p=0.12	p=0.49	**p<0.01**	p=0.85
LVEDVi	***r=0.51***	r=-0.06	r=0.02	r=-0.07	***r=0.33***
	p<0.001	p=0.48	p=0.79	p=0.43	***p<0.001***
LVMi	***r=0.39***	r=-0.08	r=-0.04	r=-0.06	***r=0.23***
	p<0.001	p=0.31	p=0.61	p=0.50	***p<0.01***
LVEF	r=0.07	r=0.31	***r=0.23***	r=0.13	***r=-0.24***
	p=0.41	p<0.001	***p<0.01***	p=0.12	***p<0.01***
LVGLS	r=-0.02	***r=-0.29***	***r=-0.23***	r=-0.13	***r=0.30***
	p=0.78	***p<0.001***	***p<0.01***	p=0.13	***p<0.001***
RVEDVi	**r=0.35**	*r=-0.04*	*r=0.05*	r=-0.09	***r=0.38***
	p<0.001	*p=0.64*	*p=0.56*	p=0.31	***p<0.001***
RVEF	r=0.067	***r=0.27***	*r=0.14*	**r=0.20**	***r=-0.24***
	p=0.45	***p<0.01***	*p=0.13*	**p<0.05**	***p<0.01***
RVFWLS	r=-0.12	***r=-0.23***	*r=-0.07*	**r=-0.21**	*r=0.03*
	p=0.22	***p<0.05***	*r=0.48*	**p<0.05**	*p=0.98*
VO_2/kg	***r=0.25***	***r=-0.23***	r=0.01	**r=-0.24**	
	p<0.01	***p<0.01***	p=0.99	**p<0.01**	

Abbreviations: LAVi: left atrial maximal volume index; LAEF: left atrial total emptying fraction; LA active EF = left atrial active emptying fraction; LA passive EF = left atrial passive emptying fraction; VO_2/kg: peak oxygen uptake; LVEDVi = left ventricular end-diastolic index; LVMi = left ventricular mass index; LVEF = left ventricular ejection fraction; LVGLS = left ventricular global longitudinal strain; RVEDVi = right ventricular end-diastolic volume index; RVEF = right ventricular ejection fraction; RVFWLS: right ventricular free wall longitudinal strain

Multiple linear regression models were built to identify independent predictors of VO_2/kg in the athlete group. In the first model (Table 13), 3D LV and LA morphological and functional parameters, such as 3D LAVi, LAEF, LA active EF, LA passive EF, LVEDVi, LVMi, LVEF, LVGLS and LVGCS along with basic demographic and morphometric data (age, gender, BSA) and HR were included in the analysis. According to our results, gender, 3D LAVi, LA passive EF, LVGLS, HR, and BSA were independent predictors of exercise capacity, with an adjusted R^2 value of 0.506 ($p<0.0001$). Male gender was associated with better exercise performance.

DOI:10.14753/SE.2021.2460

Table 13: Multivariate linear regression analysis: independent predictors of VO_2/kg

Covariate	β	p value
Age	-0.002	0.979
Gender	**-0.741**	**<0.001**
LAVi	**0.364**	**<0.001**
LAEF	0.012	0.880
LA True EF	0.034	0.621
LA Passive EF	**-0.170**	**0.03**
LVEDVi	-0.047	0.569
LVEF	0.027	0.758
LVMi	-0.054	0.480
LVGLS	**0.212**	**0.001**
LVGCS	-0.018	0.809
BSA	**-0.453**	**<0.001**
HR	**0.157**	**0.04**
Cumulative R^2:	**0.506**	
Standard error:	**4.72%**	
Cumulative p:	**<0.0000001**	

Abbreviations: LAVi: left atrial maximal volume index; LAEF: left atrial total emptying fraction; LA active EF = left atrial active emptying fraction; LA passive EF = left atrial passive emptying fraction; LVEDVi: left ventricular end-diastolic volume index, LVEF: left ventricular ejection fraction, LVMi: left ventricular mass index; LVGLS: left ventricular global longitudinal strain; LVGCS: left ventricular global circumferential strain; BSA: body surface area; HR: heart rate

In the second model, 3D RV parameters (RVEDVi, RVFWLS) replaced two non-significant predictors of the previous analysis (Table 14). In this case, gender, LAVi, LA passive EF, LVGLS, HR and BSA, and also RVEDVi and RVFWLS were independent predictors of VO_2/kg with further improvement of the model (adjusted R^2 value of 0.592, $p<0.0001$).

DOI:10.14753/SE.2021.2460

Table 14: Multivariate linear regression analysis: independent predictors of VO_2/kg

Covariate	β	p value
Age	0.096	0.162
Gender	**-0.828**	**<0.001**
LAVi	**0.222**	**<0.01**
LA True EF	0.128	0.058
LA Passive EF	**-0.190**	**<0.01**
LVEDVi	0.115	0.431
LVMi	-0.054	0.611
LVGLS	0.389	**<0.001**
LVGCS	0.055	0.42
RVEDVi	0.272	**<0.01**
RVFWLS	**-0.133**	**<0.05**
BSA	-0.671	**<0.001**
HR	**0.268**	**<0.001**
Cumulative R^2:	**0.591**	
Standard error:	**4.25%**	
Cumulative p:	**<0.0000001**	

Abbreviations: LAVi: left atrial maximal volume index; LA active EF = left atrial active emptying fraction; LA passive EF = left atrial passive emptying fraction; LVEDVi: left ventricular end-diastolic volume index, LVMi: left ventricular mass index; LVGLS: left ventricular global longitudinal strain; RVEDVi: right ventricular end-diastolic volume; RVFWLS: right ventricular free wall longitudinal strain; BSA: body surface area; HR: heart rate

DOI:10.14753/SE.2021.2460

4.4 Intra- and interobserver variability

Intra- and interobserver variability of the key parameters in our experimental and human studies demonstrated appropriate reproducibility, which corresponds to available literature data (Table 15).

Table 15: Intra- and interobserver variability of key parameters in our studies

	Intraobserver variability, ICC	Interobserver variability, ICC
GLS[1]	0.917	0.917
LSr[1]	0.973	0.970
GCS[1]	0.942	0.936
CSr[1]	0.974	0.961
RVEDV[2]	0.929	0.868
RVESV[2]	0.951	0.914
RVESV after decomposition (longitudinal motion only)[2]	0.934	0.871
RVESV after decomposition (radial motion only)[2]	0.939	0.890
LAVi[3]	0.970	0.961
LAVmin[3]	0.974	0.976
LApreAV[3]	0.974	0.882

Abbreviations:ICC = intraclass correlation; GLS = global longitudinal strain; GCS = global circumferential strain; RVEDV = right ventricular end-diastolic volume; RVESV = right ventricular end-systolic volume; LAVi = left atrial maximal volume index; LAVmin = left atrial minimal volume index; LApreAV = left atrial pre-A wave volume index

[1]: Characterization of the dynamic changes in left ventricular morphology and function induced by exercise training and detraining in a rat model of athlete's heart [2]: Assessment of the exercise-induced shift in right ventricular contraction pattern [3]: Unfolding the relationship between left atrial morphology and function and exercise capacity in elite athletes

DOI:10.14753/SE.2021.2460

5. DISCUSSION

5.1 Characterization of the dynamic changes in left ventricular morphology and function induced by exercise training and detraining

Our first study aimed to provide a detailed characterization of LV morphological and functional changes induced by long-term, intense exercise training and detraining in a rodent model using consecutive evaluation by advanced echocardiography. According to our data, LV hypertrophic response was observed even after 4 weeks of exercise training, and during the remaining weeks of the training period, further development of ventricular hypertrophy could be observed. Following the cessation of swim training, wall thickness and LV mass values showed complete morphological regression after a short period of 2 weeks. Regarding functional measures, STE-derived strain values demonstrated similar dynamic changes of myocardial deformation. As a gold standard measurement of myocardial contractility, invasive LV pressure-volume quantification was used to confirm training-induced systolic enhancement and its reversibility.

Swim-training—a prototype of dynamic, aerobic sports—has been proposed as a stimulus leading to eccentric LV hypertrophy according to the dichotomous concept of Morganroth (18). However, increased RWT values and unaltered end-diastolic dimensions suggest that concentric hypertrophy has been developed by long-term swim training in our animals. Our data might show similarity with previous research enrolling sedentary young subjects after intensive endurance training, showing a biphasic response with an initial concentric hypertrophy in the first six-month-long period, while LV dilation may occur only in the case of long-term maintained exercise (63). Along with similar HR values during anesthesia, end-diastolic chamber sizes did not differ between the control and exercised groups, while end-systolic dimensions were markedly decreased after exercise training. In addition to the heterogeneous response of the myocardial structure to exercise training (25), the role of differences in scale of cardiac dimensions and HR between rodents and humans could not be excluded.

The cessation of regular exercise (detraining) in athletes leads to the reversion of cardiovascular adaptation. This phenomenon can be used to aid the differential diagnosis between athlete's heart and primary forms of pathological hypertrophy (116). The

majority of data in this field focuses on the morphological aspects of reverse remodeling. Previous echocardiographic studies in small animals showed rapid changes (within 2-4 weeks) in response to deconditioning (117), and clinical studies also confirm a similar nature of reverse remodeling in humans (61). Consistently, the consecutive data of wall thickness and LV mass values showed complete morphological regression after 2 weeks of cessation of swim training. These results suggest a rapid reversion of training-induced myocardial growth after discontinuation of biomechanical stress caused by exercise sessions. The exercise-induced cavity dimensions also regressed to control values after the detraining period, however, with a slight delay compared to the alterations in myocardial mass. This complete regression after deconditioning was demonstrated in most of the healthy individuals participating in different sports (105). The development and regression of physiological hypertrophy was also underlined by histological analysis in accordance with the previous results of our research group (110). While the increased cardiac mass is a clear and essential feature of exercise-induced cardiovascular adaptation, the follow-up of training-induced alterations in LV myocardial function are still ambiguous. Considering that myocardial contractility is a major determinant of LV function, in the last decades, efforts have been made to describe myocardial inotropy in vivo, which led to the development of novel invasive methods (118). Particular attention has been paid to exercise-induced physiological hypertrophy because this state is associated with “supernormal” myocardial contractility. This remarkable attribution has been observed in both in vitro (isolated cardiomyocyte, papillary muscle) and in vivo experimental investigations with the development of different techniques (119,120). Our hemodynamic data, utilizing load-independent parameters (ESPVR, PRSW), underpin the “supernormal” contractility in our animals after completing a 12-week-long training plan and indicate total reversion after the detraining period. Although these parameters can describe myocardial inotropy in detail, pressure-volume analysis requires the sacrifice of experimental animals; thus, this method cannot be applied in longitudinal experimental sports cardiology projects. Novel methods of cardiovascular imaging, such as STE-derived strain values may serve as a reliable non-invasive markers of LV contractility and overcome this fundamental methodological limitation of experimental sports cardiology.

We have observed enhanced deformation parameters in response to regular training while detraining resulted in regression of the increased GLS and GCS similarly in nature with the morphological remodeling. Therefore, in the current animal experiments, strain and strain rate parameters were able to demonstrate the supernormal systolic function of the LV in the context of exercise-induced hypertrophy. Our previous study has shown that these parameters correlate well with the gold standard pressure-volume analysis-derived measurements of cardiac contractility, highlighting the usefulness of STE-derived deformation parameters in this setting (113). Of note, our rat model of an athlete's heart is characterized by a concentric type of LV hypertrophy, and the lack of the abovementioned prominent LV dilation may have prevented the “pseudonormalisation” or even decrease of strain parameters, which are frequently reported in the literature and also observed in our human studies (37).

The dynamic nature of the development and regression in LV structural versus functional remodeling is of pivotal interest. Since the regression of LV morphological remodeling (hypertrophy) is a principal feature of an athlete's heart, used even in clinical decision-making (105), the potential presence of an instant reversal of the characteristic functional changes may hold additive value.

Previous longitudinal human studies examining LV functional changes of the athlete’s heart reported a constant gain of function during the training period as assessed by LVEF and/or GLS (63,65). However, the drop back to the control level in systolic function seems to be a much more instant phenomenon after the cessation of training.

Development dynamics of athlete's heart are far better investigated compared to its reversibility. In line with our results, even the first publications suggested quite an instant drop in morphological characteristics (61,121). Thus, the time until the development of athlete's heart markedly exceeds the time until its complete morphological and functional regression. Our study is the first to characterize the effects of detraining on LV myocardial mechanics, confirming an instantaneous normalization of systolic deformation. The experiments with a prompt cessation of training may refer to a real-life scenario, where the athlete is forced to stop exercise, i.e., due to an injury.

STE-derived deformation parameters show an immediate reduction in response to deconditioning in previously exercised animals, which is more instant compared to conventional echocardiographic measurements of systolic function. This phenomenon

may provide another useful aspect of reversibility, which may support an early differential diagnosis between an athlete's heart and pathological cardiac hypertrophy in doubtful situations.

5.2 Assessment of the exercise-induced shift in right ventricular contraction pattern

In our second study, we aimed to characterize RV morphological and functional changes in response to long-term, intense exercise training in a group of elite water polo athletes. According to our results, typical features of RV mechanics include a functional shift compared to healthy, non-trained controls: the relative contribution of longitudinal motion to global function is increased, while the radial shortening is significantly decreased in athletes. Moreover, this functional pattern correlated with aerobic exercise performance measured by CPET.

Our water polo athletes showed significant RV morphological remodeling, as expected. Compared to the conventional RV linear dimensions, 3D volumetric assessment demonstrated more pronounced RV dilation in athletes. Still, from a purely clinical view, quantification of RV volumes holds low diagnostic value: along with the morphological changes of the athlete’s heart, slightly reduced RV function measured by fractional area change (FAC) or 3D RV EF are often present as well; therefore, a considerable group of athletes fulfill the Task Force criteria of ARVC (45). These similarities hamper a confident distinction of athlete’s heart and pathological conditions but also showing the need for detailed functional characterization, which may offer more specific and sensitive markers in order to differentiate these entities.

Despite the notable amount of circumferentially oriented myofibers in the subepicardial layer of the RV myocardium, data are scarce about the non-longitudinal function of the chamber (122). The complex RV contraction pattern incorporates movements along two other anatomical axes: the radial motion of free wall often referred to as the “bellows effect,” and anteroposterior shortening of the chamber by stretching of the free wall over the septum (6). The latter mechanism is significantly affected by the LV function via the interventricular septum, which highlights the role of the LV in RV function through ventricular interdependence (123). Our results comprise a functional shift in RV function

with an increased contribution of longitudinal function and a decreased importance of the free wall radial motion.

There are several underlying factors that may explain the presence of this functional shift. As previously mentioned, repetitive, vigorous exercise bouts are associated with marked hemodynamic demands, which results in a disproportionate hemodynamic load compared to the LV (84). Beyond the volume overload associated with significantly increased CO, during intense exercise, elevated RV pressures also develop, which may act as important promoting factors of RV functional remodeling (41).

In pathological states, volume and pressure overload of the RV displays distinct mechanical responses. In patients with isolated RV volume overload, such as by the consequence of atrial septal defect, it has been shown that increased preload results in higher TAPSE and RV GLS along with similar FAC (partly incorporating the radial motion), which may point at a higher contribution of longitudinal shortening to global function (124-126). Similarly, previous studies with endurance athletes also showed increased tricuspid annular kinetics (44). In parallel with the controversial findings of LV deformation imaging, the vast majority of studies found similar (48), or slightly higher RV GLS in athletes (44,127), however, decreased resting RV longitudinal function was also reported (128). Beyond methodological differences, this inconsistent data is mainly attributable to the heterogeneity of the athletes investigated.

In patients with RV pressure overload, such as primary pulmonary hypertension or chronic thromboembolic pulmonary hypertension, the loss of radial function may be a more sensitive and earlier marker of RV dysfunction (129). Impairment in longitudinal RV function may also appear with the progression of the disease; nevertheless, it may be not sensitive enough for diagnosis and to predict survival (130,131). According to our results, in athletes of mixed exercise nature the RV mechanics shares the features of both volume overload (with the increased relative contribution of longitudinal shortening) and pressure overload (decreased radial shortening). In our population of healthy young athletes, this functional shift has to be perceived as a physiological adaptation to regular, intense exercise. Evidence suggests that exercise-induced RV dysfunction develops by the varying contribution of the individual susceptibility and the hemodynamic overload of intense training (41,85). Sensitive imaging markers are still lacking to screen for athletes at risk and also for the monitoring of exercise-induced changes.

Exercise adaptation is also associated with changes in the autonomic nervous system with a higher parasympathetic tone (132). The RV is densely innervated by autonomic fibers, and the altered neural regulation may also affect ventricular function (133). The revealed gender differences may also be consequences of the significantly higher resting HR of females. Higher HR was shown to be independently associated with higher LV longitudinal deformation in a pooled population of athletes and controls (27). Considering that the frequency-dependent inotropy (Bowditch phenomenon) applies to the RV as well, it may result in higher deformation values in females. Concomitant remodeling of the LV may also play a role in the functional shift: LV contraction significantly contributes to RV function, which can also be altered by the marked morphological and functional adaptation of the ventricles (134). Previous studies suggest that RV diastolic mechanics may also play an important role in cardiac performance (135). In our study, male athletes demonstrated higher resting early diastolic SR compared to the corresponding control group, which reserve capacity may also be beneficial during exercise.

Important gender differences were also noted: in our study, male athletes developed significantly higher ventricular volumes compared to female athletes; however, global RV function underwent the same mechanical shift in both genders. Interestingly, despite the supernormal relative contribution of longitudinal motion to global RV function, females demonstrate a marked decrease in longitudinal deformation, especially at the basal level of the free wall. This result corresponds to several previous papers where the importance of the basal free wall segment was highlighted (135,136) but also showing worrisome similarity with the RV longitudinal contraction pattern reported in subclinical ARVC mutation carriers (100).

Interestingly, this unique RV functional pattern of the athlete's heart showed a correlation with exercise capacity measured by CPET. Similarly to previous findings, we found a linear relationship between LV and RV volumes and VO_2/kg (72,137). EF or other functional parameters of each ventricle failed to show any correlation with peak oxygen uptake. On the other hand, there was a significant correlation between REF/RVEF, LEF/RVEF, and VO_2/kg, indicating that the degree of this mechanical shift may be related to peak exercise capacity pointing at a continuum of training level and functional alterations seen even during resting conditions. Therefore, the increased relative

contribution of RV longitudinal function along with a decreased radial motion may be an important marker of athlete's heart.

5.3 Unfolding the relationship between left atrial morphology and function and exercise capacity in elite athletes

In our third study, we found a prominent LA enlargement with lower resting atrial function with considerable differences between genders. 3D LA and LV morphology and function showed correlation with VO_2/kg; moreover, using multivariate linear regression, LAVi and LA passive EF were independent predictors of peak exercise capacity.

Atrial remodeling in athletes represents a dynamic adaptation to the hemodynamic load associated with exercise training. Beyond volume overload, increased CO during exercise is also associated with increased LV filling pressures; therefore, the LA is also a subject of pressure overload (15,40).

In order to cope with these hemodynamic demands, the LA undergoes a complex morphological and functional remodeling. Moreover, resting bradycardia in athletes shifts the diastolic filling of the LV even more towards the early period (38). All these changes refer to a more effective LA-LV diastolic coupling mainly based on passive hemodynamics instead of active contraction. During exercise, however, this functional reserve capacity will be able to actively support adequate LV filling and systemic forward flow when HR increases (138).

In parallel with previous results, athletes demonstrated significantly higher LA volumes. Interestingly, no difference was found in LAVi between male and female athletes. Conflicting results have been reported about the influence of gender on atrial size. In opposite to our results, D'Andrea and coworkers demonstrated that LA size was greater in males compared to female athletes (139). Nevertheless, a meta-analysis using 2D echocardiography concluded that gender does not influence LA volumes, which is in line with our 3D data (51). Badano and coworkers suggested reference values for 3D LA volumes and phasic functional indices measuring a large subset of healthy Italian volunteers using the same software applied in our study (140). Comparing our controls to their reference values of the same age range, we found similar LA volumes, while the athletes demonstrated clear LA enlargement. Similarly to our results, they found that LA

volumes indexed to BSA were similar in men and women and increasing across age categories (140).

Along with LA morphology, LA functional parameters also demonstrate dynamic changes in our athlete group. Studies using 2D volumetric or speckle-tracking echocardiography approach demonstrated normal LA reservoir function and reduced contractile function along with maintained passive emptying properties compared to sedentary controls (141,142). While reservoir function in athletes was reported to be preserved in several papers, there is evidence of decreased resting reservoir function at mid-season compared to the pre-season period, suggesting that LA adaptation to exercise may also involve lower resting reservoir function of the chamber (52,142). Moreover, a recent meta-analysis found that both LA reservoir and contractile functions are lower in athletes (50). In line with these data, in our study 3D LAEF and LAGLS, markers of LA reservoir function were significantly lower in athletes compared to non-trained controls. In contrast to other LA phasic functional parameters, LA passive EF was found to be comparable between the study groups, which may be attributable to the supernormal LV early diastolic function of athletes facilitating LA emptying in conduit phase (38). These findings are consistent with a previous publication, also applying 3D echocardiography (143). Data are scarce regarding gender differences of LA functional adaptation: according to previous data using 2D speckle tracking echocardiography in runners, females exhibit similar LA functional changes, with significantly higher LA contractile function compared to males (144). According to our results, female athletes have significantly higher LAEF and LAGLS, but similar LA passive emptying and contractile properties compared to male athletes.

Besides gender, HR, and morphometric parameters such as BSA, in our multivariate linear regression model 3D, but not 2D-derived LAVmax was an independent predictor of VO_2/kg. Our findings suggest that LV and LA morphology correlate directly while resting functional parameters have an inverse relationship with peak exercise capacity in mixed trained athletes. Previous echocardiographic and also cMR studies demonstrated similar linear correlation with LV and LA volumes and VO_2/kg (72,73). Interestingly, 3D LVEDVi was not a predictor of exercise performance, suggesting that the assessment of LA morphological adaptation using 3D echocardiography may provide incremental value in the characterization of athlete's heart. Moreover, cardiac functional parameters such as

LVGLS and LA passive EF were also independent predictors of fitness. LVGLS was proven to be a strong marker of LV functional status (76), and LA passive EF may be perceived as a composite marker of LV diastolic function, LA stiffness, and filling pressures, which may explain their predictive value (145). Our second multivariate linear regression model revealed that RV morphology and function (RVEDVi, RVFWLS) are also independent predictors of VO_2/kg besides those parameters that were revealed in our first model. Interestingly, better exercise performance is associated with lower LV longitudinal deformation; however, with higher RV longitudinal deformation. This finding is consistent with our second study described in this thesis.

5.4 Limitations

There are several limitations that have to be addressed regarding the above-discussed studies. First and foremost, we were using echocardiography, which is not the gold standard for the measurement of cardiac chamber volumes and EF. Nevertheless, echocardiography is considered to be a highly reliable and reproducible method, and the largest body of data in this field are derived from this imaging modality.

In our experimental rodent study, the trained rats developed concentric-type of LV hypertrophy, which may be attributable to the nature and the longevity of the training. It is also important to mention that during our in vivo investigations, HR did not differ between trained and control animals, which might be related to the anesthesia that might influence the autonomic balance and mask exercise-induced bradycardia and the consequent chamber dilatation. Although this phenomenon could be a limitation of the study, the similar HR values might offer the advantage to obtain more comparable parameters of ventricular dimensions and mechanics. Beyond these observations, rodent and human physiology obviously differ in many aspects, which limits the applicability of our findings to the clinical setting.

In our clinical studies, the number of investigated athletes was relatively low. Our study populations were generally younger than the “typical” athlete groups in sports cardiology research. It is also important to mention that we were examining only water sport disciplines. Therefore, cardiac remodeling and subsequent functional changes may be less prominent compared to the classical ultra-endurance athletes (e.g., ultramarathon,

cycling), which may represent the absolute peak of exercise-induced cardiac adaptation. Nevertheless, our athletes still have a long training history and participate in top-level training and competition. 3D echocardiography yields lower temporal and spatial resolution compared to 2D echocardiography; however, multi-beat reconstruction was applied in both studies to achieve a higher frame rate and better spatial resolution. Moreover, 3D image acquisition and analysis require special equipment and expertise. In the second study, our method was based on 3D analysis by a custom software; therefore, absolute values of the strain and strain rate measurements are not comparable to commercially available 2D methods. Only resting echocardiographic measurements were performed in our studies. Further investigations are warranted to characterize 3D chamber mechanics during exercise. Our clinical studies are cross-sectional, while the temporal changes in RV and LA morphology and function, such as throughout a training season or dynamics of deconditioning, remain unknown.

DOI:10.14753/SE.2021.2460

6. CONCLUSIONS

In our first study, we have characterized the temporal nature of the development and the regression of exercise-induced cardiac remodeling using conventional echocardiography and STE in a rodent model. We have shown that LV hypertrophy occurs even after 4 weeks of exercise, with a gradual increase in wall thicknesses later on the training period. In parallel with the morphological changes, LV deformation measures increase in a similar manner. Suspension of the training resulted in rapid LV reverse remodeling: both morphological and functional measures were comparable in the study groups 2 weeks following the cessation of the training. We have confirmed enhanced LV contractility of the exercised group and also the deteriorating effects of deconditioning by invasive hemodynamic measurements. Histological examinations also showed the increase and regression of cardiomyocyte width with no concomitant collagen deposition. Our results suggest that STE might be an ideal method to follow-up changes induced by exercise training and detraining.

In our second study, by the 3D echocardiographic assessment of RV mechanical pattern, we have shown that beyond the well-known marked dilation and low-normal resting EF, the RV of the athlete's heart is characterized by an increased relative contribution of the longitudinal and a decreased contribution of radial wall motions at rest. While the morphological changes were less pronounced in females, the RV mechanics did not differ between genders. Moreover, this mechanical pattern shows a correlation with exercise performance measured by CPET. According to these results, this functional shift may represent a novel resting marker of athlete's heart.

Our third study showed significant LV and LA morphological and functional remodeling using 3D echocardiography in a relatively large set of elite athletes. In the face of the lower LV volumes in female athletes compared to males, LA volumes were comparable between genders. Several LV and LA measures showed a significant correlation with exercise capacity; however, 3D LAVmax and LA passive EF were independent predictors of VO_2/kg. Our results suggest that athletes' atrial enlargement and lower resting function do not represent dysfunction, but a physiological aspect of athlete's heart: less contraction in a higher volume chamber can achieve the same stroke volume as a smaller one with more pronounced shortening. Assessment of LA remodeling and phasic function by 3D echocardiography might be an important evaluating step in sports cardiology.

DOI:10.14753/SE.2021.2460

7. SUMMARY

Regular physical exercise is associated with significant hemodynamic demands inducing changes in cardiac morphology and function, also referred to as the athlete's heart. Data are scarce regarding the temporal dynamics of the physiological hypertrophy and its reversal. Moreover, in the past decades, data are also growing about the possible harmful effects of intense training. When underlying susceptibility is present, athletic training may precipitate cardiovascular diseases, emphasizing the need for in-depth characterization of the athlete's heart, which should not be confined to the LV.

Our research group characterized the development and regression of the athlete's heart in a rodent model. LV structural changes were evident after 4 weeks of training with a gradual increase throughout the exercise phase. LV remodeling was accompanied by an enhanced LV systolic function measured by STE-derived GLS and GCS. Cessation of the training was associated with rapid reverse remodeling: LV morphological and functional parameters were comparable between the exercised and the control groups even after 2 weeks.

We have also studied RV mechanics of the athlete's heart by enrolling professional water polo players examined by 3D echocardiography. Markedly higher RV volumes and low-normal RVEF were noted, as expected. However, an increased relative contribution of the longitudinal motion and a decreased contribution of radial wall motion were also detected at rest. In opposed to the RV morphological remodeling, this deformation pattern did not differ between males and females. Moreover, the degree of this functional shift also correlated with peak exercise capacity measured by CPET. LA morphology and function were also investigated by 3D echocardiography in mixed-trained athletes. Higher LV and LA volumes were established while resting functional measures were generally decreased compared to controls. 3D LV volumes in female athletes were significantly lower compared to males; LA volumes did not differ between genders. 3D LAVmax and also LA passive EF and LV GLS were independent predictors of exercise capacity, suggesting that the assessment of LA morphology and function by 3D echocardiography may have incremental value.

In summary, our results emphasize the growing clinical attention and the added value of advanced echocardiographic techniques (particularly speckle tracking and 3D echocardiography) in the arena of sports cardiology.

DOI:10.14753/SE.2021.2460

8. ÖSSZEFOGLALÁS

A rendszeres sporttevékenységgel összefüggő hemodinamikai terhelés a szív morfológiai és funkcionális változásait indukálja, melyet sportszívnek nevezünk. Ezen jellegzetes változások ellenére kevés adat áll rendelkezésre kialakulásának és visszafejlődésének pontos dinamikájáról. Újabb eredmények alapján az intenzív sporttevékenységnek káros hatásai is lehetnek: ha bizonyos genetikai hajlam jelen van, a rendszeres fizikai terhelés különféle megbetegedések megjelenését precipitálhatja, amelyek azonban nem kizárólag a bal kamrával vannak összefüggésben.

Sportszív patkánymodelljével vizsgáltuk a sportszív kialakulását, illetve a reverz remodellációt. Négy hét edzés hatására a sportoló csoport szignifikáns falvastagság növekedése mellett a GLS és GCS emelkedő nyugalmi deformációt mutatott. Az edzéstevékenység felfüggesztése gyors reverz remodellációt eredményezett: mindössze 2 hét dekondicionálódást követően a bal kamra alaki és működési sajátosságai a kontroll csoportéval összehasonlíthatóak voltak.

A jobb kamrai mechanika sajátosságait is vizsgáltuk vízilabdás élsportolókon. A sportolói csoport a várható módon jelentősen emelkedett jobb kamrai volumeneket, illetve alacsony-normális funkcionális paramétereket mutatott. Mindazonáltal, a jobb kamrai mechanika elemzése során a longitudinális rövidülés relatív dominanciájával párhuzamosan a radiális irányú kontrakció relatív csökkenése mutatkozott. Míg a jobb kamrai morfológiai átépülés nőkben kevésbé volt markáns, a deformációs mintázat jellege a két nemben hasonló volt. A deformációs mintázat paraméterei, illetve a VO_2/kg között szignifikáns korrelációt találtunk. A bal kamra és a bal pitvar sajátosságait egy kevert terhelésű sportoló populáción vizsgáltuk. Az emelkedett volumenek mellett a sportolók nyugalmi bal kamrai és pitvari funkcionális paraméterei alacsonyabbak voltak a kontroll csoporthoz képest. Míg a bal kamrai térfogatok alacsonyabbak voltak női sportolókban, a bal pitvari térfogatok tekintetében nem mutatkozott különbség a nemek között. A 3D echokardiográfiás bal pitvari volumenek, illetve funkcionális paraméterek összefüggést mutattak a VO_2/kg-mal, ezen felül a 3D bal pitvari Vmax, illetve a passzív EF és a bal kamrai GLS is független prediktorai voltak a csúcs terhelhetőségnek. Összefoglalva, eredményeink rámutatnak a modern echokardiográfiás technikák potenciális klinikai felhasználására és jelentős hozzáadott értékére a sportkardiológia területén.

9. REFERENCES

1. Henschen S. (1899) Skilanglauf und skiwettlauf: eine medizinische sportstudie. Mitt Med Klin Uppsala (Jena), 2: 15-18.
2. EA. D. (1899) The effects of training: a study of the Harvard University crews. Boston Med Surg J: 229-233.
3. NV. P. (1951) [Roentgenologic investigation of the heart in athletes]. Klin Med (Mosk): 48-54.
4. Narang A, Addetia K. (2018) An introduction to left ventricular strain. Curr Opin Cardiol, 33: 455-463.
5. Stokke TM, Hasselberg NE, Smedsrud MK, Sarvari SI, Haugaa KH, Smiseth OA, Edvardsen T, Remme EW. (2017) Geometry as a Confounder When Assessing Ventricular Systolic Function: Comparison Between Ejection Fraction and Strain. J Am Coll Cardiol, 70: 942-954.
6. Kovacs A, Lakatos B, Tokodi M, Merkely B. (2019) Right ventricular mechanical pattern in health and disease: beyond longitudinal shortening. Heart Fail Rev, 24: 511-520.
7. Hoit BD. (2014) Left atrial size and function: role in prognosis. J Am Coll Cardiol, 63: 493-505.
8. Edler I, Lindstrom K. (2004) The history of echocardiography. Ultrasound Med Biol, 30: 1565-1644.
9. Haugaa KH, Dejgaard LA. (2018) Global Longitudinal Strain: Ready for Clinical Use and Guideline Implementation. J Am Coll Cardiol, 71: 1958-1959.
10. Ayach B, Fine NM, Rudski LG. (2018) Right ventricular strain: measurement and clinical application. Curr Opin Cardiol, 33: 486-492.
11. Buggey J, Hoit BD. (2018) Left atrial strain: measurement and clinical application. Curr Opin Cardiol, 33: 479-485.
12. Wandt B, Bojo L, Tolagen K, Wranne B. (1999) Echocardiographic assessment of ejection fraction in left ventricular hypertrophy. Heart, 82: 192-198.

13. Lang RM, Badano LP, Mor-Avi V, Afilalo J, Armstrong A, Ernande L, Flachskampf FA, Foster E, Goldstein SA, Kuznetsova T, Lancellotti P, Muraru D, Picard MH, Rietzschel ER, Rudski L, Spencer KT, Tsang W, Voigt JU. (2015) Recommendations for cardiac chamber quantification by echocardiography in adults: an update from the American Society of Echocardiography and the European Association of Cardiovascular Imaging. Eur Heart J Cardiovasc Imaging, 16: 233-270.

14. Lang RM, Addetia K, Narang A, Mor-Avi V. (2018) 3-Dimensional Echocardiography: Latest Developments and Future Directions. JACC Cardiovasc Imaging, 11: 1854-1878.

15. La Gerche A, Claessen G, Van de Bruaene A, Pattyn N, Van Cleemput J, Gewillig M, Bogaert J, Dymarkowski S, Claus P, Heidbuchel H. (2013) Cardiac MRI: a new gold standard for ventricular volume quantification during high-intensity exercise. Circ Cardiovasc Imaging, 6: 329-338.

16. McDiarmid AK, Swoboda PP, Erhayiem B, Lancaster RE, Lyall GK, Broadbent DA, Dobson LE, Musa TA, Ripley DP, Garg P, Greenwood JP, Ferguson C, Plein S. (2016) Athletic Cardiac Adaptation in Males Is a Consequence of Elevated Myocyte Mass. Circ Cardiovasc Imaging, 9: e003579.

17. Mitchell JH, Haskell W, Snell P, Van Camp SP. (2005) Task Force 8: classification of sports. J Am Coll Cardiol, 45: 1364-1367.

18. Morganroth J, Maron BJ, Henry WL, Epstein SE. (1975) Comparative left ventricular dimensions in trained athletes. Ann Intern Med, 82: 521-524.

19. Haykowsky MJ, Samuel TJ, Nelson MD, La Gerche A. (2018) Athlete's Heart: Is the Morganroth Hypothesis Obsolete? Heart Lung Circ, 27: 1037-1041.

20. Prior DL, La Gerche A. (2012) The athlete's heart. Heart, 98: 947-955.

21. McMullen JR, Shioi T, Zhang L, Tarnavski O, Sherwood MC, Kang PM, Izumo S. (2003) Phosphoinositide 3-kinase(p110alpha) plays a critical role for the induction of physiological, but not pathological, cardiac hypertrophy. Proc Natl Acad Sci U S A, 100: 12355-12360.

22. Kunisada K, Tone E, Fujio Y, Matsui H, Yamauchi-Takihara K, Kishimoto T. (1998) Activation of gp130 transduces hypertrophic signals via STAT3 in cardiac myocytes. Circulation, 98: 346-352.

23. Ching GW, Franklyn JA, Stallard TJ, Daykin J, Sheppard MC, Gammage MD. (1996) Cardiac hypertrophy as a result of long-term thyroxine therapy and thyrotoxicosis. Heart, 75: 363-368.
24. Carbone A, D'Andrea A, Riegler L, Scarafile R, Pezzullo E, Martone F, America R, Liccardo B, Galderisi M, Bossone E, Calabro R. (2017) Cardiac damage in athlete's heart: When the "supernormal" heart fails! World J Cardiol, 9: 470-480.
25. Pluim BM, Zwinderman AH, van der Laarse A, van der Wall EE. (2000) The athlete's heart. A meta-analysis of cardiac structure and function. Circulation, 101: 336-344.
26. Utomi V, Oxborough D, Whyte GP, Somauroo J, Sharma S, Shave R, Atkinson G, George K. (2013) Systematic review and meta-analysis of training mode, imaging modality and body size influences on the morphology and function of the male athlete's heart. Heart, 99: 1727-1733.
27. Lo Iudice F, Petitto M, Ferrone M, Esposito R, Vaccaro A, Buonauro A, D'Andrea A, Trimarco B, Galderisi M. (2017) Determinants of myocardial mechanics in top-level endurance athletes: three-dimensional speckle tracking evaluation. Eur Heart J Cardiovasc Imaging, 18: 549-555.
28. D'Ascenzi F, Anselmi F, Piu P, Fiorentini C, Carbone SF, Volterrani L, Focardi M, Bonifazi M, Mondillo S. (2019) Cardiac Magnetic Resonance Normal Reference Values of Biventricular Size and Function in Male Athlete's Heart. JACC Cardiovasc Imaging, 12: 1755-1765.
29. Nagashima J, Musha H, Takada H, Murayama M. (2003) New upper limit of physiologic cardiac hypertrophy in Japanese participants in the 100-km ultramarathon. J Am Coll Cardiol, 42: 1617-1623.
30. Abergel E, Chatellier G, Hagege AA, Oblak A, Linhart A, Ducardonnet A, Menard J. (2004) Serial left ventricular adaptations in world-class professional cyclists: implications for disease screening and follow-up. J Am Coll Cardiol, 44: 144-149.
31. Boraita A, Sanchez-Testal MV, Diaz-Gonzalez L, Heras ME, Alcocer-Ayuga M, de la Rosa A, Rabadan M, Abdul-Jalbar B, Perez de Isla L, Santos-Lozano A, Lucia A. (2019) Apparent Ventricular Dysfunction in Elite Young Athletes: Another Form of Cardiac Adaptation of the Athlete's Heart. J Am Soc Echocardiogr, 32: 987-996.

32. Beaumont A, Grace F, Richards J, Hough J, Oxborough D, Sculthorpe N. (2017) Left Ventricular Speckle Tracking-Derived Cardiac Strain and Cardiac Twist Mechanics in Athletes: A Systematic Review and Meta-Analysis of Controlled Studies. Sports Med, 47: 1145-1170.

33. Vitarelli A, Capotosto L, Placanica G, Caranci F, Pergolini M, Zardo F, Martino F, De Chiara S, Vitarelli M. (2013) Comprehensive assessment of biventricular function and aortic stiffness in athletes with different forms of training by three-dimensional echocardiography and strain imaging. Eur Heart J Cardiovasc Imaging, 14: 1010-1020.

34. Utomi V, Oxborough D, Ashley E, Lord R, Fletcher S, Stembridge M, Shave R, Hoffman MD, Whyte G, Somauroo J, Sharma S, George K. (2014) Predominance of normal left ventricular geometry in the male 'athlete's heart'. Heart, 100: 1264-1271.

35. Caselli S, Montesanti D, Autore C, Di Paolo FM, Pisicchio C, Squeo MR, Musumeci B, Spataro A, Pandian NG, Pelliccia A. (2015) Patterns of left ventricular longitudinal strain and strain rate in Olympic athletes. J Am Soc Echocardiogr, 28: 245-253.

36. Kneffel Z, Varga-Pinter B, Toth M, Major Z, Pavlik G. (2011) Relationship between the heart rate and E/A ratio in athletic and non-athletic males. Acta Physiol Hung, 98: 284-293.

37. Caselli S, Di Paolo FM, Pisicchio C, Pandian NG, Pelliccia A. (2015) Patterns of left ventricular diastolic function in Olympic athletes. J Am Soc Echocardiogr, 28: 236-244.

38. Kovacs A, Apor A, Nagy A, Vago H, Toth A, Nagy AI, Kovats T, Sax B, Szeplaki G, Becker D, Merkely B. (2014) Left ventricular untwisting in athlete's heart: key role in early diastolic filling? Int J Sports Med, 35: 259-264.

39. Maufrais C, Doucende G, Rupp T, Dauzat M, Obert P, Nottin S, Schuster I. (2017) Left ventricles of aging athletes: better untwisters but not more relaxed during exercise. Clin Res Cardiol, 106: 884-892.

40. Reeves JT, Groves BM, Cymerman A, Sutton JR, Wagner PD, Turkevich D, Houston CS. (1990) Operation Everest II: cardiac filling pressures during cycle exercise at sea level. Respir Physiol, 80: 147-154.

41. La Gerche A, Rakhit DJ, Claessen G. (2017) Exercise and the right ventricle: a potential Achilles' heel. Cardiovasc Res, 113: 1499-1508.

42. Bohm P, Schneider G, Linneweber L, Rentzsch A, Kramer N, Abdul-Khaliq H, Kindermann W, Meyer T, Scharhag J. (2016) Right and Left Ventricular Function and Mass in Male Elite Master Athletes: A Controlled Contrast-Enhanced Cardiovascular Magnetic Resonance Study. Circulation, 133: 1927-1935.

43. Major Z, Csajagi E, Kneffel Z, Kovats T, Szauder I, Sido Z, Pavlik G. (2015) Comparison of left and right ventricular adaptation in endurance-trained male athletes. Acta Physiol Hung, 102: 23-33.

44. Ujka K, Bastiani L, D'Angelo G, Catuzzo B, Tonacci A, Mrakic-Sposta S, Vezzoli A, Giardini G, Pratali L. (2017) Enhanced Right-Chamber Remodeling in Endurance Ultra-Trail Athletes Compared to Marathon Runners Detected by Standard and Speckle-Tracking Echocardiography. Front Physiol, 8: 527.

45. D'Ascenzi F, Pisicchio C, Caselli S, Di Paolo FM, Spataro A, Pelliccia A. (2017) RV Remodeling in Olympic Athletes. JACC Cardiovasc Imaging, 10: 385-393.

46. Vos M, Hauser AM, Dressendorfer RH, Hashimoto T, Dudlets P, Gordon S, Timmis GC. (1985) Enlargement of the right heart in the endurance athlete: a two-dimensional echocardiographic study. Int J Sports Med, 6: 271-275.

47. Venlet J, Piers SR, Jongbloed JD, Androulakis AF, Naruse Y, den Uijl DW, Kapel GF, de Riva M, van Tintelen JP, Barge-Schaapveld DQ, Schalij MJ, Zeppenfeld K. (2017) Isolated Subepicardial Right Ventricular Outflow Tract Scar in Athletes With Ventricular Tachycardia. J Am Coll Cardiol, 69: 497-507.

48. Pagourelias ED, Kouidi E, Efthimiadis GK, Deligiannis A, Geleris P, Vassilikos V. (2013) Right atrial and ventricular adaptations to training in male Caucasian athletes: an echocardiographic study. J Am Soc Echocardiogr, 26: 1344-1352.

49. P BS, Khakha DC, Mahajan S, Gupta S, Agarwal M, Yadav SL. (2008) Effect of cryotherapy on arteriovenous fistula puncture-related pain in hemodialysis patients. Indian J Nephrol, 18: 155-158.

50. Cuspidi C, Tadic M, Sala C, Gherbesi E, Grassi G, Mancia G. (2019) Left atrial function in elite athletes: A meta-analysis of two-dimensional speckle tracking echocardiographic studies. Clin Cardiol, 42: 579-587.

51. Iskandar A, Mujtaba MT, Thompson PD. (2015) Left Atrium Size in Elite Athletes. JACC Cardiovasc Imaging, 8: 753-762.

52. D'Ascenzi F, Pelliccia A, Natali BM, Zaca V, Cameli M, Alvino F, Malandrino A, Palmitesta P, Zorzi A, Corrado D, Bonifazi M, Mondillo S. (2014) Morphological and functional adaptation of left and right atria induced by training in highly trained female athletes. Circ Cardiovasc Imaging, 7: 222-229.

53. D'Ascenzi F, Anselmi F, Focardi M, Mondillo S. (2018) Atrial Enlargement in the Athlete's Heart: Assessment of Atrial Function May Help Distinguish Adaptive from Pathologic Remodeling. J Am Soc Echocardiogr, 31: 148-157.

54. Gjerdalen GF, Hisdal J, Solberg EE, Andersen TE, Radunovic Z, Steine K. (2015) Atrial Size and Function in Athletes. Int J Sports Med, 36: 1170-1176.

55. McClean G, George K, Lord R, Utomi V, Jones N, Somauroo J, Fletcher S, Oxborough D. (2015) Chronic adaptation of atrial structure and function in elite male athletes. Eur Heart J Cardiovasc Imaging, 16: 417-422.

56. Colombo C, Finocchiaro G. (2018) The Female Athlete's Heart: Facts and Fallacies. Curr Treat Options Cardiovasc Med, 20: 101.

57. Turkbey EB, Jorgensen NW, Johnson WC, Bertoni AG, Polak JF, Diez Roux AV, Tracy RP, Lima JA, Bluemke DA. (2010) Physical activity and physiological cardiac remodelling in a community setting: the Multi-Ethnic Study of Atherosclerosis (MESA). Heart, 96: 42-48.

58. McClean G, Riding NR, Ardern CL, Farooq A, Pieles GE, Watt V, Adamuz C, George KP, Oxborough D, Wilson MG. (2018) Electrical and structural adaptations of the paediatric athlete's heart: a systematic review with meta-analysis. Br J Sports Med, 52: 230.

59. Pavlik G, Major Z, Csajagi E, Jeserich M, Kneffel Z. (2013) The athlete's heart. Part II: influencing factors on the athlete's heart: types of sports and age (review). Acta Physiol Hung, 100: 1-27.

60. Chandra N, Papadakis M, Sharma S. (2012) Cardiac adaptation in athletes of black ethnicity: differentiating pathology from physiology. Heart, 98: 1194-1200.

61. Maron BJ, Pelliccia A, Spataro A, Granata M. (1993) Reduction in left ventricular wall thickness after deconditioning in highly trained Olympic athletes. Br Heart J, 69: 125-128.

62. Luthi P, Zuber M, Ritter M, Oechslin EN, Jenni R, Seifert B, Baldesberger S, Attenhofer Jost CH. (2008) Echocardiographic findings in former professional cyclists after long-term deconditioning of more than 30 years. Eur J Echocardiogr, 9: 261-267.
63. Arbab-Zadeh A, Perhonen M, Howden E, Peshock RM, Zhang R, Adams-Huet B, Haykowsky MJ, Levine BD. (2014) Cardiac remodeling in response to 1 year of intensive endurance training. Circulation, 130: 2152-2161.
64. Opondo MA, Aiad N, Cain MA, Sarma S, Howden E, Stoller DA, Ng J, van Rijckevorsel P, Hieda M, Tarumi T, Palmer MD, Levine BD. (2018) Does High-Intensity Endurance Training Increase the Risk of Atrial Fibrillation? A Longitudinal Study of Left Atrial Structure and Function. Circ Arrhythm Electrophysiol, 11: e005598.
65. Weiner RB, DeLuca JR, Wang F, Lin J, Wasfy MM, Berkstresser B, Stohr E, Shave R, Lewis GD, Hutter AM, Jr., Picard MH, Baggish AL. (2015) Exercise-Induced Left Ventricular Remodeling Among Competitive Athletes: A Phasic Phenomenon. Circ Cardiovasc Imaging, 8.
66. Baggish AL, Wang F, Weiner RB, Elinoff JM, Tournoux F, Boland A, Picard MH, Hutter AM, Jr., Wood MJ. (2008) Training-specific changes in cardiac structure and function: a prospective and longitudinal assessment of competitive athletes. J Appl Physiol (1985), 104: 1121-1128.
67. Sharma S, Drezner JA, Baggish A, Papadakis M, Wilson MG, Prutkin JM, La Gerche A, Ackerman MJ, Borjesson M, Salerno JC, Asif IM, Owens DS, Chung EH, Emery MS, Froelicher VF, Heidbuchel H, Adamuz C, Asplund CA, Cohen G, Harmon KG, Marek JC, Molossi S, Niebauer J, Pelto HF, Perez MV, Riding NR, Saarel T, Schmied CM, Shipon DM, Stein R, Vetter VL, Pelliccia A, Corrado D. (2018) International recommendations for electrocardiographic interpretation in athletes. Eur Heart J, 39: 1466-1480.
68. Vidal A, Agorrody V, Abreu R, Viana P, Dodera A, Vidal L. (2017) Vagal third-degree atrioventricular block in a highly trained endurance athlete. Europace, 19: 1863.
69. Pereira F, de Moraes R, Tibirica E, Nobrega AC. (2013) Interval and continuous exercise training produce similar increases in skeletal muscle and left ventricle microvascular density in rats. Biomed Res Int, 2013: 752817.

70. Green DJ, Spence A, Rowley N, Thijssen DH, Naylor LH. (2012) Vascular adaptation in athletes: is there an 'athlete's artery'? Exp Physiol, 97: 295-304.
71. Paolillo S, Agostoni P. (2017) Prognostic Role of Cardiopulmonary Exercise Testing in Clinical Practice. Ann Am Thorac Soc, 14: S53-S58.
72. La Gerche A, Burns AT, Taylor AJ, Macisaac AI, Heidbuchel H, Prior DL. (2012) Maximal oxygen consumption is best predicted by measures of cardiac size rather than function in healthy adults. Eur J Appl Physiol, 112: 2139-2147.
73. Rundqvist L, Engvall J, Faresjo M, Carlsson E, Blomstrand P. (2017) Regular endurance training in adolescents impacts atrial and ventricular size and function. Eur Heart J Cardiovasc Imaging, 18: 681-687.
74. Lazic JS, Tadic M, Antic M, Radovanovic D, Nesic D, Rakocevic R, Mazic S. (2019) The relationship between right heart and aerobic capacity in large cohort of young elite athletes. Int J Cardiovasc Imaging, 35: 1027-1036.
75. Gianturco L, Bodini BD, Gianturco V, Lippo G, Solbiati A, Turiel M. (2017) Left ventricular longitudinal strain in soccer referees. Oncotarget, 8: 39766-39773.
76. Hasselberg NE, Haugaa KH, Sarvari SI, Gullestad L, Andreassen AK, Smiseth OA, Edvardsen T. (2015) Left ventricular global longitudinal strain is associated with exercise capacity in failing hearts with preserved and reduced ejection fraction. Eur Heart J Cardiovasc Imaging, 16: 217-224.
77. Vina J, Sanchis-Gomar F, Martinez-Bello V, Gomez-Cabrera MC. (2012) Exercise acts as a drug; the pharmacological benefits of exercise. Br J Pharmacol, 167: 1-12.
78. Reimers CD, Knapp G, Reimers AK. (2012) Does physical activity increase life expectancy? A review of the literature. J Aging Res, 2012: 243958.
79. Corrado D, Basso C, Rizzoli G, Schiavon M, Thiene G. (2003) Does sports activity enhance the risk of sudden death in adolescents and young adults? J Am Coll Cardiol, 42: 1959-1963.
80. Harmon KG, Asif IM, Klossner D, Drezner JA. (2011) Incidence of sudden cardiac death in National Collegiate Athletic Association athletes. Circulation, 123: 1594-1600.
81. Emery MS, Kovacs RJ. (2018) Sudden Cardiac Death in Athletes. JACC Heart Fail, 6: 30-40.

82. Corrado D, Basso C, Schiavon M, Thiene G. (1998) Screening for hypertrophic cardiomyopathy in young athletes. N Engl J Med, 339: 364-369.
83. Elmaghawry M, Alhashemi M, Zorzi A, Yacoub MH. (2012) A global perspective of arrhythmogenic right ventricular cardiomyopathy. Glob Cardiol Sci Pract, 2012: 81-92.
84. La Gerche A, Heidbuchel H, Burns AT, Mooney DJ, Taylor AJ, Pfluger HB, Inder WJ, Macisaac AI, Prior DL. (2011) Disproportionate exercise load and remodeling of the athlete's right ventricle. Med Sci Sports Exerc, 43: 974-981.
85. Sanz-de la Garza M, Rubies C, Batlle M, Bijnens BH, Mont L, Sitges M, Guasch E. (2017) Severity of structural and functional right ventricular remodeling depends on training load in an experimental model of endurance exercise. Am J Physiol Heart Circ Physiol, 313: H459-H468.
86. Cruz FM, Sanz-Rosa D, Roche-Molina M, Garcia-Prieto J, Garcia-Ruiz JM, Pizarro G, Jimenez-Borreguero LJ, Torres M, Bernad A, Ruiz-Cabello J, Fuster V, Ibanez B, Bernal JA. (2015) Exercise triggers ARVC phenotype in mice expressing a disease-causing mutated version of human plakophilin-2. J Am Coll Cardiol, 65: 1438-1450.
87. La Gerche A, Burns AT, Mooney DJ, Inder WJ, Taylor AJ, Bogaert J, Macisaac AI, Heidbuchel H, Prior DL. (2012) Exercise-induced right ventricular dysfunction and structural remodelling in endurance athletes. Eur Heart J, 33: 998-1006.
88. Maron BJ, Epstein SE, Roberts WC. (1986) Causes of sudden death in competitive athletes. J Am Coll Cardiol, 7: 204-214.
89. Bohm P, Scharhag J, Meyer T. (2016) Data from a nationwide registry on sports-related sudden cardiac deaths in Germany. Eur J Prev Cardiol, 23: 649-656.
90. Ayinde H, Schweizer ML, Crabb V, Ayinde A, Abugroun A, Hopson J. (2018) Age modifies the risk of atrial fibrillation among athletes: A systematic literature review and meta-analysis. Int J Cardiol Heart Vasc, 18: 25-29.
91. Mohanty S, Mohanty P, Tamaki M, Natale V, Gianni C, Trivedi C, Gokoglan Y, L DIB, Natale A. (2016) Differential Association of Exercise Intensity With Risk of Atrial Fibrillation in Men and Women: Evidence from a Meta-Analysis. J Cardiovasc Electrophysiol, 27: 1021-1029.

92. Calvo N, Brugada J, Sitges M, Mont L. (2012) Atrial fibrillation and atrial flutter in athletes. Br J Sports Med, 46 Suppl 1: i37-43.
93. Fatkin D, Cox CD, Huttner IG, Martinac B. (2018) Is There a Role for Genes in Exercise-Induced Atrial Cardiomyopathy? Heart Lung Circ, 27: 1093-1098.
94. Noakes T, Opie L, Beck W, McKechnie J, Benchimol A, Desser K. (1977) Coronary heart disease in marathon runners. Ann N Y Acad Sci, 301: 593-619.
95. Mohlenkamp S, Lehmann N, Breuckmann F, Brocker-Preuss M, Nassenstein K, Halle M, Budde T, Mann K, Barkhausen J, Heusch G, Jockel KH, Erbel R, Marathon Study I, Heinz Nixdorf Recall Study I. (2008) Running: the risk of coronary events : Prevalence and prognostic relevance of coronary atherosclerosis in marathon runners. Eur Heart J, 29: 1903-1910.
96. Roberts WO, Schwartz RS, Garberich RF, Carlson S, Knickelbine T, Schwartz JG, Peichel G, Lesser JR, Wickstrom K, Harris KM. (2017) Fifty Men, 3510 Marathons, Cardiac Risk Factors, and Coronary Artery Calcium Scores. Med Sci Sports Exerc, 49: 2369-2373.
97. Lin J, DeLuca JR, Lu MT, Ruehm SG, Dudum R, Choi B, Lieberman DE, Hoffman U, Baggish AL. (2017) Extreme Endurance Exercise and Progressive Coronary Artery Disease. J Am Coll Cardiol, 70: 293-295.
98. Mont L, Pelliccia A, Sharma S, Biffi A, Borjesson M, Terradellas JB, Carre F, Guasch E, Heidbuchel H, Gerche A, Lampert R, McKenna W, Papadakis M, Priori SG, Scanavacca M, Thompson P, Sticherling C, Viskin S, Wilson M, Corrado D, Lip GY, Gorenek B, Lundqvist CB, Merkely B, Hindricks G, Hernandez-Madrid A, Lane D, Boriani G, Narasimhan C, Marquez MF, Haines D, Mackall J, Marques-Vidal PM, Corra U, Halle M, Tiberi M, Niebauer J, Piepoli M. (2017) Pre-participation cardiovascular evaluation for athletic participants to prevent sudden death: Position paper from the EHRA and the EACPR, branches of the ESC. Endorsed by APHRS, HRS, and SOLAECE. Europace, 19: 139-163.
99. Yoerger DM, Marcus F, Sherrill D, Calkins H, Towbin JA, Zareba W, Picard MH, Multidisciplinary Study of Right Ventricular Dysplasia I. (2005) Echocardiographic findings in patients meeting task force criteria for arrhythmogenic right ventricular dysplasia: new insights from the multidisciplinary study of right ventricular dysplasia. J Am Coll Cardiol, 45: 860-865.

100. Teske AJ, Cox MG, Te Riele AS, De Boeck BW, Doevendans PA, Hauer RN, Cramer MJ. (2012) Early detection of regional functional abnormalities in asymptomatic ARVD/C gene carriers. J Am Soc Echocardiogr, 25: 997-1006.
101. Pelliccia A, Lemme E, Maestrini V, Di Paolo FM, Pisicchio C, Di Gioia G, Caselli S. (2018) Does Sport Participation Worsen the Clinical Course of Hypertrophic Cardiomyopathy? Clinical Outcome of Hypertrophic Cardiomyopathy in Athletes. Circulation, 137: 531-533.
102. Sheikh N, Papadakis M, Schnell F, Panoulas V, Malhotra A, Wilson M, Carre F, Sharma S. (2015) Clinical Profile of Athletes With Hypertrophic Cardiomyopathy. Circ Cardiovasc Imaging, 8: e003454.
103. Schnell F, Matelot D, Daudin M, Kervio G, Mabo P, Carre F, Donal E. (2017) Mechanical Dispersion by Strain Echocardiography: A Novel Tool to Diagnose Hypertrophic Cardiomyopathy in Athletes. J Am Soc Echocardiogr, 30: 251-261.
104. Narula S, Shameer K, Salem Omar AM, Dudley JT, Sengupta PP. (2016) Machine-Learning Algorithms to Automate Morphological and Functional Assessments in 2D Echocardiography. J Am Coll Cardiol, 68: 2287-2295.
105. Weiner RB, Wang F, Berkstresser B, Kim J, Wang TJ, Lewis GD, Hutter AM, Jr., Picard MH, Baggish AL. (2012) Regression of "gray zone" exercise-induced concentric left ventricular hypertrophy during prescribed detraining. J Am Coll Cardiol, 59: 1992-1994.
106. Wang Y, Wisloff U, Kemi OJ. (2010) Animal models in the study of exercise-induced cardiac hypertrophy. Physiol Res, 59: 633-644.
107. Natali AJ, Turner DL, Harrison SM, White E. (2001) Regional effects of voluntary exercise on cell size and contraction-frequency responses in rat cardiac myocytes. J Exp Biol, 204: 1191-1199.
108. Bellafiore M, Sivverini G, Palumbo D, Macaluso F, Bianco A, Palma A, Farina F. (2007) Increased cx43 and angiogenesis in exercised mouse hearts. Int J Sports Med, 28: 749-755.
109. Kemi OJ, Ceci M, Condorelli G, Smith GL, Wisloff U. (2008) Myocardial sarcoplasmic reticulum Ca2+ ATPase function is increased by aerobic interval training. Eur J Cardiovasc Prev Rehabil, 15: 145-148.

110. Radovits T, Olah A, Lux A, Nemeth BT, Hidi L, Birtalan E, Kellermayer D, Matyas C, Szabo G, Merkely B. (2013) Rat model of exercise-induced cardiac hypertrophy: hemodynamic characterization using left ventricular pressure-volume analysis. Am J Physiol Heart Circ Physiol, 305: H124-134.
111. Evangelista FS, Brum PC, Krieger JE. (2003) Duration-controlled swimming exercise training induces cardiac hypertrophy in mice. Braz J Med Biol Res, 36: 1751-1759.
112. Strickland JC, Smith MA. (2016) Animal models of resistance exercise and their application to neuroscience research. J Neurosci Methods, 273: 191-200.
113. Kovacs A, Olah A, Lux A, Matyas C, Nemeth BT, Kellermayer D, Ruppert M, Torok M, Szabo L, Meltzer A, Assabiny A, Birtalan E, Merkely B, Radovits T. (2015) Strain and strain rate by speckle-tracking echocardiography correlate with pressure-volume loop-derived contractility indices in a rat model of athlete's heart. Am J Physiol Heart Circ Physiol, 308: H743-748.
114. Mosteller RD. (1987) Simplified calculation of body-surface area. N Engl J Med, 317: 1098.
115. Lakatos B, Toser Z, Tokodi M, Doronina A, Kosztin A, Muraru D, Badano LP, Kovacs A, Merkely B. (2017) Quantification of the relative contribution of the different right ventricular wall motion components to right ventricular ejection fraction: the ReVISION method. Cardiovasc Ultrasound, 15: 8.
116. Maron BJ, Maron BA. (2017) Revisiting Athlete's Heart Versus Pathologic Hypertrophy: ARVC and the Right Ventricle. JACC Cardiovasc Imaging, 10: 394-397.
117. Bocalini DS, Carvalho EV, de Sousa AF, Levy RF, Tucci PJ. (2010) Exercise training-induced enhancement in myocardial mechanics is lost after 2 weeks of detraining in rats. Eur J Appl Physiol, 109: 909-914.
118. Pacher P, Nagayama T, Mukhopadhyay P, Batkai S, Kass DA. (2008) Measurement of cardiac function using pressure-volume conductance catheter technique in mice and rats. Nat Protoc, 3: 1422-1434.
119. Kemi OJ, Haram PM, Wisloff U, Ellingsen O. (2004) Aerobic fitness is associated with cardiomyocyte contractile capacity and endothelial function in exercise training and detraining. Circulation, 109: 2897-2904.

120. Olah A, Kellermayer D, Matyas C, Nemeth BT, Lux A, Szabo L, Torok M, Ruppert M, Meltzer A, Sayour AA, Benke K, Hartyanszky I, Merkely B, Radovits T. (2017) Complete Reversion of Cardiac Functional Adaptation Induced by Exercise Training. Med Sci Sports Exerc, 49: 420-429.

121. Martin WH, 3rd, Coyle EF, Bloomfield SA, Ehsani AA. (1986) Effects of physical deconditioning after intense endurance training on left ventricular dimensions and stroke volume. J Am Coll Cardiol, 7: 982-989.

122. Haddad F, Hunt SA, Rosenthal DN, Murphy DJ. (2008) Right ventricular function in cardiovascular disease, part I: Anatomy, physiology, aging, and functional assessment of the right ventricle. Circulation, 117: 1436-1448.

123. Buckberg G, Hoffman JI. (2014) Right ventricular architecture responsible for mechanical performance: unifying role of ventricular septum. J Thorac Cardiovasc Surg, 148: 3166-3171 e3161-3164.

124. Dragulescu A, Grosse-Wortmann L, Redington A, Friedberg MK, Mertens L. (2013) Differential effect of right ventricular dilatation on myocardial deformation in patients with atrial septal defects and patients after tetralogy of Fallot repair. Int J Cardiol, 168: 803-810.

125. Eroglu E, Cakal SD, Cakal B, Dundar C, Alici G, Ozkan B, Yazicioglu MV, Tigen K, Esen AM. (2013) Time course of right ventricular remodeling after percutaneous atrial septal defect closure: assessment of regional deformation properties with two-dimensional strain and strain rate imaging. Echocardiography, 30: 324-330.

126. Vitarelli A, Sardella G, Roma AD, Capotosto L, De Curtis G, D'Orazio S, Cicconetti P, Battaglia D, Caranci F, De Maio M, Bruno P, Vitarelli M, De Chiara S, D'Ascanio M. (2012) Assessment of right ventricular function by three-dimensional echocardiography and myocardial strain imaging in adult atrial septal defect before and after percutaneous closure. Int J Cardiovasc Imaging, 28: 1905-1916.

127. Esposito R, Galderisi M, Schiano-Lomoriello V, Santoro A, De Palma D, Ippolito R, Muscariello R, Santoro C, Guerra G, Cameli M, Mondillo S, De Simone G. (2014) Nonsymmetric myocardial contribution to supranormal right ventricular function in the athlete's heart: combined assessment by speckle tracking and real time three-dimensional echocardiography. Echocardiography, 31: 996-1004.

128. Teske AJ, Prakken NH, De Boeck BW, Velthuis BK, Martens EP, Doevendans PA, Cramer MJ. (2009) Echocardiographic tissue deformation imaging of right ventricular systolic function in endurance athletes. Eur Heart J, 30: 969-977.
129. Swift AJ, Rajaram S, Capener D, Elliot C, Condliffe R, Wild JM, Kiely DG. (2015) Longitudinal and transverse right ventricular function in pulmonary hypertension: cardiovascular magnetic resonance imaging study from the ASPIRE registry. Pulm Circ, 5: 557-564.
130. Moceri P, Duchateau N, Baudouy D, Schouver ED, Leroy S, Squara F, Ferrari E, Sermesant M. (2017) Three-dimensional right-ventricular regional deformation and survival in pulmonary hypertension. Eur Heart J Cardiovasc Imaging.
131. Moceri P, Bouvier P, Baudouy D, Dimopoulos K, Cerboni P, Wort SJ, Doyen D, Schouver ED, Gibelin P, Senior R, Gatzoulis MA, Ferrari E, Li W. (2017) Cardiac remodelling amongst adults with various aetiologies of pulmonary arterial hypertension including Eisenmenger syndrome-implications on survival and the role of right ventricular transverse strain. Eur Heart J Cardiovasc Imaging, 18: 1262-1270.
132. Coote JH, White MJ. (2015) CrossTalk proposal: bradycardia in the trained athlete is attributable to high vagal tone. J Physiol, 593: 1745-1747.
133. Machhada A, Trapp S, Marina N, Stephens RCM, Whittle J, Lythgoe MF, Kasparov S, Ackland GL, Gourine AV. (2017) Vagal determinants of exercise capacity. Nat Commun, 8: 15097.
134. Santamore WP, Gray L, Jr. (1995) Significant left ventricular contributions to right ventricular systolic function. Mechanism and clinical implications. Chest, 107: 1134-1145.
135. Sanz de la Garza M, Grazioli G, Bijnens BH, Pajuelo C, Brotons D, Subirats E, Brugada R, Roca E, Sitges M. (2016) Inter-individual variability in right ventricle adaptation after an endurance race. Eur J Prev Cardiol, 23: 1114-1124.
136. Sanz-de la Garza M, Giraldeau G, Marin J, Grazioli G, Esteve M, Gabrielli L, Brambila C, Sanchis L, Bijnens B, Sitges M. (2017) Influence of gender on right ventricle adaptation to endurance exercise: an ultrasound two-dimensional speckle-tracking stress study. Eur J Appl Physiol, 117: 389-396.
137. Swoboda PP, Erhayiem B, McDiarmid AK, Lancaster RE, Lyall GK, Dobson LE, Ripley DP, Musa TA, Garg P, Ferguson C, Greenwood JP, Plein S. (2016)

Relationship between cardiac deformation parameters measured by cardiovascular magnetic resonance and aerobic fitness in endurance athletes. J Cardiovasc Magn Reson, 18: 48.

138. Wright S, Sasson Z, Gray T, Chelvanathan A, Esfandiari S, Dimitry J, Armstrong S, Mak S, Goodman JM. (2015) Left atrial phasic function interacts to support left ventricular filling during exercise in healthy athletes. J Appl Physiol (1985), 119: 328-333.

139. D'Andrea A, Riegler L, Cocchia R, Scarafile R, Salerno G, Gravino R, Golia E, Vriz O, Citro R, Limongelli G, Calabro P, Di Salvo G, Caso P, Russo MG, Bossone E, Calabro R. (2010) Left atrial volume index in highly trained athletes. Am Heart J, 159: 1155-1161.

140. Badano LP, Miglioranza MH, Mihaila S, Peluso D, Xhaxho J, Marra MP, Cucchini U, Soriani N, Iliceto S, Muraru D. (2016) Left Atrial Volumes and Function by Three-Dimensional Echocardiography: Reference Values, Accuracy, Reproducibility, and Comparison With Two-Dimensional Echocardiographic Measurements. Circ Cardiovasc Imaging, 9.

141. Gabrielli L, Bijnens BH, Butakoff C, Duchateau N, Montserrat S, Merino B, Gutierrez J, Pare C, Mont L, Brugada J, Sitges M. (2014) Atrial functional and geometrical remodeling in highly trained male athletes: for better or worse? Eur J Appl Physiol, 114: 1143-1152.

142. D'Ascenzi F, Pelliccia A, Natali BM, Cameli M, Lisi M, Focardi M, Padeletti M, Palmitesta P, Corrado D, Bonifazi M, Mondillo S, Henein M. (2015) Training-induced dynamic changes in left atrial reservoir, conduit, and active volumes in professional soccer players. Eur J Appl Physiol, 115: 1715-1723.

143. Nemes A, Domsik P, Kalapos A, Orosz A, Oszlanczi M, Torok L, Balogh L, Marton J, Forster T, Lengyel C. (2017) Volumetric and functional assessment of the left atrium in young competitive athletes without left ventricular hypertrophy: the MAGYAR-Sport Study. J Sports Med Phys Fitness, 57: 900-906.

144. Sanchis L, Sanz-de La Garza M, Bijnens B, Giraldeau G, Grazioli G, Marin J, Gabrielli L, Montserrat S, Sitges M. (2017) Gender influence on the adaptation of atrial performance to training. Eur J Sport Sci, 17: 720-726.

145. Leite L, Mendes SL, Baptista R, Teixeira R, Oliveira-Santos M, Ribeiro N, Coutinho R, Monteiro V, Martins R, Castro G, Ferreira MJ, Pego M. (2017) Left atrial mechanics strongly predict functional capacity assessed by cardiopulmonary exercise testing in subjects without structural heart disease. Int J Cardiovasc Imaging, 33: 635-642.

10. BIBLIOGRAPHY OF THE CANDIDATE

10.1 Bibliography related to the present thesis

1. Olah A, Kovacs A, Lux A, Tokodi M, Braun S, **Lakatos BK**, Matyas C, Kellermayer D, Ruppert M, Sayour AA, Barta BA, Merkely B, Radovits T. (2019) Characterization of the dynamic changes in left ventricular morphology and function induced by exercise training and detraining. Int J Cardiol, 277: 178-185.
   IF: 3.229
2. **Lakatos BK**, Kiss O, Tokodi M, Toser Z, Sydo N, Merkely G, Babity M, Szilagyi M, Komocsin Z, Bognar C, Kovacs A, Merkely B. (2018) Exercise-induced shift in right ventricular contraction pattern: novel marker of athlete's heart? Am J Physiol Heart Circ Physiol.
   IF: 4.048
3. **Lakatos BK**, Molnar AA, Kiss O, Sydo N, Tokodi M, Solymossi B, Fabian A, Dohy Z, Vago H, Babity M, Bognar C, Kovacs A, Merkely B. (2020) Relationship between Cardiac Remodeling and Exercise Capacity in Elite Athletes: Incremental Value of Left Atrial Morphology and Function Assessed by Three-Dimensional Echocardiography. J Am Soc Echocardiogr, 33: 101-109 e101.
   IF: 5.508

10.2 Bibliography not related to the present thesis

1. **Lakatos B**, Toser Z, Tokodi M, Doronina A, Kosztin A, Muraru D, Badano LP, Kovacs A, Merkely B. (2017) Quantification of the relative contribution of the different right ventricular wall motion components to right ventricular ejection fraction: the ReVISION method. Cardiovasc Ultrasound, 15: 8.
   IF: 2.051
2. Matyas C, Kovacs A, Nemeth BT, Olah A, Braun S, Tokodi M, Barta BA, Benke K, Ruppert M, **Lakatos BK**, Merkely B, Radovits T. (2018) Comparison of speckle-tracking echocardiography with invasive hemodynamics for the detection of characteristic cardiac dysfunction in type-1 and type-2 diabetic rat models. Cardiovasc Diabetol, 17: 13.

IF: 7.332

3. **Lakatos BK**, Tokodi M, Assabiny A, Toser Z, Kosztin A, Doronina A, Racz K, Koritsanszky KB, Berzsenyi V, Nemeth E, Sax B, Kovacs A, Merkely B. (2018) Dominance of free wall radial motion in global right ventricular function of heart transplant recipients. Clin Transplant, 32: e13192.
   IF: 1.667
4. Molnar AA, Kovacs A, **Lakatos BK**, Polos M, Merkely B. (2018) Sinus of Valsalva aneurysm protruding intramurally into right ventricle: does size really matter? Eur Heart J Cardiovasc Imaging, 19: 234.
   IF: 4.841
5. Kovacs A, Molnar AA, Kolossvary M, Szilveszter B, Panajotu A, **Lakatos BK**, Littvay L, Tarnoki AD, Tarnoki DL, Voros S, Jermendy G, Sengupta PP, Merkely B, Maurovich-Horvat P. (2018) Genetically determined pattern of left ventricular function in normal and hypertensive hearts. J Clin Hypertens (Greenwich), 20: 949-958.
   IF: 2.719
6. Doronina A, Edes IF, Ujvari A, Kantor Z, **Lakatos BK**, Tokodi M, Sydo N, Kiss O, Abramov A, Kovacs A, Merkely B. (2018) The Female Athlete's Heart: Comparison of Cardiac Changes Induced by Different Types of Exercise Training Using 3D Echocardiography. Biomed Res Int, 2018: 3561962.
   IF: 2.276
7. Kovacs A, **Lakatos B**, Nemeth E, Merkely B. (2018) Response to Ivey-Miranda and Farrero-Torres "Is there dominance of free wall radial motion in global right ventricular function in heart transplant recipients or in all heart surgery patients?". Clin Transplant, 32: e13286.
   IF: 1.665
8. Kovacs A, **Lakatos B**, Tokodi M, Merkely B. (2019) Right ventricular mechanical pattern in health and disease: beyond longitudinal shortening. Heart Fail Rev, 24: 511-520.
   IF: 3.538
9. Csecs I, Czimbalmos C, Toth A, Dohy Z, Suhai IF, Szabo L, Kovacs A, **Lakatos B**, Sydo N, Kheirkhahan M, Peritz D, Kiss O, Merkely B, Vago H. (2020) The

impact of sex, age and training on biventricular cardiac adaptation in healthy adult and adolescent athletes: Cardiac magnetic resonance imaging study. Eur J Prev Cardiol, 27: 540-549.
IF: 5.864

10. Tokodi M, Schwertner WR, Kovacs A, Toser Z, Staub L, Sarkany A, **Lakatos BK**, Behon A, Boros AM, Perge P, Kutyifa V, Szeplaki G, Geller L, Merkely B, Kosztin A. (2020) Machine learning-based mortality prediction of patients undergoing cardiac resynchronization therapy: the SEMMELWEIS-CRT score. Eur Heart J. May 7;41(18):1747-1756.
IF: 22.673
11. Tokodi M, Németh E, **Lakatos BK**, Kispál E, Tősér Z, Staub L, Rácz K, Soltész Á, Szigeti S, Varga T, Gál J, Merkely B, Kovács A. (2020) Right ventricular mechanical pattern in patients undergoing mitral valve surgery: a predictor of post-operative dysfunction? ESC Heart Failure, 2020 Jun;7(3):1246-1256. Epub 2020 Mar 26.
IF: 3.902
12. **Lakatos BK**, Kovacs A (2020) Global Longitudinal Strain in Moderate Aortic Stenosis: A Chance to Synthesize It All? Circ Cardiovasc Imaging 2020 Apr;13(4):e010711.
IF: 5.691
13. **Lakatos BK**, Nabeshima Y, Tokodi M, Nagata Y, Toser Z, Otani K, Kitano T, Fabian A, Ujvari A, Boros AM, Merkely B, Kovacs A, Takeuchi M (2020) Importance of non-longitudinal motion components in right ventricular function: 3D echocardiographic study in healthy volunteers J Am Soc Echocardiogr. 2020 Aug;33(8):995-1005.e1. Epub 2020 Jun 30
IF: 5.508
14. Ruppert M, **Lakatos BK**, Braun S, Tokodi M, Karime C, Olah A, Sayour AA, Hizoh I, Barta BA, Merkely B, Kovacs A, Radovits T (2020) Longitudinal strain reflects ventriculo-arterial coupling rather than mere contractility in rat models of hemodynamic overload-induced heart failure J Am Soc Echocardiogr. 2020 Oct;33(10):1264-1275.e4. Epub 2020 Aug 7.
IF: 5.508

DOI:10.14753/SE.2021.2460

Hungarian articles:

1. **Lakatos B**, Kovács A, Tokodi M, Doronina A, Merkely B. (2016) A jobb kamrai anatómia és funkció korszerű echokardiográfiás vizsgálata: patológiás és fiziológiás eltérések. Orv Hetil. 157(29):1139-46.
   IF: 0.497
2. Ujvári A, Komka Z, Kántor Z, **Lakatos BK**, Tokodi M, Doronina A, Babity M, Bognár C, Kiss O, Merkely B, Kovács A (2018) Kajakos és kenus élsportolók bal és jobb kamrai analízise 3D echokardiográfia segítségével Cardiol Hung 48: 13–19
3. Suhai FI, Sax B, Assabiny A, Király Á, Czimbalmos C, Csécs I, Kovács A, **Lakatos B**, Németh E, Becker D, Szabolcs Z, Hubay M, Merkely B, Vágó Hajnalka (2018) A szív MR-vizsgálat szerepe kevert típusú (humorális és celluláris) kardiális allograft rejekció esetén Cardiol Hung 48: 44–51
4. Fábián A, **Lakatos BK**, Kiss O, Sydó N, Vágó H, Czimbalmos C, Tokodi M, Kántor Z, Bognár C, Major D, Kovács A, Merkely B (2019) A jobb kamrai kontrakciós mintázat változása élsportolókban: háromdimenziós echokardiográfiás vizsgálat Cardiol Hung 49: 17–23

DOI:10.14753/SE.2021.2460

12. ACKNOWLEDGEMENTS

This present work would not have been possible without the tremendous support and help of several individuals. First and foremost, I would like to express my sincere gratitude to my mentors: Dr. Attila Kovács showed me incredible depths of cardiology. His guidance in research, clinical work, and also in many valuable lessons of life truly helped me to grow not only as a scientist but also as a human being. I am especially grateful to Professor Béla Merkely for his professional guidance and his constant support, providing me outstanding opportunities during the years of my PhD research. Their ever-lasting enthusiasm towards the field always stood as an inspiration for me. I am very grateful to Dr. Violetta Kékesi for the many help and advice from my PhD application till the submission of this thesis.

I would like to thank Dr. Orsolya Kiss, and all the other members and co-workers of the Sports Cardiology Research Group for their many useful advice and for their exceptional work, which were substantial for my scientific work. Also many thanks to Dr. Nóra Sydó for her great contribution.

I am particularly grateful to Dr. Andrea Molnár and all the other members of the Echocardiography Working Group of the Institute for their great help during my research projects.

Many thanks to Dr. Márton Tokodi and Zoltán Tősér for their help in many technical aspects of my research, giving me aid in numerous issues during my studies.

I am also incredibly grateful to Dr. Tamás Radovits, Dr. Attila Oláh, and the whole Experimental Cardiology Research Group for showing me the beauty of basic research and giving me the opportunity to participate in such projects.

I would like to thank Ágnes Pfeifer for the echo lab assistance, bearing dozens of hours of additional work due to the scientific projects only with patience, support, and good mood.

DOI:10.14753/SE.2021.2460

Many thanks to all the fellow PhD students and student researchers: Dr. Szilvia Herczeg, Dr. Miklós Vértes, Dr. Mihály Ruppert, Dr. Adrienn Ujvári, Mónika Szilágyi, Alexandra Fábián, Erika Kispál and also to all my former and current co-workers at the Heart and Vascular Center not only for their scientific contribution to this work but also for their friendship.

A very special word of thanks to my significant other, Zita, for her constant emotional support, love, and inexhaustible patience in many difficult times when those were the only things that kept me go on.

Last but not least, I would like to express my gratitude for my family, providing me a careless and supporting environment. I cannot describe how grateful I am for all the sacrifices that they made in order to help me any time, every time.